

VYSOKÉ UČENÍ TECHNICKÉ V BRNĚ

BRNO UNIVERSITY OF TECHNOLOGY



FAKULTA CHEMICKÁ
ÚSTAV CHEMIE MATERIÁLŮ

FACULTY OF CHEMISTRY
INSTITUTE OF MATERIALS SCIENCE

THE SYNTHESIS AND CHARACTERISATION OF COMPOSITE MATERIALS FOR POTENTIAL APPLICATION IN MEDICINE

SYNTEZA A VLASTNOSTI BIOKOMPOZITNÍCH MATERIÁLŮ S POTENCIÁLNÍM VYUŽITÍM V MEDICÍNĚ

DIZERTAČNÍ PRÁCE

DOCTORAL THESIS

AUTOR PRÁCE

AUTHOR

Ing. ZUZANA BALGOVÁ

VEDOUCÍ PRÁCE

SUPERVISOR

prof. Dr. Ing. MARTIN T. PALOU

BRNO 2013

ABSTRACT

The work is focused on the synthesis and the study of biocomposite materials for potential medical application. The theoretical part is a literature overview focused on different types of biomaterials especially on polyvinyl alcohol - hydroxyapatite (PVA/HA) composites.

A set of polyvinyl alcohol (PVA) membranes with various weight percent - 0%, 10%, 20%, 30%, 40% and 50% of hydroxyapatite (HA) were prepared. Hydroxyapatite was prepared by precipitation procedure using starting materials of diammonium hydrogen phosphate and calcium nitrate tetrahydrate in water alkaline environment and then mixed with solution of polyvinyl alcohol, which was prepared by dissolving it in water at 85°C. The different mixtures were casted in a mould and evaporated for 7 days at temperature 30 °C to obtain 0,5 mm thin membranes. The ATR-FTIR spectroscopy was used to identify the different functional groups in composite membranes, XRD testing was carried out to identify crystallized hydroxyapatite. The tensile testing and TGA measurement were realised to find the effect of HA amount on the mechanical properties and thermal stability of the membranes. The *in vitro* bioactivity tests in Simulated Blood Fluid (SBF) were performed for 2 hours, 7 and 28 days. SEM was used to characterise surface microstructure of biocomposite membranes before and after immersion in SBF. The surface of the tested membranes were analysed to investigate the formation of apatite, the characteristic of bioactivity. It was observed a formation of clusters within membranes with increasing amount of HA particles due to hydrogen bond and also the agglomeration and crystal growth of HA particles during drying of membranes. The bioactivity was found increasing with time immersion of biocomposite materials.

KEYWORDS:

biocomposites, polyvinyl alcohol, hydroxyapatite, microstructure, SBF bioactivity

ABSTRAKT

Dizertační práce se zabývá syntézou a studiem kompozitních materiálů pro potenciální lékařské využití. Teoretická část je zaměřena na biomateriály, zejména na kompozity složené z polyvinylalkoholu a hydroxyapatitu (PVA/HA).

Byly připraveny kompozitní membrány složené z polyvinylalkoholu s různým hmotnostním zastoupením hydroxyapatitu - 0%, 10%, 20%, 30%, 40% a 50%. Hydroxyapatit (HA) byl připraven srážecí metodou z hydrogenfosforečnanu amonného a tetrahydrátu dusičnanu vápenatého ve vodném alkalickém prostředí. Vzniklá suspenze se smísila s roztokem polyvinylalkoholu, který byl připraven rozpuštěním ve vodě o teplotě 85° C. Jednotlivé směsi byly odlity do formy a sušeny po dobu 7 dní při teplotě 30 ° C, vzniklé 0,5 mm tenké membrány byly analyzovány ATR-FTIR spektroskopii k identifikaci funkčních skupin v kompozitu, dále byla provedena XRD analýza. Zkouška tahem a TGA měření byly realizovány k určení vlivu HA na mechanické vlastnosti, respektive změnu tepelné odolnosti kompozitů ve srovnání s čistým PVA. Byla provedena zkouška bioaktivity v simulovaném krevním roztoku (SBF) po dobu 2h, 7 a 28 dnů. SEM byla použita k charakterizaci povrchové mikrostruktury biokompozitních membrán před a po ponoření do SBF. Na povrchu testovaných membrán vznikla vrstva apatitu, která je charakteristická pro bioaktivní materiály. Bylo zjištěno, že s rostoucím množstvím HA v kompozitu docházelo ke vzniku aglomerátů, které vznikly mimo jiné jako důsledek růstu krystalů HA během sušení membrán. Bioaktivita rostla s delším působením SBF na vzorky.

KLÍČOVÁ SLOVA:

biokompozity, polyvinylalkohol, hydroxyapatit, mikrostruktura, SBF bioaktivita

BALGOVÁ, Z. *Syntéza a vlastnosti biokompozitních materiálů s potenciálním využitím v medicíně*. Brno: Vysoké učení technické v Brně, Fakulta chemická, 2013. 84 s. Vedoucí dizertační práce prof. Dr. Ing. Martin Palou.

DECLARATION

I declare that the diploma thesis has been worked out by myself and that all the quotations from the used literary sources are accurate and complete. The content of the diploma thesis is the property of the Faculty of Chemistry of Brno University of Technology and all commercial uses are allowed only if approved by both the supervisor and the dean of the Faculty of Chemistry, BUT.

.....
student's signature

ACKNOWLEDGEMENT

I would like to express my deepest appreciation to all those who supported and helped me during my doctoral study.

My special thanks goes to prof. Dr. Ing. Martin Tchingnabe Palou for his supervision, help, expert support and patience.

I wish to thank my family for encouragement and support.

Martin & Olga, thank you for giving me the strength.

CONTENTS

1	THE AIM OF THE WORK	9
2	INTRODUCTION	10
3	THEORETICAL PART	13
3.1	Biomaterials of first generation	14
3.1.1	Metals	14
3.1.2	Ceramics	14
3.1.3	Polymers	14
3.1.4	Composites	14
3.2	Biomaterials of second generation	14
3.2.1	Ceramics	15
3.2.1.1	Calcium phosphates	15
3.2.1.2	Bioactive glasses	15
3.2.1.3	Glass ceramics	15
3.2.2	Metals	16
3.2.3	Polymers	16
3.3	Composites	16
3.4	Biomaterials of third generation	17
3.4.1	Scaffolds for tissue engineering	17
3.4.2	In situ tissue regeneration.	17
3.5	Composites	18
3.5.1	Nanocomposites	18
3.6	Hydroxyapatite	21
3.6.1	HA mechanical properties	23
3.6.2	HAP preparation	24
3.7	Poly(vinyl alcohol)	24
3.7.1	Manufacture of poly(vinyl alcohol)	24
3.7.2	Properties based on degree of polymerization	25
3.7.3	Dissolving properties based on degree of hydrolysis	25
3.7.3.1	Manufacture of polyvinylacetate	25
3.7.4	Polymer chain	26
3.7.5	Poly(vinyl alcohol) in medical application	26
3.7.6	In vivo toxicity status	27
3.8	Poly(vinyl alcohol) – Hydroxyapatite composite	27
3.8.1	Interaction between HA and PVA	27
3.8.2	Mechanical properties of HA/PVA	28
3.8.3	PVA/HA composite application	30
3.9	Bioactivity testing	30
3.9.1	Simulated body fluids	31
3.9.2	Mechanism of apatite layer formation in SBF	32
3.9.3	HA bioceramics in vivo behaviour	33
4	EXPERIMENTAL PART	34
4.1	Samples preparation	34
4.1.1	Chemicals used	34
4.1.2	Preparation of hydroxyapatite	34

4.1.3	Preparation of poly(vinyl alcohol)	34
4.1.4	Composite membranes preparation	35
4.1.5	Simulated body fluid preparation	35
4.2	Testing methods	36
4.2.1	FTIR-ATR	36
4.2.2	Morphological characterization with scanning electron microscopy	36
4.2.3	XRD diffraction analysis	36
4.2.4	Tensile properties	37
4.2.5	Thermogravimetric Analysis (TGA)	38
4.2.6	Bioactivity testing	39
5	RESULTS AND DISCUSSION	40
5.1	XRD analysis	40
5.2	FTIR-ATR	41
5.3	Morphological characterisation with SEM	43
5.4	Tensile properties	47
5.5	Thermogravimetric analysis	52
5.5.1	PVA thermal decomposition	52
5.5.2	HA thermal decomposition	54
5.5.3	PVA thermogravimetry analysis	54
5.5.4	Hydroxyapatite thermogravimetry analysis	55
5.5.5	PVA/HA composite thermogravimetry analysis "	56
5.6	Bioactivity testing	58
5.6.1	Surface Roughness	62
6	CONCLUSION	65
7	FUTURE WORK	67
8	REFERENCES	68
9	LIST OF FIGURES	76
10	LIST OF TABLES	78
11	LIST OF SYMBOLS	79
12	APPENDIX	80
12.1	TGA results	80
12.2	List of publications	83

1 THE AIM OF THE WORK

- Draw up a literature overview focused on biomaterials especially on poly(vinyl alcohol)- hydroxyapatite (PVA/HA) composites; current state-of the-art.
- Preparation of PVA/HA composites by precipitation method with variable amounts of HA in PVA matrix.
- Characterisation of the composite properties.
- Soaking samples in Simulated Body Fluid (SBF); detection of new structures created on sample surfaces after soaking; clarification of new structures formation.
- To realise the aims of the PhD study the following methods will be used
 - Scanning Electron Microscopy (SEM)
 - Infrared spectroscopy by ATR (FTIR-ATR)
 - X-ray Diffraction (XRD)
 - Thermogravimetric analysis (TGA)
 - Tensile properties testing
 - Bioactivity in microincubator with SBF

2 INTRODUCTION

People tried to replace bone tissue long time ago, the oldest proof is the neolithic golden slide found in Peru which was used as forehead bone replacement. About more then 1000 years ago bone implants were point of interest in Arabian countries, five hundred years ago the Aztecs were dealing with this question.

Biological materials are used as replacement, increasingly non-biological materials as metals, metal alloys, ceramics, polymers and composites are applied. The required feature of materials used as implants is non-toxicity for living cells, non-inflammatory, non-teratogenicity, non-mutagenicity and non-cancerous. In the present times ceramic surface bioactive materials are used as they successfully imitate the advantages of biological materials [1].

The development and use of biomaterials as implants in biomedicine is gaining in intensity since the end of the 20th century, as the life expectancy in developed countries exceeds the 80. Those values are spectacular if compared with those corresponding to early 20th century, around 40 years, while in Imperial Rome the life expectancy was only 22 years. Therefore, 19 centuries passed before the expected lifespan doubled and then, in just one century, the 20th century, it doubled again. This spectacular rise is still ongoing, increasing the demand and the need for biomaterials. The ageing of the population involves certain problems that were not so generic some time ago, since fewer people reached those ages where the incidence of such diseases is more evident [2].

The definition of biomaterials is: "A biomaterial is a substance that has been engineered to take a form which, alone or as part of a complex system, is used to direct, by control of interactions with components of living systems, the course of any therapeutic or diagnostic procedure, in human or veterinary medicine"[3].

In any case, biomaterials are intended to interface with biological systems to evaluate, treat, augment or replace any tissue, organ or function of the body and are now used in a number of different applications throughout the body [4]. The major difference between biomaterials and other classes of materials is the ability of biomaterials to remain in a biological environment without damaging the surroundings and without being damaged themselves in the process. Thus, biomaterials are solely associated with the health care domain and they must have an interface with tissues or tissue components. One should stress that any artificial materials that are simply in contact with skin, such as hearing aids and wearable artificial limbs, are not included in the definition of biomaterials since the skin acts as a protective barrier between the body and the external world. The biomaterials discipline is founded in the knowledge of the synergistic interaction of material science, biological science, chemical science, medical science and mechanical science and requires input and comprehension from all these areas so that implanted biomaterials perform adequately in a living body and interrupt normal body functions as little as possible [5].

Engineering materials could be classified as metals, polymers ceramics and composites. In the same way, biomaterials are divided into biometals, biopolymers, bioceramics and biocomposites [5, 6].

When a synthetic material is placed within the human body, tissue reacts towards the implant in a variety of ways depending on the material type. The mechanism of tissue interaction (if any) depends on the tissue response to the implant surface. In general, there are three terms in

which a biomaterial may be described in or classified into representing the tissues responses. These are bioinert, bioresorbable and bioactive [7].

The term bioinert refers to any materials that once placed in the human body have minimal interaction with its surrounding tissue. Examples of these are stainless steel, titanium, alumina, partially stabilised zirconia, and ultra high molecular weight polyethylene. Generally a fibrous capsule might form around bioinert implants hence its biofunctionality relies on tissue integration through the implant (Figure 1a). Bioactive refers to a material, which upon being placed within the human body interacts with the surrounding bone and in some cases, even soft tissue. This occurs through a time - dependent kinetic modification of the surface, triggered by their implantation within the living bone. An ion exchange reaction between the bioactive implant and surrounding body fluids results in the formation of a biologically active carbonate apatite (CHAp) layer on the implant that is chemically and crystallographically equivalent to the mineral phase in bone. Prime examples of these materials are synthetic hydroxyapatite [8, 9]. ($\text{Ca}_{10}(\text{PO}_4)_6(\text{OH})_2$), glassceramics A-W [9] and bioglass® [10], (Figure 1b and c)). Bioresorbable refers to a material that upon placement within the human body starts to dissolve (resorbed) and slowly replaced by advancing tissue (such as bone). Common examples of bioresorbable materials are tricalcium phosphate ($\text{Ca}_3(\text{PO}_4)_2$) and polylactic–polyglycolic acid copolymers. Calcium oxide, calcium carbonate and gypsum are other common materials that have been utilised during the last three decades (Figure 1d) [12].

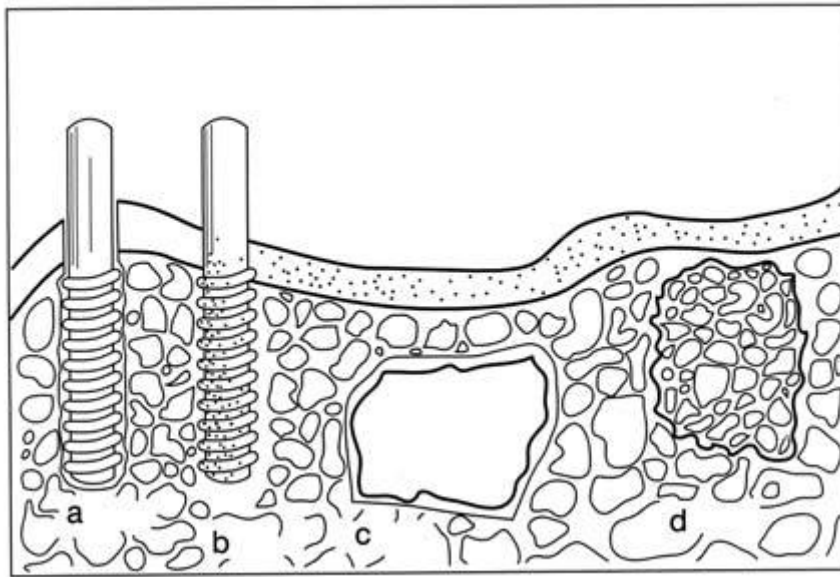


Figure 1: Classification of bioceramics according to their bioactivity; (a) bioinert, alumina dental implant, (b) bioactive, hydroxyapatite ($\text{Ca}_{10}(\text{PO}_4)_2(\text{OH})_2$) coating on a metallic dental implant, (c) surface active, bioglass, (d) bioresorbable tri-calcium phosphate implant ($\text{Ca}_3(\text{PO}_4)_2$) [12]

Depending on the function to perform, they can be manufactured from very different materials. It is known that the reactivity of solids begins on their surface. This general statement is of particular importance in the field of biomaterials, since they will be in contact with an aqueous medium and in presence of cells and proteins.

Nowadays, it is possible to manufacture implants for any part of our body, except for the brain. Obviously, different types of materials are in use depending on the tissue to be replaced. If we focus on functional artificial biomaterials, the choice has to be made among metals, polymers and ceramics. Each group exhibits some a priori advantages and drawbacks. Ceramics, for instance, are the most biocompatible materials and can be obtained with bioinert, bioactive or bioresorbable properties, but their main drawbacks are their hardness and fragility.

Metals exhibit problems of corrosion and toxicity, but their mechanical behaviour is optimum. Polymers offer many possibilities depending on their chemical composition and structure (biodegradability degree, hydrophilic/hydrophobic ratio, toughness/flexibility, etc.), but very few have shown good bioactive properties to ensure the implant osteo-integration.

It is quite usual to use the three types of materials in the same implant. This is the case of a total hip joint prosthesis which presents a metal beam, partially coated with a bioactive ceramic, while the head is made of an inert ceramic and the socket is made of polymer [13].

3 THEORETICAL PART

The searching for ceramic bone substitutes started in the 1950s, and the first aim was to use inert materials which had no reaction with living tissues. Later on, in the 1980s, the trend changed towards exactly the opposite; the idea is to implant ceramics that react with the environment and produce newly formed bone. And then, in the current century, we are searching for new ceramics [5].

Table 1 shows different types of materials that are employed as bone substitutes. Basically, only metalloid materials, of the commercially available synthetic biomaterials, are mechanically good enough to reconstruct large cortical bone defects. Of donor materials, autograft is bone that is removed from the patient's own body, whereas allograft is bone that is removed from the same species (i.e. other humans). In addition, xenograft is also of biological origin; it is extracted from the inorganic phase of mammal bone but of some other species, typically e.g. that of neat. In fact, the use of autograft is drastically limited, because of the lack of availability and donor site morbidity limits. On the other hand, the risk of infection [14].

Table 1: The main material categories to reconstruct bone, and some of their typical disadvantages[14]

ALLOGRAFT	AUTOGRAFT
Infection Risk Management of bone bank is difficult Expensive	Lack of availability Damage to healthy bone tissues Secondary surgical procedure needed
METALLIC MATERIALS	POLYMER-BASED MATERIALS
Metal-bone interface mechanical Loosening risk Stress shielding High elasticity moduli not optimal for bone Release of nanoparticles	Residual toxic monomers, e.g. Risk of exothermic effects, hypotonia, or heart and lung complications Risk of wear debris
BIOCERAMICS AND BIOACTIVE GLASSES	OTHER, e.g. Xenografts
Brittleness Stress shielding High modulus of elasticity	Infection risk Low strength

The biomaterials for the biomedical applications have evolved through three different generations, namely first generation (bioinert materials), second generation (bioactive and biodegradable materials) and third generation (materials designed to stimulate specific responses at the molecular level) [16].

3.1 Biomaterials of first generation

When synthetic materials were first used in biomedical applications, the only requirement was to ‘achieve a suitable combination of physical properties to match those of the replaced tissue with a minimal toxic response of the host’ [15]. They were the first-generation biomaterials, according to Hench’s classification, because they were inert so as to reduce the immune response and the foreign body reaction to a minimum [16].

3.1.1 Metals

The first metallic materials successfully used during the twentieth century in orthopaedic applications were stainless steel and cobalt-chrome-based alloys. Ti and Ti alloys were introduced by the 1940s. NiTi shape memory alloys were developed by the 1960s and they seemed to open a whole new range of applications, due to their special mechanical behaviour, but the properly unsolved allergenic effect of Ni has hampered their use. Ti and its alloys, originally used in aeronautics, became materials of great interest in the biomedical field, due to their excellent properties that include a moderate elastic modulus of approximately 110 GPa, a good corrosion resistance and a low density [16].

3.1.2 Ceramics

The first generation of ceramics as biomaterials, called inert ceramics, were focused on natural bone substitution. Well known examples are zirconia, titanium and alumina. which are primarily used in fabrication of femoral heads to substitute the damaged bones. These ceramics are biocompatible, but the living body reacts against the implants because they are of foreign nature and the implant made of this artificial material never transforms into bone [17].

3.1.3 Polymers

Some examples of polymer biomaterials of the first generation are silicone rubber, PE, acrylic resins, polyurethanes, polypropylene (PP) and polymethylmethacrylate (PMMA) [16]. PMMA is typically used as a filler material (bone cement) for joint replacement surgical procedures [18]. PE, and more specifically UHMWPE, is particularly attractive for applications such as the liner of acetabular cups in total hip arthroplasties, in the tibial insert and patellar component in total knee arthroplasties and as a spacer in intervertebral artificial disc replacement. Its unique properties of high abrasion resistance, low friction and high impact strength, excellent toughness and low density, ease of fabrication, biocompatibility and biostability make it an ideal candidate for application as an implant [16, 19, 20].

3.1.4 Composites

Polymer matrix composites are being increasingly studied for different applications ranging from coatings, load-bearing implants or biosensors [21]. Examples of polymers proposed as matrices in biomedical composites include poly(methylmethacrylate) (PMMA), polysulfone (PSU), poly(etheretherketone) PEEK or Epoxy resins [22].

3.2 Biomaterials of second generation

The mechanism of bonding of bioactive glasses (composed of $\text{Na}_2\text{O}-\text{CaO}-\text{P}_2\text{O}_5-\text{SiO}_2$) to living tissue, was established in 1971 by L. Hench [23]. In 1984 L.Hench and J. Wilson [24]

successfully developed a new biomaterial, which was defined as bioactive., i.e. material with a specific response on interaction with living tissue [25].

3.2.1 Ceramics

Ceramics of the second generation, when react with the physiological fluids, the layer of biological-type apatite on their surface is formed. Among these ceramics it could be mentioned some calcium phosphates and several compositions of glasses and ceramic glasses, which are manufactured as powders, porous pieces, dense pieces, injectable mixtures and coatings for the medical applications. They have an excellent features in terms of biocompatibility and bioactivity, but their mechanical properties are very poor [26].

The thermal and chemical stability of ceramics and durability makes ceramics good materials for inert implants. Ceramics are one of the few materials that are durable and inert enough to withstand the corrosive effect of body fluids. Ceramics are used for applications such as heart valves, orthopaedic implants and dental applications [27].

Ceramics have many wanted properties such as hardness, chemical stability and corrosion-resistivity, but they are brittle. Therefore combinations with polymers, metals and other ceramics have been developed to achieve properties such as strength and elasticity. Ceramic coated, biocompatible metals have the strength and flexibility of metals and the ability of ceramics to function with biological systems [26].

3.2.1.1 Calcium phosphates

HA ($\text{Ca}_{10}(\text{PO}_4)_6(\text{OH})_2$), β -tricalcium phosphate (β -TCP, $\text{Ca}_3(\text{PO}_4)_2$), their derivatives and their combinations are the mostly used ceramics. Depending on their synthesis process, these materials show different physical and chemical properties. HA shows excellent bioactive properties, after implantation HA remains integrated into the regenerated bone tissue, whereas TCPs are completely reabsorbed. There is a range of suitable CaPs that can be used as CaP cements (CPCs). These materials are injectable, harden inside the damaged bone tissue and generate low heat transfer that avoids the premature death of surrounding cells [16, 28, 29, 30].

3.2.1.2 Bioactive glasses

Profesor L. Hench designed in 1968 an imaginative route to obtain new bone from a glass [31]. A piece of glass was soaked in an aqueous solution with the same ions present in the human plasma. The reaction product of the glass and the fluid was an apatite similar to biological ones. Although their bioactivity is excellent, the great problem of glasses is that their mechanical properties are very poor, which limits their application in the filling of small defects [11].

3.2.1.3 Glass ceramics

In the 1960s the original work on Bioglass® by L. Hench was being undertaken. Kokubo et al. were developing a new glass-ceramic material in Japan and they first reported the production and behaviour of A-W glass-ceramic in 1982 [32].

Glasses also can be used as precursors in the production of glass ceramics [33]. The specific microstructure of glass ceramics reinforces the mechanical properties of the whole piece.

Therefore, it is possible to obtain bioactive glass ceramics with mechanical properties much closer now to those of the natural teeth [34].

Apatite-wollastonite (A-W) glass-ceramic became one of the most extensively studied glass ceramics for use as a bone substitute. Apatite-wollastonite glass-ceramic is an assembly of small apatite particles effectively reinforced by wollastonite. The bending strength, fracture toughness and Young's modulus of A-W glass-ceramic are the highest among bioactive glass and glass-ceramics, enabling it to be used in some major compression load bearing applications, such as vertebral prostheses and iliac crest replacement. It combines high bioactivity with suitable mechanical properties [35].

3.2.2 Metals

None of the metallic materials used in orthopaedics is bioactive per se. However, two methods can be considered to obtain bioactive metals. The first one consists of coating the surface of the implant with a bioactive ceramic (HA and BGs). The second one is to chemically modify the surface of the material so as to obtain the deposition of a bioactive ceramics *in vivo* or to induce proteins and cell adhesion and other tissue/material interactions. Some of the coating methods of the first approach include electrophoretic deposition, plasma spraying, radio frequency or ionic ray sputtering, laser ablation or hot isostatic pressure. None of these methods produce covalent links with the substrate, and the majority are not cost-effective. However, HA coating by plasma spray deposition is at present the most common method used for clinical applications. In this process, HA in its plasma state (greater than 1000°C) is projected against a colder material metallic surface (100–150°C). By cooling down rapidly, a mechanical interaction is created between the ceramic and the substrate [16].

3.2.3 Polymers

This second generation is classified as group of resorable polymers. Biodegradable polymers of synthetic and natural origin such as polyglycolide (PGA), polylactide (PLA), polyvinylalcohol (PVA), hyaluronic acid and other hydrogels are greatly studied currently. Biodegradability is mainly originated by hydrolysis of the polymer chain backbone and to a lesser extent by enzymatic activity [16, 36, 37]

3.3 Composites

Composite materials reinforced with ceramic particles or fibres both biodegradable and inert can be considered to have been developed during the last 30 years. The well known composite of this generation is HAPEX, which consists of PE and HA particles as the filler, which is clinically used for middle ear and orbital floor implants [12].

Bioabsorbable composites for bone repair applications were developed following the first generation so-called bone-analogue concept proposed by [38] and [39]. It is necessary to point out that in the case of Bonfield's composite, as well as some others, the concept is a bioactive non-biodegradable material: HAPEX consists of a PE matrix reinforced with HA particles. HA acts as the bioactive agent that promotes osteoblast attachment, while PE, the matrix, is a stable, non-biodegradable inert polymer. It is worth mentioning that HAPEX has been successfully commercialized for middle-ear implant applications [40]. PVA/HA composite has been extensively studied as implant [16].

3.4 Biomaterials of third generation

Whereas second-generation biomaterials were designed to be either resorbable or bioactive, the next generation of biomaterials is combining these two properties, with the aim of developing materials that, once implanted, will help the body heal itself. Two alternative routes of repair are now available with the use of these tailored biomaterials - Tissue engineering and *in situ* tissue regeneration [41].

3.4.1 Scaffolds for tissue engineering

Tissue engineering attempts to develop artificial materials able to replace biological tissues in situations where the human body cannot perform replacement by itself. One attempt consists on designing biomimetic materials that combine synthetic materials with cellular recognizing positions. These hybrid materials can yield surfaces with better properties. There are some difficulties to choose the specific type of cell from the huge universe of them. It is also difficult to induce functionality and architectures in multiple cells when they react with the surface of a biomimetic material [26].

Progenitor cells are seeded onto modified resorbable scaffolds. The cells grow outside the body and become differentiated and mimic naturally occurring tissues. These tissue engineered constructs are then implanted into the patients to replace diseased or damaged tissues. With time the scaffolds are resorbed and replaced by host tissues that include a viable blood supply and nerves [41]. The design of scaffolds able to guide cell growth is an important challenge in tissue engineering. The aim is to fabricate pieces that support and structure the newly formed tissue and said pieces have to be made of the most suitable materials for these tasks. Biological cells must be cultured onto this support and subsequently give rise to the growth of new tissue. At present, the aim is to find biomaterials which induce the regeneration of hard tissues stimulating the response of the cells involved. The requirements for these ceramics are to act as a scaffold and also to be porous so that the cells can do their job. It is worth recalling the concept of porosity and its range of order. Those materials with mesoporosity between 2 and 50 nm are of interest for applications where drugs or biologically active molecules are loaded, and later released to help in the bone regeneration process. Macroporous materials, where the pore sizes are in the order of microns, are adequate as scaffolds for tissue engineering [42].

3.4.2 In situ tissue regeneration.

This approach involves the use of biomaterials in the form of powders, solutions, or doped microparticles to stimulate local tissue repair. Bioactive materials release chemicals in the form of ionic dissolution products, or growth factors such as bone morphogenic protein (BMP), at controlled rates, by diffusion or network breakdown, that activate the cells in contact with the stimuli. The cells produce additional growth factors that in turn stimulate multiple generations of growing cells to self-assemble into the required tissues *in situ* along the biochemical and biomechanical gradients that are present [41]. The development of materials for any replacement application should be based on the understanding of the structure to be substituted. This is true in many fields, but particularly exigent in substitution medicine. The demands upon the material properties largely depend on the site of application and the function it has to restore. Ideally, a replacement material should mimic the living tissue from a mechanical, chemical, biological and functional point of view [22].

3.5 Composites

A composite material consists at least two chemically identified phases which are separated by interface(s). The properties of composites are strongly influenced by a number of factors e.g. filler shape, size and size distribution, properties and volume percentage of filler, matrix properties (e.g. molecular weight), dispersion of filler particles in the polymer matrix and the state of the filler/matrix interface. In the case of biocomposites, other factors such as biocompatibility of the filler or matrix, the degradation rate of matrix and non-toxicity [43] must be considered. Physical characteristics such as shape, size, and size distribution of filler particles are very important in determining the mechanical properties of a composite.

Irregular shape of the filler is preferred to the spherical, as the molten polymer can easily penetrate onto the particle surface and forms a mechanical interlock with the particle, contrarily the smooth surface of spherical particles does not allow such a joining to form a locking mechanism. Consequently, the absence of chemical bonding between the polymer and the particle will influence the mechanical properties of the composite [44].

The composites can be divided into groups according to connecting interaction between the components of composite. Commonly one of these compounds is inorganic and the other one organic in nature. The first class are those that show weak interactions between the two phases (van der Waals, hydrogen bonding or weak electrostatic interactions). The second class of hybrid materials have strong chemical interactions between the components (covalent, coordination, ionic) or without chemical interactions between the two components [45].

Kickelbick designed four types of mutual arrangements of nano-sized particles to a polymer chain.

- (1) inorganic particles embedded in inorganic polymer,
- (2) incorporation of particles by bonding to the polymer backbone,
- (3) an interpenetrating network with chemical bonds,
- (4) an inorganic-organic hybrid polymer.

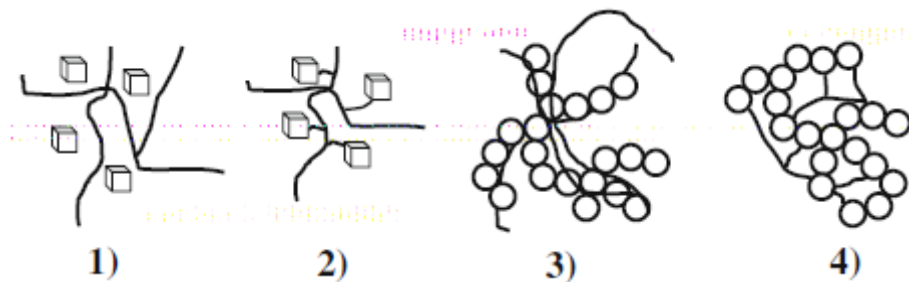


Figure 2: Four types of mutual arrangements of nanoparticles to a polymer chain according to Kickelbick: (1) inorganic particles embedded in an inorganic polymer, (2) incorporation of particles by bonding to the polymer backbone, (3) interpenetrating network with chemical bonds, (4) inorganic-organic hybrid polymer [45]

3.5.1 Nanocomposites

Nanocomposites are materials defined as composites being reinforced with particles having at least one dimension in a nano meter size range. Common example of nanocomposites is the structure of bones. A bone has a complex arrangement of materials and structures at different length-scales, which work in synergy to perform diverse mechanical, biological and chemical functions, such as: structural support, protection and storage of healing cells, and mineral ion

homeostasis. The structure of bone can be described as a hierarchical organisation. The different levels of this structure are: (1) the macrostructure: cancellous and cortical bone; (2) the microstructure (from 10 to 500 μm): Haversian systems, osteons, single trabeculae; (3) the sub-microstructure (1–10 μm): lamellae; (4) the nanostructure (from a few hundred nanometres to 1 μm): fibrillar collagen and embedded mineral; and (5) the sub nanostructure (below a few hundred nanometres): molecular structure of constituent elements, such as mineral, collagen, and non-collagenous organic proteins (Fig.3). The structure is made more complex by the 3D arrangement and orientations of the different components.

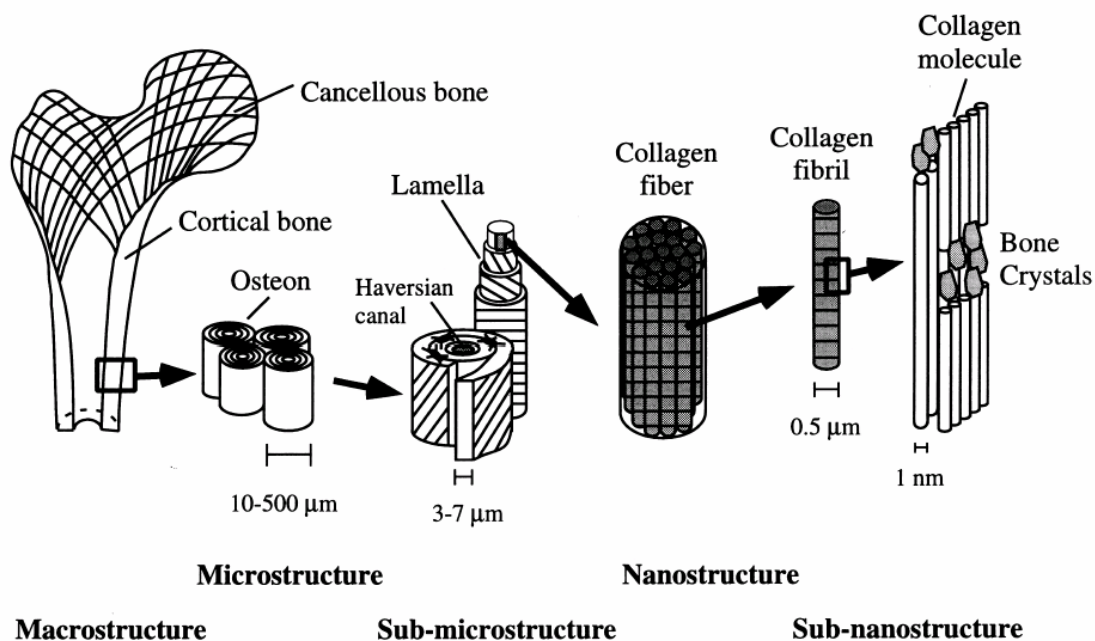


Figure 3: Hierarchical structure of bones: a) cortical and cancellous bone; b) osteons with Haversian systems; c) lamellae; d) collagen fibre assemblies of collagen fibrils; e) bone mineral crystals, collagen molecules and non-collagenous proteins. From [46, 47]

Nanoparticles were firstly introduced in the 90th of last century, since then the most of the effort was focused on the preparation and understanding the behavior of nanocomposites. It has been reported that at the nanoscale (below about 100 nm), a material's property can change dramatically. With only a reduction in size and no change in the substance itself, materials can exhibit new properties such as electrical conductivity, insulating behavior, elasticity, greater strength, different color, and greater reactivity-characteristics that the very same substances do not exhibit at the micro or macroscale [48].

First concepts to characterise nanocomposite behaviour were established for microcomposite and were just scaled three orders of magnitude lower to describe and understand the nanocomposite behavior. It was shown by Jancar et al. [49, 50, 51], this approach might not be correct. With decreasing particle size, the specific surface area increases. The large portion of polymer is in an intimate contact with the filler surface and takes a maximum advantage of interphase area. This has a strong influence of several composite properties like stiffness. Particles with high specific surface area tend to form aggregates easily (Fig. 4).

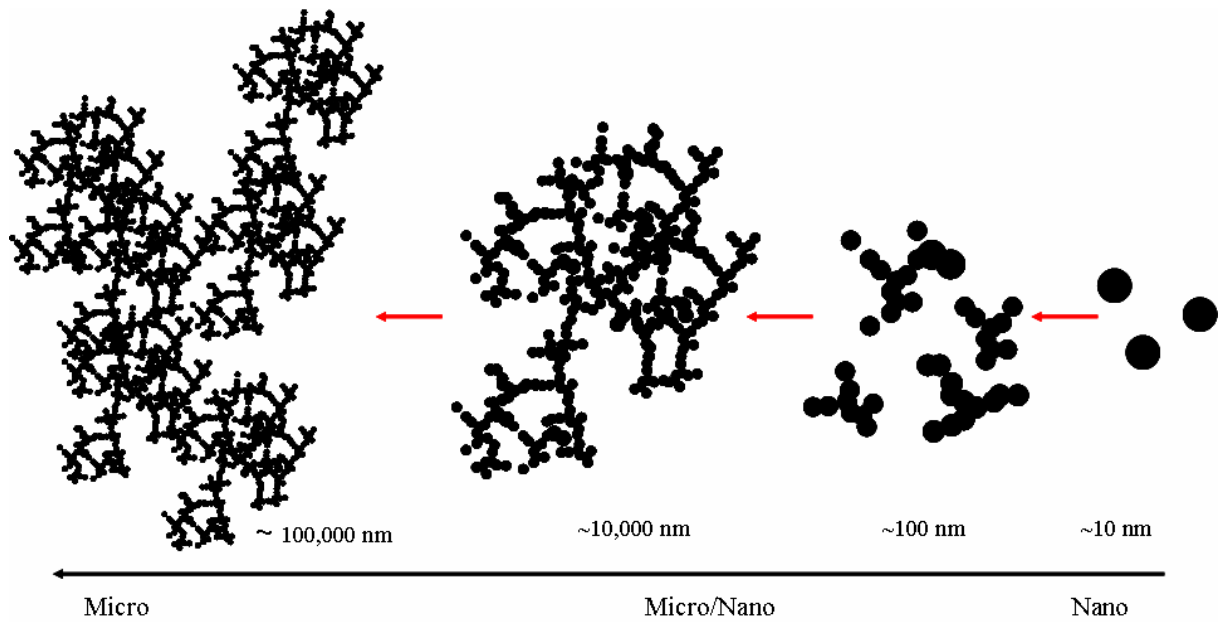


Figure 4: Increasing size and decreasing specific surface area of nanoparticles - From nanocomposites on the right to a micro composite on the left. Simplified example of hierarchically organized structures found in nanocomposites [52].

The aggregates formation is managed by the need for an optimal surface to volume ratio. Several methods exist to avoid the agglomeration. These procedures are focused on preventing the aggregation applying a surface treatment and with using an external field. However, nano spheres tend to form agglomerates easily unless a protective colloid is used to keep them separate. It was shown that spherical nanoparticles can assemble into stripes under a loading [52].

Akcora *et al.* [59] showed a broad effect of self-assembled nanoparticles under a broad range of conditions into a variety of superstructures. By varying the quality of solvent, annealing time, chain length and grafting density, a various super-organized structures were found. The effect of aggregates on the deformation behavior was always considered as negative. It was believed that the deformation behavior for well separated particles yields to the largest mechanical response, for example - stiffness. However, the question of reinforcement efficiency for well-dispersed or percolated particles is not fully answered, yet. There is no doubt that the incorporation of nano-spherical particles with large specific surface area leads to the amplification of several molecular processes resulting in an enhanced macroscopic properties.

The effect of nanoparticles on the matrix properties and the relationship between nano-scale structural variables and the macro-scale properties of polymer nanocomposites remains in its infancy [51].

Aggregation and agglomeration phenomena are very important points. It can be simply calculated that for particles below approximately 10 μm thermally activated Brownian motion prevails gravitation forces. Particular characteristic of colloidal particles is very large surface area of the interface region.

Stability of colloidal dispersion can be viewed in sense of thermodynamics by free energy, G , at constant temperature and pressure as [53]

$$dG = \gamma d\sigma \quad (1)$$

where γ is surface tension and $d\sigma$ is surface area change ($d\sigma = \sum_i^N d\sigma_i$).

Thus, the increase in the interface area causes increase of the free energy. Due to surface tension the interface is connected with positive additional Gibbs free energy [54] and as inner surface area of particles increases the stability of suspension becomes thermodynamically inconvenient. In suspension where interparticle collisions take place, the interaction between two particles may be formalized according familiar Leonard-Jones potential U , and interparticle distance, r .

$$U \approx U_{\text{repulsion}} - U_{\text{attraction}} \approx r^{-12} - r^{-6} \quad (2)$$

Long-range attraction forces, which cause aggregation, can be disturbed by creating a shell around each particle that supports dispersion stability (from thermodynamics point of view the system become metastable). It is usually carried out by adsorption of molecules or ions on the particle surface [53, 55].

3.6 Hydroxyapatite

Hydroxyapatite is described as one of the most bioactive ceramics widely used as powder or in particulate forms in various bone repairs and as coating for metallic prostheses to improve their biological properties. It has excellent biocompatibility, bioactivity and osteo-conduction properties. HA is thermodynamically the most stable calcium phosphate ceramic compound nearest to the pH, temperature and composition of the physiological fluid [56].

Contrarily HA is fragile and has low tensile strength, due to those it can not be use to replace bone in load bearing sites.

HA is the main inorganic mineral constituent of bones, enamel, dentine and pathologically calcified tissues. Hydroxyapatites are naturally-occurring forms of calcium apatites with chemical formula of $\text{Ca}_5(\text{PO}_4)_3(\text{OH})$, but it is usually written as $\text{Ca}_{10}(\text{PO}_4)_6(\text{OH})_2$ because the crystal unit cell is made up of two molecules. The pure HA powder is white in colour [57].

Apatites belong to the family of calcium phosphates and are represented by the general formula $\text{Me}_{10}(\text{XO}_4)_6\text{Y}_2$. The Me atoms correspond for divalent cations (Ca, Ba, Pb) suitable for substitution by monovalent (Na, Rb, Cs) or trivalent (Al, Nd, La) cations, while the XO_4 group is a trivalent anion (PO_4^{3-} , VO_4^{3-}) able to be substituted by tetravalent or divalent groups (SiO_4^{4-} , GeO_4^{4-} or SO_4^{2-} , CO_3^{2-} , HPO_4^{2-}). The charge is balanced by monovalent anions Y such as F^- (fluorapatite), Cl^- (chlorapatite), OH^- (HA). The structure makes apatites chemically and thermally stable [58].

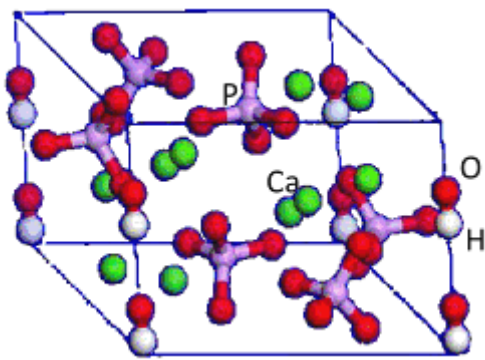


Figure 5: Crystal structure of hydroxyapatite [59].

The bone consists of organic components (mostly collagen fibres) and inorganic mineral phase, known as biological hydroxyapatite which represents 65-70 wt% of natural bone [60]. Collagen fibres keep bones resilient, while mineral component is responsible for the bone stiffness (Fig. 6). The most compatible with bone mineral phase is non-stoichiometric calcium phosphate of “apatitic structure”. It differs from stoichiometric hydroxyapatite of formula $\text{Ca}_{10}(\text{PO}_4)_6(\text{OH})_2$ with molar ratio of $\text{Ca/P} = 1.67$ [61]. Bone contains carbonated HA crystals in the form of plates and needles with length about 40–60 nm, width 20 nm and thickness 1.5–5 nm [58].

Biological apatites are non-stoichiometric, mostly Ca-deficient with respect to phosphate ($\text{Ca/P} < 1.67$) unless carbonate ion is incorporated, then Ca/P is higher than 1.67. The difference between stoichiometric hydroxyapatite and bone mineral is founded in the impurity content, which is associated mostly with ions substitution for calcium sites in the bone hydroxyapatite structure [61]. This ratio can be an important factor in cell adhesion, proliferation and in bone remodelling and formation. Calcium-deficient HA is of greater biological interest because the mineral portion of the hard tissue is primarily carbonate substituted calcium-deficient HA, with a Ca/P ratio of about 1.5, which is chemically and compositionally similar to tricalciumphosphate but structurally similar to stoichiometric hydroxyapatite [44].

The natural sources of HA are animal bones and corals or can be synthesized from appropriate substrates. HA materials made from animal bones inherit some properties such as chemical composition and structure [62, 63].

HA is a crystal of hexagonal structure with the space group $\text{P6}_3/\text{m}$. The lower crystallographic symmetry induces mechanical anisotropy along each axis. The a, b plane is bio-active, the c plane is bioinert. That's why a specific crystal orientation is required HA should be used as a biomaterial [44].

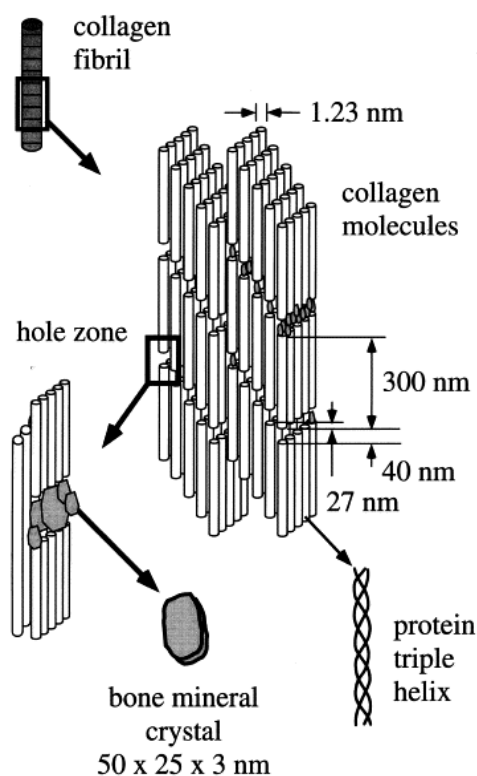


Figure 6: A schematic diagram illustrating the assembly of collagen fibers and bone minerals crystals [71].

3.6.1 HA mechanical properties

Ideally, a bone substitute should be replaced by a mature bone without transient loss of mechanical support. Unfortunately for material scientists, a human body provides one of the most inhospitable environments for implanted materials. It is warm, wet and both chemically and biologically active. Furthermore, the body is capable of generating quite massive force concentrations and the variance in such characteristics among individuals might be enormous. All types of potential biomaterials and bioceramics must sustain attacks of a great variety of aggressive conditions. Regrettably, there is presently no material fulfilling all these requirements. On the other hand, any ceramics, when they fail, tend to do so in a dramatic manner. The brittle nature of calcium orthophosphate bioceramics is attributed to high strength ionic bonds. Thus, it is not possible for plastic deformation to happen prior to failure, as a slip cannot occur. Consequently, if a crack is initiated, its progress will not be hindered by the deformation of material ahead of the crack, as would be the case in a ductile material (e.g., a metal). The crack will continue to propagate, rapidly resulting in a catastrophic failure [64, 65].

From the mechanical point of view, calcium orthophosphate bioceramics are brittle polycrystalline materials for which the mechanical properties are governed by crystallinity, grain size, grain boundaries, porosity and composition [66]. The mechanical properties decrease significantly with increasing content of an amorphous phase, microporosity and grain size, while a high crystallinity, a low porosity and small grain size tend to give a higher stiffness, a higher compressive and tensile strength and a greater fracture toughness. Thus, calcium orthophosphate bioceramics possess poor mechanical properties that do not allow use in load-bearing areas, such as artificial teeth or bones [65, 67, 68].

3.6.2 HAP preparation

Techniques to prepare HA include mechano-chemical synthesis and combustion preparation. Often used methods of HA preparation are wet chemistry techniques such as direct precipitation from aqueous solutions, electrochemical deposition, sol-gel method, hydrothermal synthesis and emulsion or micro-emulsion routes are often used [69]. The solid state synthesis of HA from oxide or inorganic salt powders usually requires extensive mechanical mixing and long heat treatments at high temperatures. These processing conditions, however, do not allow facile control over micro-structure, grain size and grain size distribution in the resulting powders or shapes [70]. This reason makes the wet chemistry techniques for HAP more suitable [71].

3.7 Poly(vinyl alcohol)

Polyvinyl alcohol was discovered in 1915 by F. Klatte. The stoichiometric saponification of polyvinyl acetate with caustic soda to yield polyvinyl alcohol was first described in 1924 by W. O. Herrmann and W. Haehnel. The monomer „vinyl alcohol“ is theoretically the enol form of acetaldehyde but can not exist as a monomer in practice. [72].

Polyvinyl alcohol is a water soluble and biodegradable synthetic polymer. For food use it is an odourless and tasteless, translucent, white or cream coloured granular powder. PVA is slightly soluble in ethanol, but insoluble in other organic solvent [73].

PVA is an excellent adhesive with superior bonding strength, film forming and emulsifying properties. The film of PVA exhibits outstanding resistance to oil, grease and solvents. In addition to its film forming property, it has excellent adhesion to both hydrophilic and hydrophobic materials. PVA has been extensively used in textile industry for warp sizing and resin finishing, in paper industry for surface sizing and pigment coating, in the production of PVAc emulsion as protective colloid, in the suspension polymerization of PVC as a dispersion agent; as binder for ceramics, magnet, foundry cores and pigments [74]. Polyvinyl alcohol is used in cosmetics as a binder, film former and viscosity-increasing agent. It is used at various concentrations up to 25% of the formulation in 1994 according to the FDA. PVA is also used by the plastic industry for various applications and in pharmaceutical products as a viscosity increasing agent as well as a lubricant in ophthalmic solutions. It is also used for several clinical applications and has been investigated as a potential carrier molecule for internal tumour investigations [75].

3.7.1 Manufacture of poly(vinyl alcohol)

The material used in the manufacture of polyvinyl alcohol is vinyl acetate monomer, which unlike vinyl alcohol, is stable. The polyvinyl acetate produced then undergoes alcoholysis. As the technical properties of polyvinyl alcohol depend in the first place on the molar mass and residual acetyl group content, industrial manufacturing processes are designed to ensure exact adherence to these parameters [76].

The most important properties which the most of applications depend on are degree of polymerization and degree of hydrolysis. The degree of polymerization is an expression of the size of polymer. The higher the degree of polymerization of polymer is, the bigger the size and the longer the length of polymer is. Similarly, the degree of hydrolysis is an expression of the ratio of hydrophilic alcohol group and hydrophobic acetate group [74].

3.7.2 Properties based on degree of polymerization

The higher degree of polymerization of polymer is, the higher viscosity of solution and adhesion strength of film are.

The higher degree of polymerization of polymer is, the less water solubility and the higher solvent resistance are.

The higher the degree of polymerization of polymer is, the higher tensile strength of PVA film is.

The higher the degree of polymerization of polymer is, the less penetration and softness of film is.

The higher the degree of polymerization of polymer is, the better protective ability is [74].

3.7.3 Dissolving properties based on degree of hydrolysis

Fully hydrolyzed grade PVA can be easily dissolved in over 90°C water, but it only swells in room temperature water [74].

Partially hydrolyzed grade PVA can be slowly dissolved in room temperature water. But in normal uses, raising temperature to 90°C is necessary for saving dissolving time. Super low hydrolyzed grade PVA can be dissolved in 25°C to 50°C water [76].

3.7.3.1 Manufacture of polyvinylacetate

Polymerisation takes place on the principle of radical chain polymerisation in an organic solvent, usually methanol. The necessary radicals are provided by initiators with peroxy- or azo groups as a result of decomposition in the reaction mixture. The methanol in this performs several functions. During polymerisation it acts as a chain transfer agent and, together with the type and quantity of initiator, enables the molar masses to be adjusted to various values. By evaporative cooling it also serves to remove the heat produced in polymerisation, and finally it is used for alcoholysis of the polyvinyl acetate. At present both continuous and discontinuous processes are still in use for vinyl acetate polymerisation.

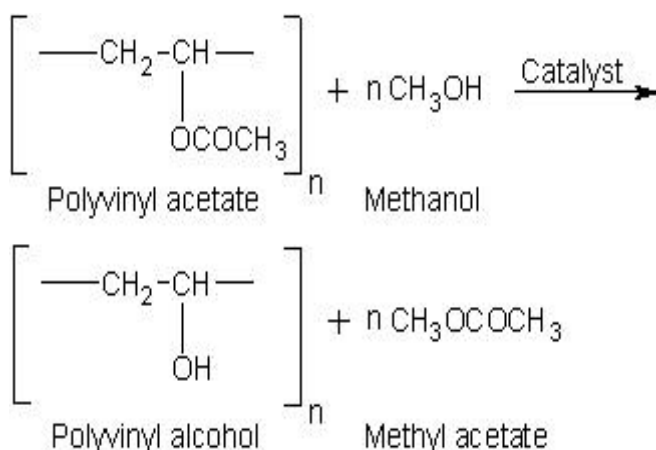


Figure 7: Preparation route of polyvinyl alcohol from polyvinyl acetate

The polyvinyl acetate dissolved in methanol is converted to polyvinyl alcohol by hydrolysis (alcoholysis), the reaction is catalysed by sodium hydroxide [72, 77].

3.7.4 Polymer chain

The polyvinyl alcohol has the following structural formula (Fig. 8) [78].

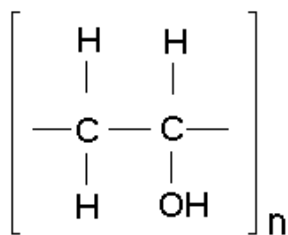


Figure 8: Polyvinyl (alcohol) structure formula

There is a strongly marked tendency towards mutual orientation in polyvinyl alcohol chains because of their polarity, both in aqueous solution and in the solid state. I. Sakurada has designed a structural model for such behavior [79].

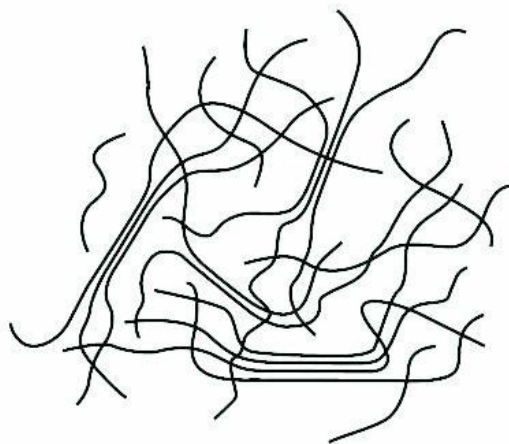


Figure 9: Sakurada's structural model of polyvinyl alcohol [79].

Depending on the origin, type and thermal history of a polyvinyl alcohol, it is possible to determine the glass transition temperature [T_g] and crystallite melting point [T_k] by differential scanning calorimetry. T_g ranges between 40 and 80 °C, and T_k between 180 and 240°C [79].

3.7.5 Poly(vinyl alcohol) in medical application

Polyvinyl alcohol hydrogel has been recognized as a substitute material for the artificial articular cartilage due to its hydrophilicity and microporous structure, high elasticity, mechanical properties of absorption and exudation of body fluid. These properties of PVA hydrogel are closer to human body cartilage tissue than those of other artificial materials. On the other hand, PVA hydrogel presents poor strength and bioactivities. The shortcomings are overcome by adding hydroxyapatite as the reinforced phase to PVA composite hydrogel. PVA/HA composite hydrogel has been extensively studied as a cartilage substitute material [5, 80, 81].

3.7.6 *In vivo* toxicity status

The critical evaluation of PVAs reported that PVA was of low oral toxicity, poorly absorbed by the gastro-intestinal tract, did not accumulate in the body after oral administration, was not mutagenic or clastogenic and had a reported NOAEL of 5000 mg/kg bw/day in a 90-day dietary study and in a two-generation reproduction study (which was the highest dose tested). The authors concluded that „the existing information on PVA supports its safe use as a coating agent for pharmaceutical and dietary supplement products“ [82].

3.8 Poly(vinyl alcohol) – Hydroxyapatite composite

Biocomposite materials based on polymer matrix reinforced with (nano)hydroxyapatite (gel) have been developed as an alternative biomaterial to titanium alloy in the replacement of diseased or damaged cartilage [83 - 85].

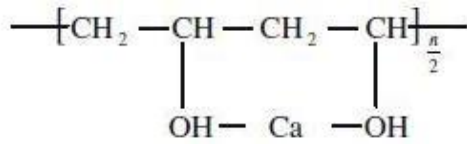
The use of PVA became very promising in the last years for its excellent biocompatibility and biotribological properties [86 - 89]. Also, the characteristic that make it a potential biomaterial to replace the natural articular cartilage is its high porous structure with high content of free water, which is similar to that found in this soft tissue.

The clinical application of the pure polymer brings some problems. The first problem is the durability of PVA. Attempts to improve hydrogel properties for load-bearing biomedical applications have included the introduction of composite materials such as rubber or glass, the use of cross-linking agents, and the use of freeze thawing procedures to induce partial crystallinity. The other major problem in clinical application is the articular cartilage fixation method. Since PVA-H itself does not adhere to tissue, longterm fixation of PVA implant by sutures is difficult.

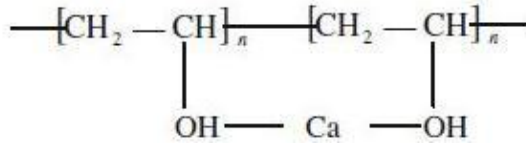
Therefore, a complex type artificial articular cartilage consists of PVA and a tissue-inducing material. Hydroxyapatite ceramic has already been used in the clinic for filling of bone defects due to its good biocompatibility and bioactivity. It can form bone-bonding with living tissue through osteoconduction mechanism [88].

3.8.1 Interaction between HA and PVA

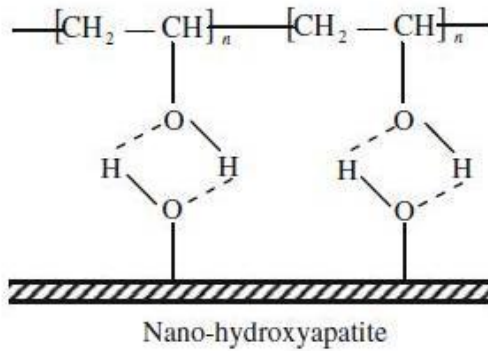
The results of Fenglan [88] showed that two binding modes between hydroxyapatite and PVA molecules existed in the composites (Fig. 10): (1), The Ca^{2+} cation in the hydroxyapatite and inter-PVA molecules or intra-PVA molecule forms bond bridge band, and this can improve the rigidity of the network in the composites. (2), The hydroxyl group of hydroxyapatite and the free hydroxyl group in PVA molecules linked by the forms of hydrogen bond, and this can improve the interfacial bonding strength between hydroxyapatite and PVA polymer. It can be concluded that PVA polymer can provide a lot of free hydroxyl group to act with hydroxyl group on the surface of hydroxyapatite while the PVA concentration increases. As a result, the compressive strength of PVA gel increased with the rise of concentration of PVA solution [90].



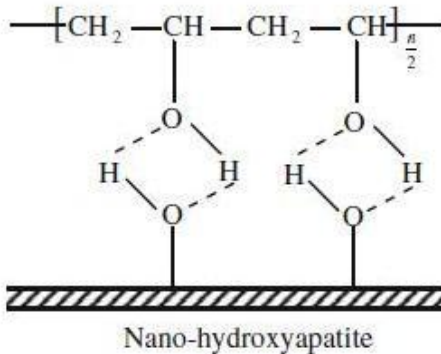
a) The interaction between Ca^{2+} cation and intra-PVA molecule



(b) The interaction between Ca^{2+} cation and inter-PVA molecules



(c) The hydrogen bond between nano-hydroxyapatite and inter-PVA molecules



(d) The hydrogen bond between nano-hydroxyapatite and intra-PVA molecules

Figure 10: The schematic diagrams of the interaction between hydroxyapatite and PVA polymers [88].

3.8.2 Mechanical properties of HA/PVA

The unique mechanical behavior of nano-HA/PVA composites depends significantly on its special structure, which is composed of four parts such as amorphous region formed by PVA molecule, microcrystalline region by hydrogen bonding of intra- and inter-PVA molecular chains, nano-HA particles reinforcing phase and lots of free water among three-dimensional network structure of PVA gel. The elastic properties of the composites are attributed to the microcrystalline region of the composites and nano-HA particles. Both free water and amorphous region in the composites are beneficial to the viscous characteristics of the composites [90, 91].

Generally, tissues are grouped into soft and hard tissues. Bone and tooth are examples of hard tissue whereas skin, blood vessels and cartilage are examples of soft tissue. Accordingly, hard tissues are intended to support loads, being stiffer (higher elastic modulus) and stronger (higher tensile strength) than soft tissues. The need for mechanical compatibility with hard tissue makes metals and ceramics to be many times considered more suitable than polymers for those type of applications. However, this is not true in many cases, basically because metals are much stiffer than human hard tissues and ceramics are not only more brittle but also stiffer than natural mineralised tissues. On the other hand unreinforced polymers are typically more ductile but not stiff enough to be used to replace hard tissues in load-bearing applications. Nevertheless, polymer based composites can be designed to meet stiffness and strength requirements for hard tissue substitution [22].

Matching the mechanical properties of implant with the ones of host tissue is the key mechanical compatibility factor in the biomaterial selection as bone replacements. Mismatching of stiffness will lead to a major load bearing on the implant device, and the surrounding bone tissue will experience less stress even after the fracture has been repaired. This phenomenon is called stress shielding or stress protection, which affects the bone remodeling and healing process. The underloaded bone adapts to the low stress environment and becomes less dense and consequently weak. Thus, failure of the implantation system is often found to be at the weak interface of the implant and the newly grown high porosity bone tissue [18, 89, 92]. Mechanical properties of some materials depicted in Fig. 11 and Table 2.

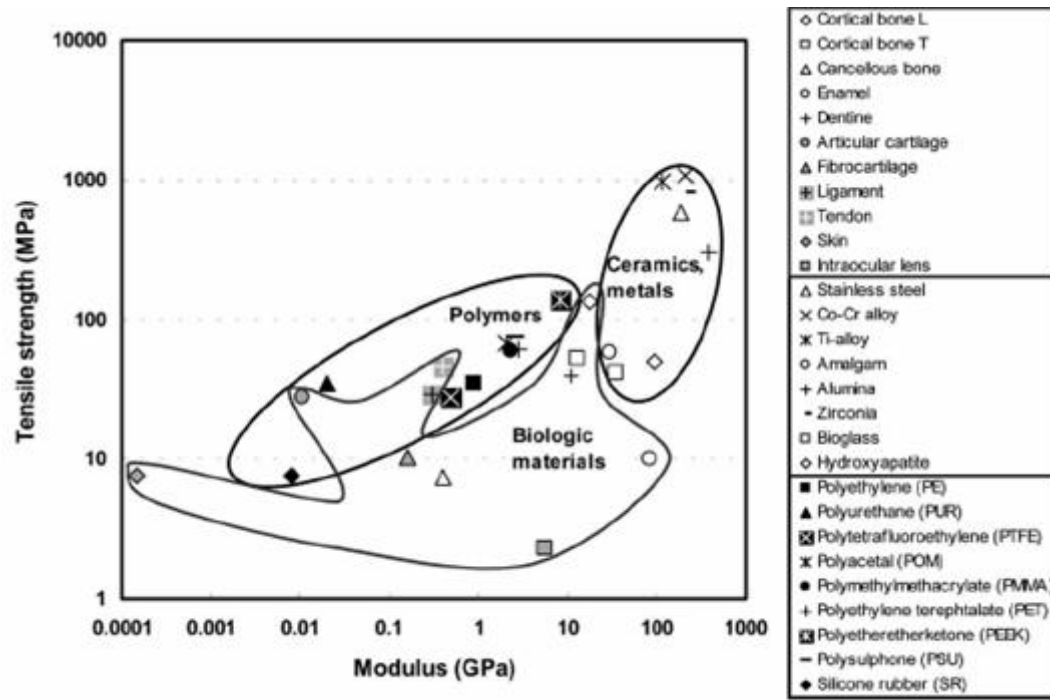


Figure 11: Tensile strength vs. modulus of materials with relevance for composite design when considering biomedical applications [93]

Table 2: List of mechanical properties of some materials [94]

Material	Flexural strength [MPa]	Elastic modulus [GPa]	Hardness [GPa]
Cortical bone	50 - 150	7 - 30	2 - 12
Human tooth enamel	8 - 35	9 - 90	0.52 - 1.3
Human tooth dentin	31 - 104	11 - 20	2.8 - 3.1
Sintered HA	115 - 120	80 - 110	1.0

3.8.3 PVA/HA composite application

Poly vinyl alcohol - hydrogel (PVA-H) is widely used in biomedical fields, such as soft tissue replacement, drug delivery, and hemodialysis membranes for its excellent biocompatibility [95, 96]. The mechanical properties of PVA-H/HA composites have also been studied for use as an artificial blood vessel the most important properties of biomaterials used for artificial joints [97].

Porous composites may be used as drug delivery system because of ability to take in the drug molecules [98, 99]. An artificial cornea consisted of a porous nano-HA/PVA hydrogel skirt and a transparent center of PVA hydrogel has been prepared as well. The results displayed a good biocompatibility and interlocking between artificial cornea and host tissues [100, 101].

3.9 Bioactivity testing

The materials developed for implants are tested by *in vivo* methods (in live animal organism) and by *in vitro* ones (in media simulating the body fluid). The tests are focused on their physical, chemical and mechanical properties and thus provide the basic information allowing the suitability of a material for implanting into the human organism to be assessed [102].

Biomaterials used in implantological applications have to demonstrate besides the appropriate mechanical properties their bioactivity, hence the ability to promote bone tissue growth. Their bioactivity is attributed to the formation on their surfaces of a hydroxycarbonated apatite (HCA) layer similar to a large extent to the mineral part of bone. The rate of tissue bonding appears to depend on the rate of HCA formation, which follows a sequence of reactions between the implanted material and the surrounding tissues and physiological fluids [103].

Kokubo proposed a mechanism of the HCA layer nucleation and growth. It consists in the interchange between Ca^{2+} ions of the glass and the H_3O^+ of the solution. This gives rise to the formation of Si-OH functional groups on the glass surface inducing thus apatite nucleation. The nuclei thus formed grow at the expense of the ions in the solution saturated with respect to the apatite [104]. *In vitro* tests are intended for use in screening bone bioactive materials before animal testing. The number of animals used and the duration of experiments can be significantly reduced by using these methods, which can assist in the efficient development of new types of bioactive materials [105]. Unfortunately, the *in vitro* test proposed by Kokubo is realised in static condition that is far from the biological realities in human body. The concentration of ions in SBF decreases with time and thus apatite formation can be stopped. These facts are illustrated by the results of investigations realized by [102] on the influence of SBF composition upon the formation of carbonated hydroxyapatite on the glass surface. The ion concentrations and pH of aqueous solution varied with testing period. It results from this study that the kinetics and mechanism of hydroxyapatite formation are influenced, not only by immersion time, but also by the variation of ion concentrations and pH of SBF in static regime [103, 105].

3.9.1 Simulated body fluids

Simulated body fluids (SBF) are solutions that the chemical composition is similar to that of the human fluid (Table 3). These solutions are used for *in vitro* tests of artificially prepared medical implants and the results serve to determine their properties such as biocompatibility, biodegradability, bio-availability, may use time, etc. The used SBF solutions are Ringer's solution, Hank's solution and variously modified solutions abbreviated as SBF. The SBF solutions began to be used in assessing the effects of bioactive glass on human organism. SBF solution was prepared for the first in 1995. This original SBF solution contained a high concentration of Cl^- ions and low concentration of HCO_3^- ions compared to the plasma, consequently, it was necessary to adjust the solution [105].

Isotonic Ringer's solution (RS) can be used to simulate plasma, hemolymph environment or other extracellular fluid, which differ in the ion concentration, pH and osmotic pressure. The composition of the RS vary according to the type of animal (fish, birds) or tissues (muscle, bone) [106].

Hank's solution (HBSS) is a balanced saline and physiological solution (Table 3). There is a reduced level of calcium and regulated phosphate concentration. In some cases artificially there is magnesium in the form of sulphate (MgSO_4) added. The solution may also be enriched with D-glucose. Balanced salt solutions(e.g. HBSS) were designed mainly for short-term preservation of viable cells. It can also be used to wash the tissues and cells [107].

Table 3: The ion concentrations (mol/l) of SBF in comparison with ions in blood plasma (BP), Ringer's solution (RS) and Hank's solution (HBSS).

Solution	Na ⁺	K ⁺	Mg ²⁺	Ca ²⁺	Cl ⁻	HCO ₃ ⁻	HPO ₄ ²⁻	SO ₄ ²⁻
BP	142.0	5.0	1.5	2.5	103.0	27.0	1.0	0.5
SBF	142.0	5.0	1.5	2.5	148.8	4.2	1.0	0.5
RS	39.1	1.4	0	0.4	40.7	0.6	0	0
HBSS	141.7	5.7	0.8	1.7	147.6	4.2	0.7	0.8

3.9.2 Mechanism of apatite layer formation in SBF

The process of formation of apatite depends on the negativity of the surface, i.e. PO_4^{3-} and OH^- constitutes the negative group while Ca^{2+} constitutes the positive group of HAp (Fig. 12(a)). The more the PO_4^{3-} and OH^- are exposed on the surface, the greater the negativity of the surface. These negative ions attract the positive Ca^{2+} ions from the SBF, thereby forming a layer of positive charge i.e. calcium-rich amorphous calcium phosphate (ACP) (Fig. 12(b)). Now the layer becomes positive with respect to the surrounding SBF, which is enough to attract negative PO_4^{3-} and OH^- from the SBF and thereby forming calcium - poor ACP (Fig. 12(c)). This gradually crystallizes to bone-like apatite (Fig. 12(d)) [108].

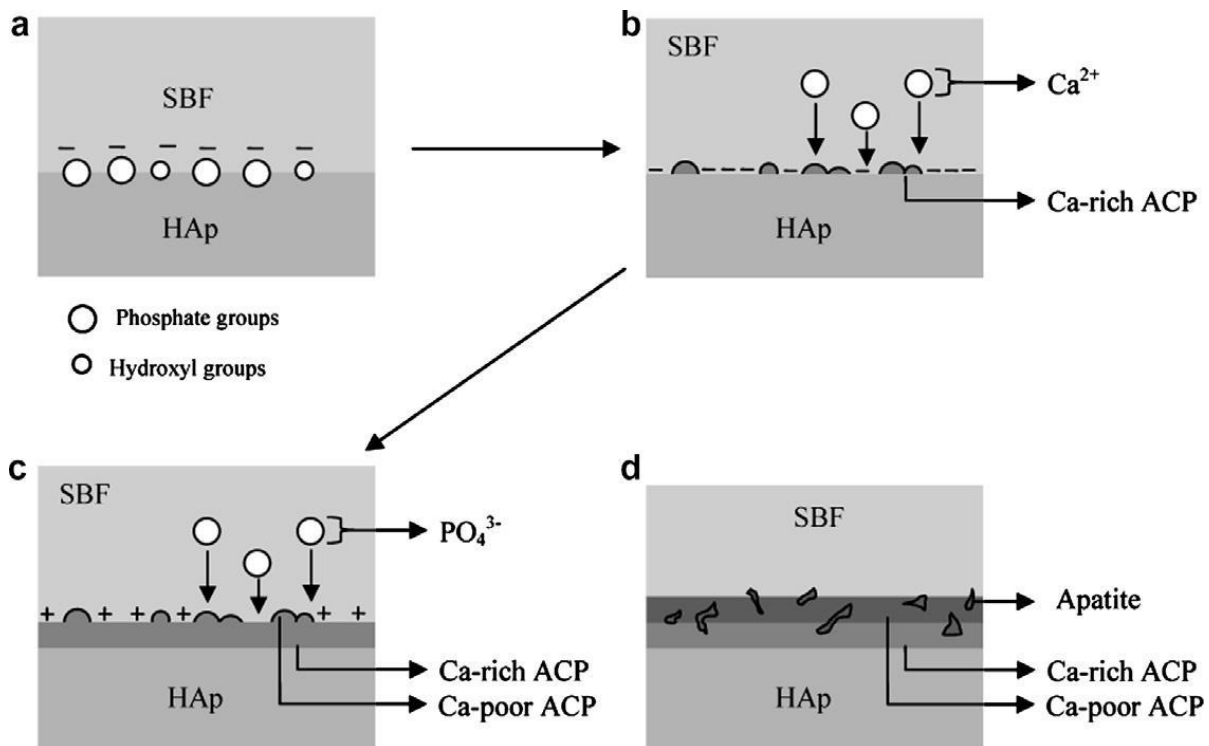
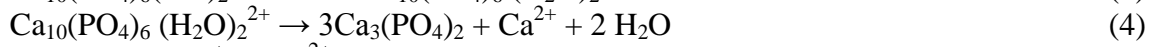
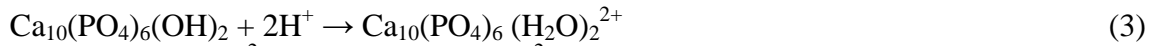


Figure 12: Schematic diagram of the process of formation of apatite on HAp surface. (a) HAp surface exposed to SBF under normal conditions, (b) calcium ions settle on HAp surface from the SBF to form Ca-rich ACP, (c) calcium-rich HAp surface attracts phosphate groups from SBF to form Ca-poor ACP and (d) ageing produces apatite on the HAp surface [108]

3.9.3 HA bioceramics *in vivo* behaviour

Shortly after implantation, a healing process is initiated by compositional changes of the surrounding bio-fluids and adsorption of biomolecules. Following this, various types of cells reach the bioceramic surface and the adsorbed layer dictates the ways the cells respond. Further, a biodegradation of the implanted bioceramics begins. This process can occur by either physicochemical dissolution with a possibility of phase transformation or cellular activity (so called, bioresorption), as well as by a combination of both processes. Dissolution is a physical chemistry process, which is controlled by some factors, such as solubility of the implant matrix, surface area to volume ratio, local acidity, fluid convection and temperature. For HA, the dissolution process in acids has been described by a sequence of four successive chemical equations:



With few exceptions, dissolution rates of calcium orthophosphates are inversely proportional to the Ca/P ratio, phase purity and crystalline size, as well as being directly related to the porosity and surface area. Bioresorption is a biological process mediated by cells (mainly osteoclasts and to a lesser extent, macrophages). It depends on the response of cells to their environment. Osteoclasts attach firmly to the implant and dissolve calcium orthophosphates by secreting an enzyme carbonic anhydrase or any other acid, leading to a local pH drop to ~4–5 [5, 109].

4 EXPERIMENTAL PART

4.1 Samples preparation

4.1.1 Chemicals used

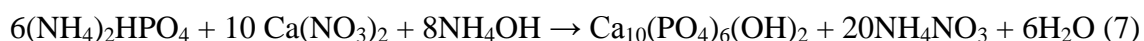
Polyvinyl alcohol Mowiol 10-98 with Mw 61 000 from Clariant
Diammonium hydrogen phosphate $(\text{NH}_4)_2\text{HPO}_4$ from Sigma-Aldrich
Calcium nitrate tetrahydrate $\text{Ca}(\text{NO}_3)_2 \cdot 4\text{H}_2\text{O}$ from Sigma-Aldrich
Ammonium hydroxide NH_4OH from Sigma-Aldrich
Distilled water for all the procedures was used.
SBF – Simulated Body Fluid

4.1.2 Preparation of hydroxyapatite

In this work hydroxyapatite was prepared by the reaction using diammonium hydrogen phosphate and calcium nitrate tetrahydrate in distilled water in presence of additional NH_4OH , which acts to conduct reaction to form nanoparticles (Equation 7). The suspension obtained can not easily sediment and the white yoghurt form is like gel. The pH was kept at high value around 13 - 14, this was controlled by ammonium hydroxide. Formed HA solution was rinsed to separate OH^- ions until the pH of suspension was neutral. That was checked by simple pH paper indicator.

The weighed portion of the precursors was calculated to maintain required molar ratio Ca:P at 1, 67. It is necessary for biological response and producing a pure HA without minor fraction. Slight imbalances in the ratio of Ca/P can lead to the appearance of extraneous phases. If the Ca/P ratio is lower than 1.67, then alpha or beta tricalcium phosphate may be present after processing. If the Ca/P is higher than 1.67, calcium oxide (CaO) may be present with the HA phase [110].

Via this precipitation reaction hydroxyapatite with spherical particles were synthesised:



The sol-gel routine was the other way, which was HA prepared. The used solvent was ethanol. Diammonium hydrogen phosphate and calcium nitrate tetrahydrate were dissolved in ethanol, then mixed together. The temperature was kept at 80 °C and the pH was maintained at about 9 - 10 with ammonium hydroxide. The mixture was stirred for several hours until the high viscosity gel was obtained. This gel was dried and the newly formed HA was mixed with PVA solution. The mixture was found to be difficult to homogenise with PVA solution and the membranes created with this HA were not used for further testing, because the HA phase was separated during drying and it was not possible to disperse in the membrane body.

4.1.3 Preparation of poly(vinyl alcohol)

Clariant poly(vinyl alcohol) was dissolved in distilled water during constant stirring at the temperature 85 °C for 4 hours until all the solid polymer was dissolved. The amount of polymer used was 21 g dissolved in 400 ml of distilled water.

Table 4: Characterisation of used PVA Mowiol 10-98 [76]

	Viscosity (4% solution at 20°C) mPa s	Degree of hydrolysis mol %	Residual acetyl wt. %
Mowiol 10-98	10 ± 1.0	98.4 ± 0.4	1.5 ± 0.4

4.1.4 Composite membranes preparation

Set of polyvinyl alcohol and hydroxyapatite composite membranes were made with various HA weight percent - 0%, 10%, 20%, 30%, 40% and 50%. Polyvinyl alcohol solution with temperature around 85 °C was stirred while adding calculated and weighed quantity of hydroxyapatite gel. This blend was mixed for 15 minutes to homogenise. Then 40 ml of the mixture was dosed into a mould with pipette. The mould has dimension 8 x 8 cm. This way prepared mixtures were dried at 30 °C for 7 days. After drying process, membranes of thickness near to 0,5 mm were removed and were ready for further testing.

Table 5: Designation of prepared composites

Composite components [in wt%]	Designation
0 HA + 100 PVA	0HA
10 HA + 90 PVA	10HA
20 HA + 80 PVA	20HA
30 HA + 70 PVA	30HA
40 HA + 60PVA	40HA
50 HA + 50 PVA	50HA
100HA + 0 PVA	100HA

4.1.5 Simulated body fluid preparation

In in vitro studies, the pH of the SBF solution is often buffered to 7.25-7.4 at 37°C using tris(hydroxymethyl) aminomethane and hydrochloric acid. SBF is a highly saturated solution, thus precipitation of calcium phosphate can easily take place during preparation, storage and use. Simulated body fluid is an acellular, aqueous medium that has inorganic ion concentrations similar to those of human extracellular fluid, in order to reproduce formation of apatite on bioactive materials *in vitro*. This fluid can be used for not only evaluation of bioactivity of artificial materials *in vitro*, but also coating of apatite on various materials under biomimetic conditions. The composition of prepared SBF was in mmol/l: 142.0 Na⁺, 5.0 K⁺, 1.5 Mg²⁺, 2.5 Ca²⁺, 148.8 Cl⁻, 0.5 SO₄²⁻, 1.0 HPO₄²⁻ and 4.2 HCO₃⁻).

SBF was prepared by dissolving the components 8.035 g NaCl, 0.355 g NaHCO₃, 0.225 g KCl, 0.231 g K₂HPO₄·3H₂O, 0.311 g MgCl₂·6H₂O, 0.292 g CaCl₂·6H₂O, 0.072 g Na₂SO₄ per litre of ultrapure water in a beaker according to the protocol given by Kokubo [111].

The medium was buffered to pH 7.3-7.4 at 36.5 ± 0.5 °C with 6.118 g tris(hydroxymethyl) aminomethane ((HOCH₂)₃CNH₂) and hydrochloric acid (HCl) to achieve the buffering capacity of blood. In preparation of SBF, each chemical was added after assuring the previous chemical dissolved fully to avoid any unexpected chemical reactions among them. Each small undesired variance in the preparation steps and the storage temperatures, may drastically affect the phase purity and high temperature stability of the produced HA on the surface, as well as the kinetics of the precipitation processes.

Sodium azide (NaN_3) was added to inhibit bacterial growth. The microbiological assay of SBF medium indicated the necessity of NaN_3 addition to inhibit the growth of bacteria. Gil [135] stated that the use of SBF without of NaN_3 addition led to enormous increase of cells (10^4 - 10^5 /ml) in the form of coliform bacterium, bacterium bacillus and Pseudomonas after cultivation in culture media at 37 °C. These anaerobic bacteria consume phosphorus and thus reduce its concentration in the medium. Furthermore, it was observed that these bacteria may have a negative impact on human health.

4.2 Testing methods

4.2.1 FTIR-ATR

Attenuated total internal reflectance (ATR) spectroscopy is a versatile and powerful technique for infrared sampling. Minimal or no sample preparation is usually required for rapid analysis. ATR is ideal for those materials which are strong absorbers.

The phenomenon of internal reflection was first reported in infrared spectroscopy in 1959. It was observed that if certain conditions were met, infrared radiation entering a prism made of a high refractive index infrared transmitting material (ATR crystal) will be totally internally reflected. This internal reflectance creates an evanescent wave which extends beyond the surface of the crystal into the sample held in contact with the crystal. In regions of the infrared spectrum where the sample absorbs energy, the evanescent wave will be attenuated.

The condition which must exist to obtain total internal reflectance is that the angle of the incident radiation θ , must exceed the critical angle, θ_c . The critical angle is a function of the refractive indices of the sample and ATR crystal and is defined as:

$$\theta_c = \sin^{-1} \frac{n_2}{n_1} \quad (8)$$

where n_1 is the refractive index of the ATR crystal and n_2 is the refractive index of the sample. High refractive index materials are chosen for the ATR crystal to minimize the critical angle.

A property of the evanescent wave which makes ATR a powerful technique is that the intensity of the wave decays exponentially with distance from the surface of the ATR crystal. The distance, which is on the order of microns, makes ATR generally insensitive to sample thickness, allowing for the analysis of thick or strongly absorbing samples.

The factors which effect the results obtained in an ATR experiment are the: wavelength of infrared radiation, refractive index of the ATR crystal, angle of incidence, efficiency of sample contact and area of sample contact with ATR crystal material [112].

4.2.2 Morphological characterization with scanning electron microscopy

The surface morphology was examined through scanning electron microscope (JEOL JSM-7600F).

4.2.3 XRD diffraction analysis

X-ray diffraction (XRD) is a basic method for determining the structure of solids. Each crystalline substance has a characteristic diffraction pattern by which we are able to identify it. This method is based on the interaction of X-rays with the electrons of atoms consisting of

a flexible variance. With regular periodic arrangement of atoms in a crystalline phase occurs after dispersion and subsequent interference of X-rays to the formation of diffraction peaks, the position, intensity and shape depend on the kind of atoms and their arrangement in 3D space. This process is governed by Bragg's law:

$$2d \sin\theta = n\lambda \quad (9)$$

where d is spacing between the planes in the atomic lattice, θ is the angle between the incident ray and the scattering planes, n is an integer characteristic and λ is the wavelength of incident wave. The diffraction pattern obtained allows to study of crystalline sample composition and microstructure [113].

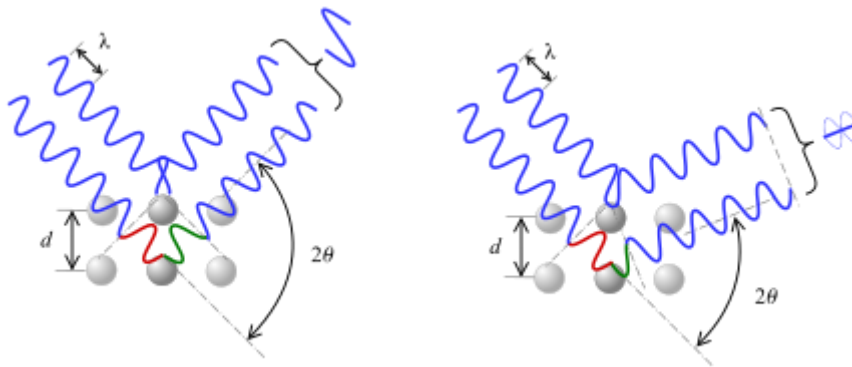


Figure 13: Two cases of the impact of X-ray beam at the crystal lattice: left Bragg condition is fulfilled - the emergence of diffraction maxima, the right is not fulfilled - destructive interference [113].

For the XRD analysis was testing device Empyrean made by Panalytical used, measurement conditions were set as follows:

• Scan Axis	Gonio
• Start Position [°2Th.]	5.0066
• End Position [°2Th.]	89.9876
• Step Size [°2Th.]	0.0130
• Scan Step Time [s]	55.08
• Anode Material	Cu
• K-Alpha1 [Å]	1.54060
• K-Alpha2 [Å]	1.54443
• Generator Settings	30 mA, 40 kV

4.2.4 Tensile properties

In this study were tested 0HA, 10HA, 20HA, 30HA, 40HA and 50HA membranes. Samples were cut out into shape of dog-bone according to ISO system standard ISO 527 (Fig. 14) The edges of the specimens were smooth, there was not requirement of any further treatment. Each sample used was previously inspected and those containing any defect such as air bubbles, holes. Width was constantly 4mm and thickness were gauged on 3 different points and averaged. The specimens were fixed into the grips of the testing machine. The

distance between sample holders was 40 mm. Each specimen was tested for 5 times and finally characteristic curves were chosen.

For the investigation it was used universal materials testing machine ZWICK Z010/TH2A made by Zwick-Roell company (Germany). The tensile testing machine pulls the sample from both ends and measures the force required to pull the specimen apart and how is the strain before breaking. The speed of the measurements was constantly set at 20 mm/min.

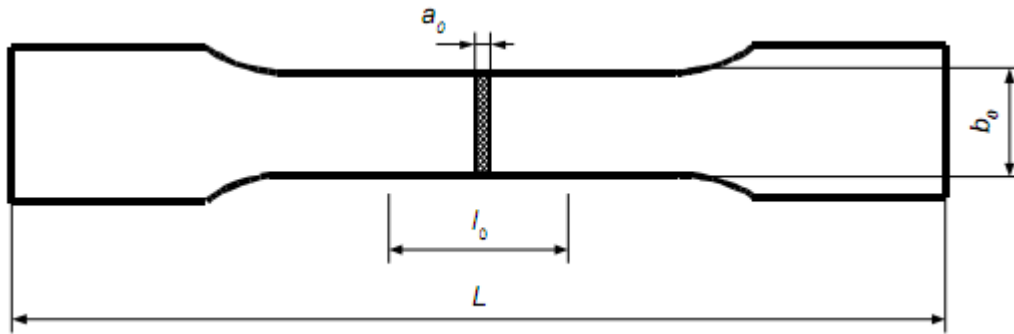


Figure 14: Dog-bone sample for tensile properties testing according to standard (ISO 527-2)

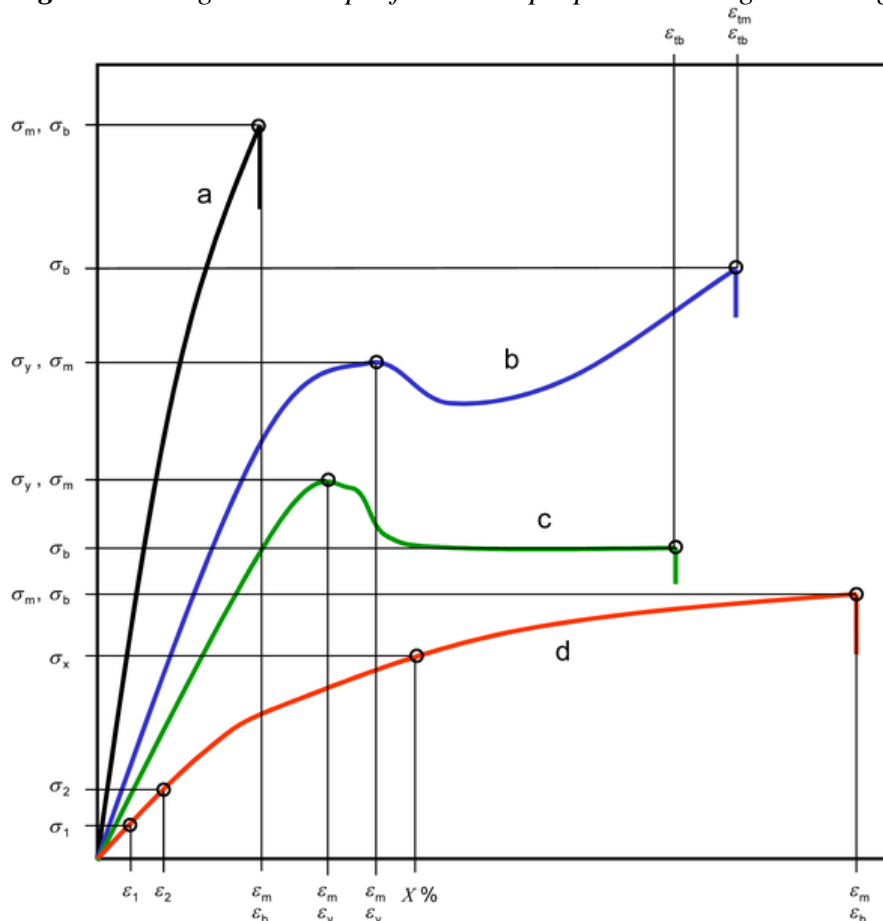


Figure 15: Typical stress strain curves [114]

Curve a –Brittle materials; Curves b and c – Tough materials with yield point; Curve d - Tough materials without yield point

4.2.5 Thermogravimetric Analysis (TGA)

The thermogravimetry analysis (TGA) is a technique which has been defined by ICTAC (the International Confederation for Thermal Analysis and Calorimetry) as a technique in which

the mass change of a substance is measured as a function of temperature whilst the substance is subjected to a controlled temperature programme [115].

Thermogravimetric analysis is the most widely used thermal method. It is based on the measurement of mass loss of material as a function of temperature. In thermogravimetry a continuous graph of mass change against temperature is obtained when a substance is heated at a uniform rate or kept at constant temperature. A plot of mass change versus temperature (T) is referred to as the thermogravimetric curve (TG curve). For the TG curve, we generally plot mass (m) decreasing downwards on the y axis (ordinate), and temperature (T) increasing to the right on the x axis [116].

Thermogravimetry is also widely used both in studies of degradation mechanism and for methods for service lifetime prediction measurements [117]. Thermogravimetry could be used for obtaining information of desorption, decomposition and oxidation processes. Thermogravimetry provides the accelerated aging experiments; information on chemical groups or morphological characteristics susceptible to attack, attacking agents and factors accelerating the deterioration [114, 117, 119].

Thermogravimetry analysis was carried out on composite samples and single components (PVA, HA) non-isothermally using a $20^{\circ}\text{C min}^{-1}$ heating rate up to 900°C .

The TGA Q500 TA Instruments research-grade thermogravimetric analyzer was used. The measurement went under N_2 condition and results were analysed with Universal V4.7A TA Instruments analyzer.

The main goal of this measurement was to assess the effect of content of hydroxyapatite in PVA matrix on thermal stability. A derivative weight loss curve was used to determine the temperature at which weight loss was most apparent.

4.2.6 Bioactivity testing

The bioactivity of the membranes with various content of HA in PVA matrix were tested with *in vitro* SBF method. The SBF was prepared in laboratory. Cleaned samples of size 1x1 cm were immersed and stored in the incubation apparatus (Binder BD 115) for 2 hours, 7 and 28 days at the temperature of 37.0°C . The microstructure of membranes surface were tested before and after soaking in SBF by SEM. The samples were weighed before and after immersion to determine the extent of biodegradation or bioactivity.

5 RESULTS AND DISCUSSION

5.1 XRD analysis

Hydroxyapatite prepared by precipitation method was further analysed by XRD analysis. The analysis depicted in Fig.16 shows that synthesized sample was a pure HA and it crystallized in the hexagonal crystal system p63/m. No other impurities were observed in the pattern.

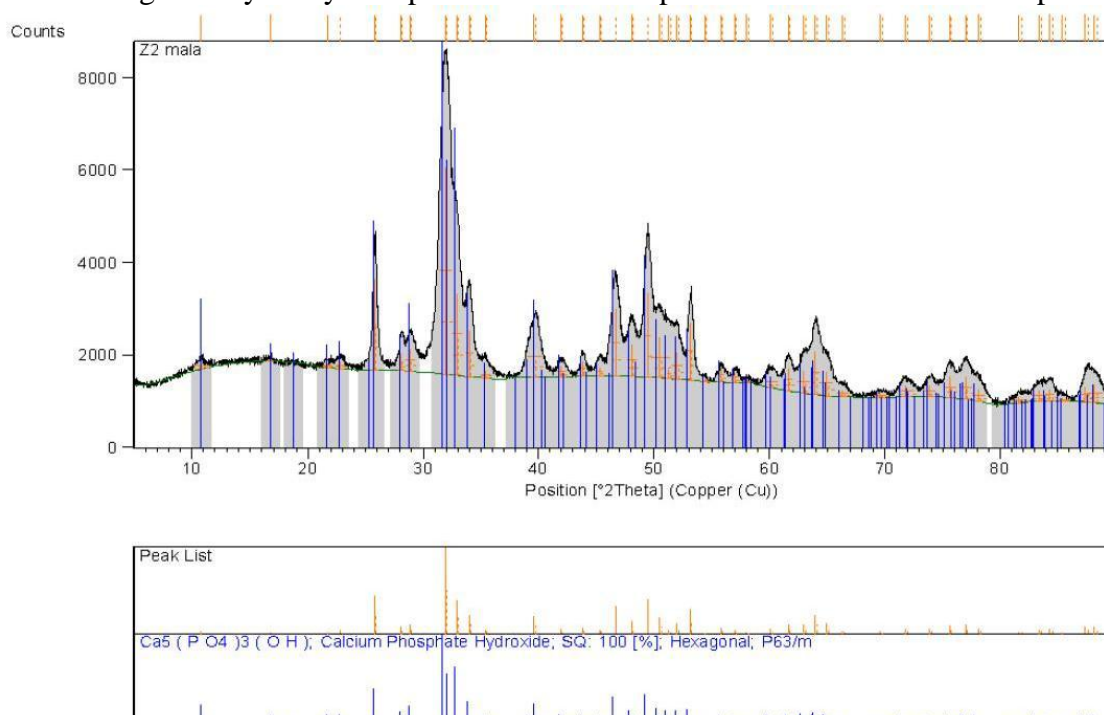


Figure 16: XRD analysis of synthesized hydroxyapatite

X ray diffraction pattern of pure PVA membrane is displayed in Fig.17. The observed maxima intensity diffraction peaks were at 11; 19,5; 23 and 40,5 ° 2theta and belonged to PVA XRD pattern. The calcite has been identified as it was used to fix the sample to the measurement target.

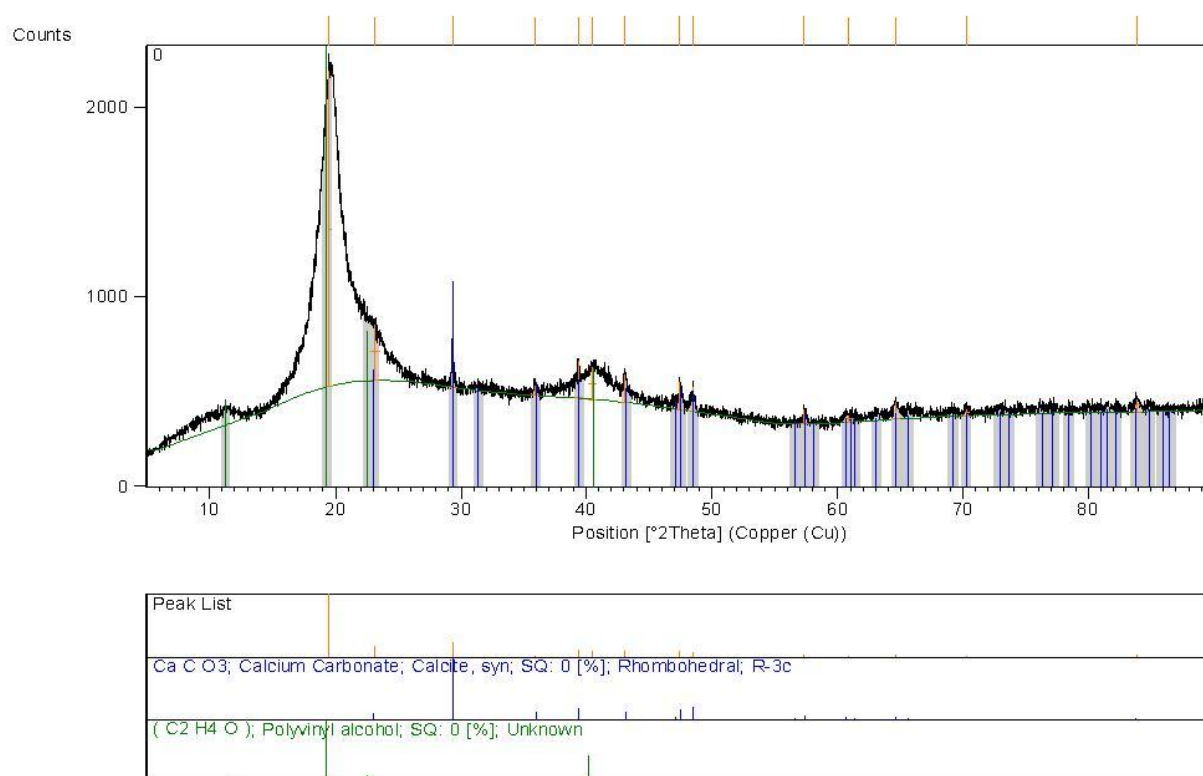


Figure 17: XRD pattern of poly(vinyl alcohol) used in membrane preparation

5.2 FTIR-ATR

The functional groups in PVA, HA and composite samples were identified and the nature of bonding between the particles and the polymer matrix were analyzed by FTIR-ATR spectroscopy analysis. The used apparatus was Nicolet i50 FTIR spectrometer with single bounce diamond crystal ATR accessory within the scanning range 4 000–400 cm^{-1} . Spectra show several bands characteristic of stretching and bending vibrations of different functional groups like O-H, C-H, C=C and C-O groups.

The FTIR spectra of different biocomposite membranes and the pure HA powder are depicted in Fig.18. The spectra are aligned from pure HA(100HA) powder, pure PVA (0HA) to 50HA composite.

The spectrum of the pure HA powder: Bands at 630 and 3570 cm^{-1} indicate structural O-H groups in the HAp crystals. Bands located at about 1000 - 1100 and 560 - 570 cm^{-1} are attributed to the ν_3 and ν_4 P-O vibration modes of regular tetrahedral PO_4^{3-} groups.

The observed bands at 604 cm^{-1} correspond to O-P-O bending and ν_1 symmetric P stretching modes. The ν_1 symmetric stretching mode of phosphate group is observed at 957 cm^{-1} . Band at 1641 cm^{-1} indicates the presence of H_2O in HAp crystals [119].

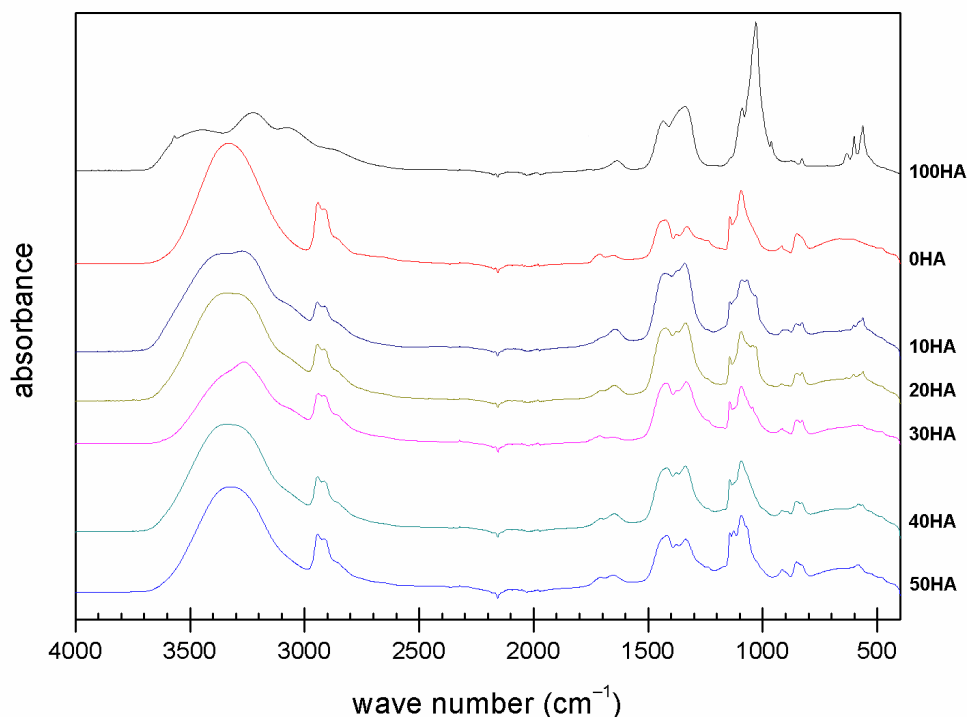


Figure 18: Spectra of HA powder(100HA), pure PVA(0HA) and PVA/HA composites with various amount of hydroxyapatite (10HA, 20HA, 30HA, 40HA, 50HA)

The PVA spectrum indicates a wide and intense band due to the presence of hydroxyl groups (O-H) at 3441 cm^{-1} . The bands corresponding to the (-CH₂-) asymmetric and the symmetric stretching at around 2900 cm^{-1} . The band at 1400 cm^{-1} can be attributed to O-H and C-H bending. The absorption peaks at 1110 cm^{-1} are related to C-O stretching.

The band at 900 cm^{-1} results from an angular deformation outside the plan of O-H bond. The absorption bands at 1625 cm^{-1} are due to symmetric stretching of carboxylate anion (-COO-) [120].

The PVA spectrum and composites spectrum show an increasing intensity of absorbance varying with the amount of HA in the samples in the adsorption range from 3000 cm^{-1} to 3500 cm^{-1} . Broad and strong band at 3360 cm^{-1} which characterizes O-H stretching frequency is well detected due the increasing presence of HA in composite materials.

The intensity of spectrum at around 1330 cm^{-1} increases with increasing content of HA in samples and is assigned to the phosphate group PO_4^{3-} .

There were detected changes in spektra after composite formation, the variation and shift in the band around $3300 - 3400\text{ cm}^{-1}$. The band observed between $2942\text{--}2944\text{ cm}^{-1}$ corresponds to C-H stretching band of PVA. A new peak of C-H stretching band is observed at 2944 cm^{-1} , when the PVA is added. These changes mark the chemical bond interactions between HA and PVA in the composite.

5.3 Morphological characterisation with SEM

The set of samples was arranged from 0HA, 10HA, 20HA, 30HA, 40HA and 50HA to compare the transparency of the samples (Fig. 19). The expectancy was the transparency decreases with increasing amount of the filler in PVA matrix, which was proved to be true. The samples with increasing HA in PVA changes their colour into white.

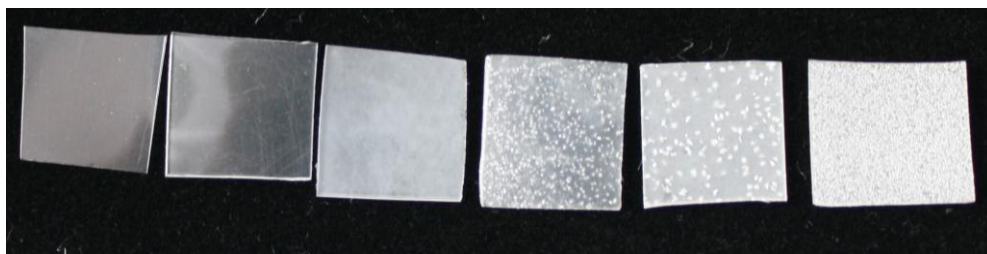


Figure 19: Membranes with various HA content in PVA matrix, from left to right 0HA, 10HA, 20HA, 30HA, 40HA and 50HA

The microstructure of PVA/HA composites with different weight percentages of HA in polyvinyl alcohol matrix, pure HA and pure PVA was analysed using scanning electron microscope (SEM). The SEM pictures are displayed in Fig. 20 - 26. The PVA matrix is continuous without bubbles. Hydroxapatite in composite is present in rod-like particles, which create various structures - agglomerates. All the results show emerging of HA agglomerates which in the case of 40HA and 50HA hydroxyapatite crystals grow into surfaces and cause the roughness of the samples. The pure PVA membrane was clear (not present). The 10HA contains small and rare occurring plates-like agglomerates, which consist of HA needles. A few solitary HA needles can be found too. The 20HA contains differently shaped agglomerates from 10HA. Short agglomerated clusters of HA needles were found in 20HA samples as well as plenty of HA needles distributed itself in the PVA matrix. The 30HA contains plenty of very similar structures as the 10HA, but in multiple amount. The long shaped clusters were observed and alone HA needles as well. The 40HA specimen shows that the matrix is saturated with the HA filler. The HA is dispersed all over the testing area and obviously the HA grows into the surface of the membrane and causes its roughness. The 50HA specimen was difficult to observe, because electron beam did interact with the sample during scanning, that's why the surface was gilded. The 50HA shows huge agglomerates, which grow through the surface and made the specimen very rough. The detailed view of HA spherical particles used to form the PVA/HA composites is displayed in Fig. 25. The particles were of micro and nano size.

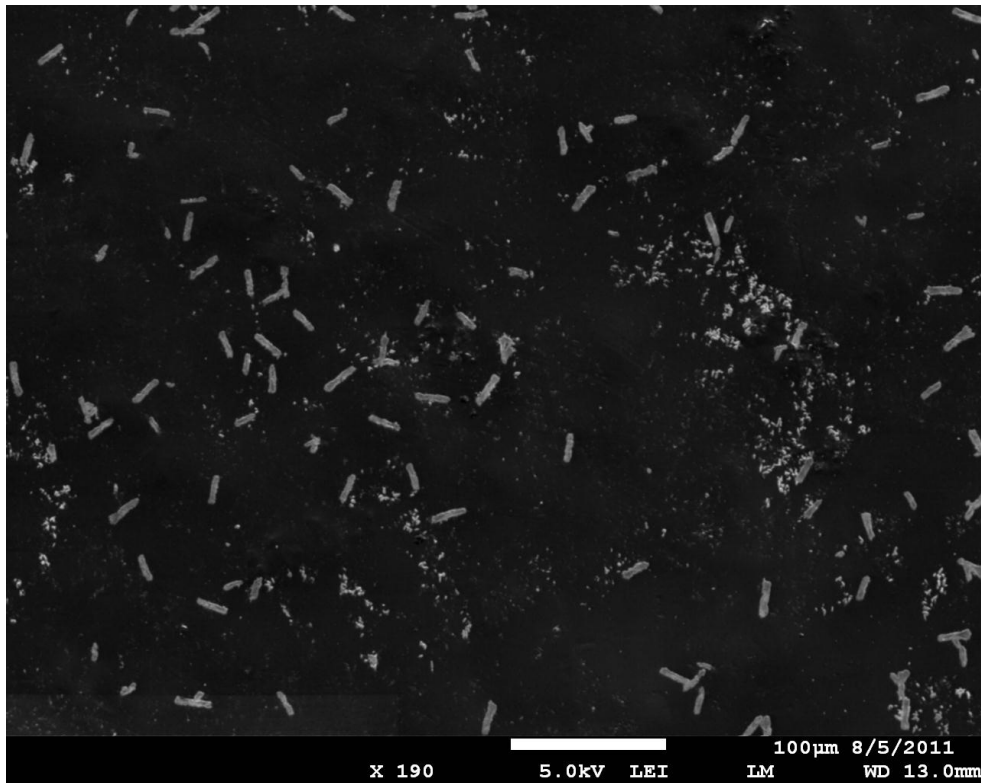


Figure 20: SEM image of 10HA at 150x magnification

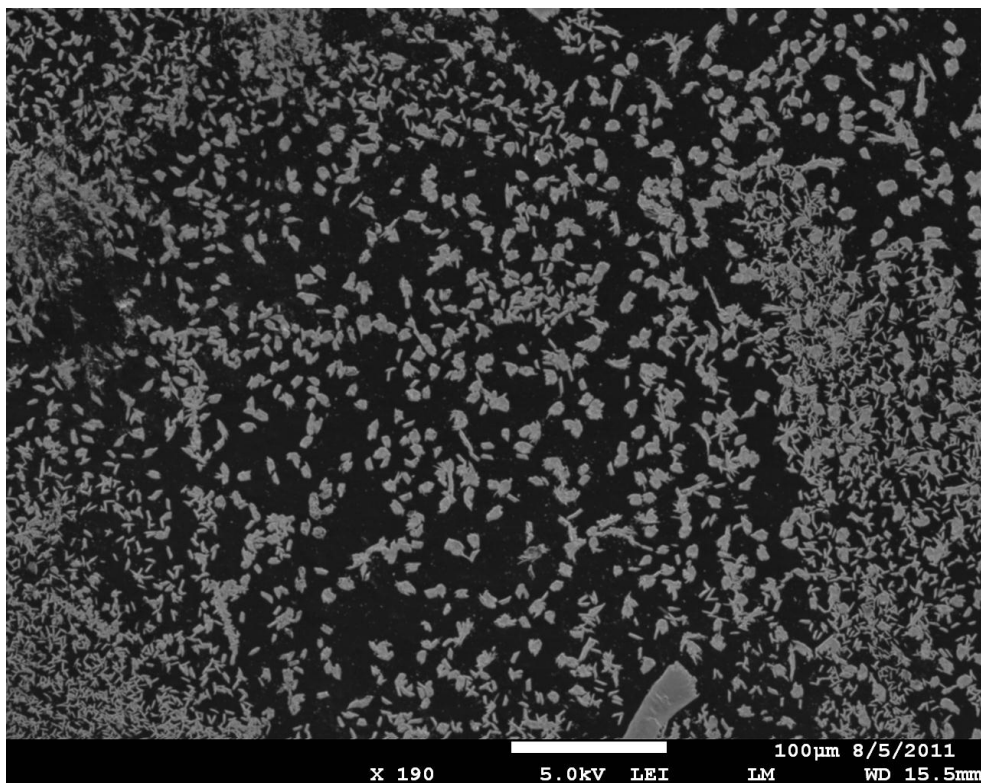


Figure 21: SEM image of 20HA at 150x magnification

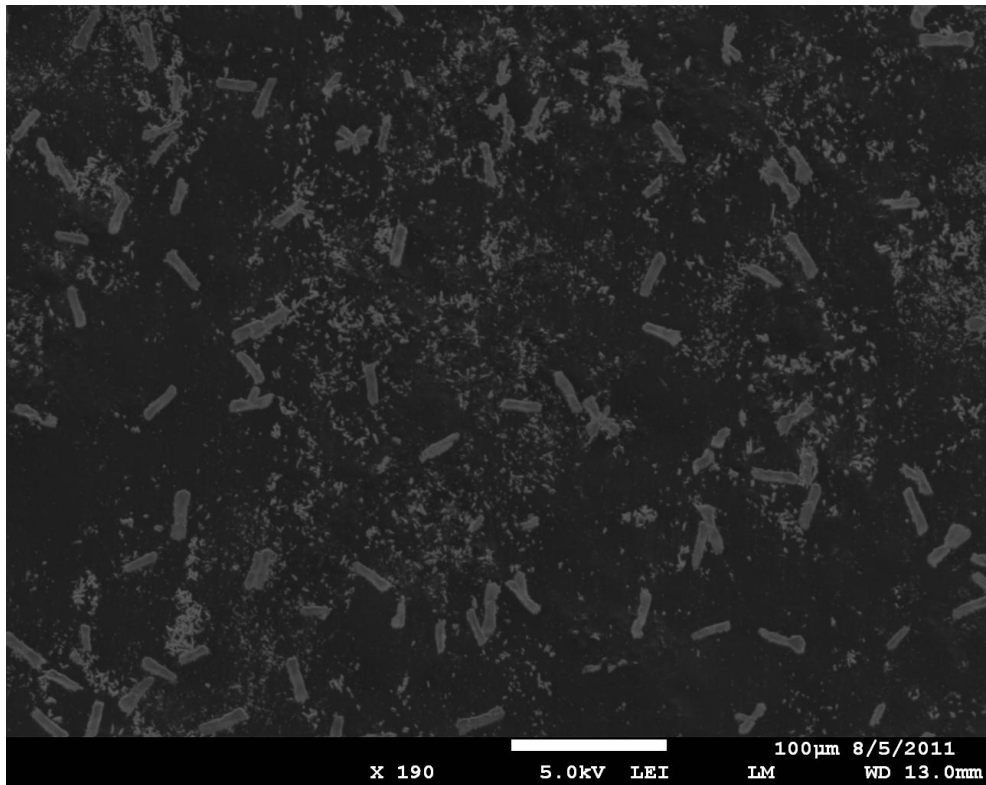


Figure 22: SEM image of 30HA at 150x magnification

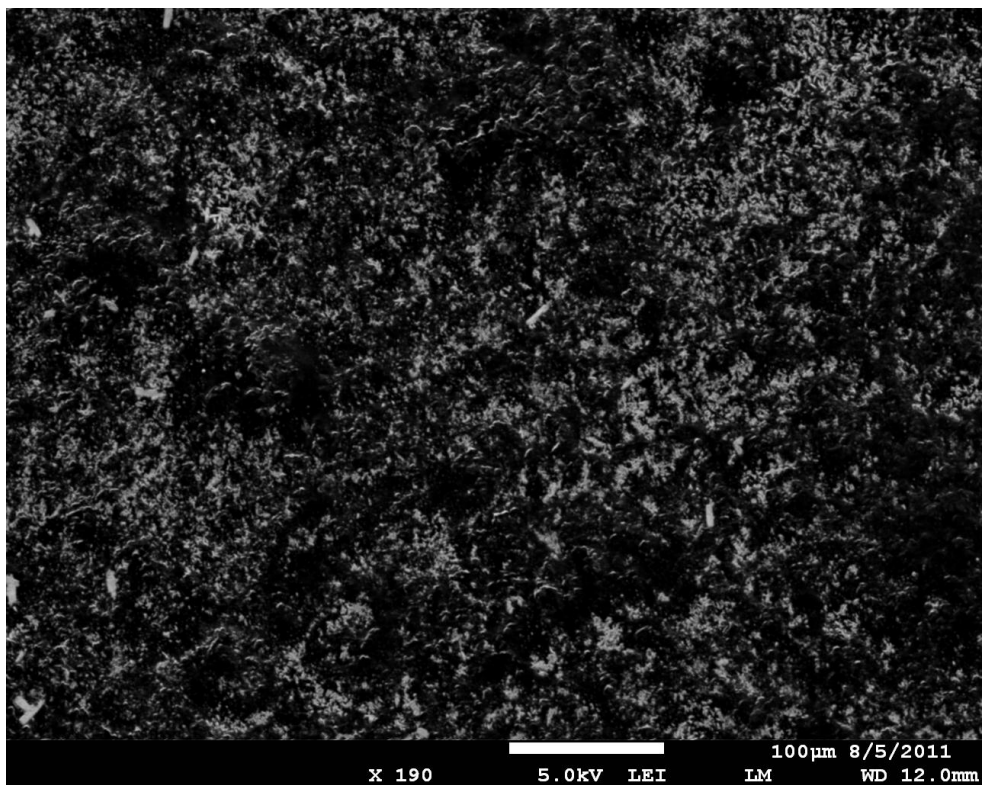


Figure 23: SEM image of 40HA at 150x magnification

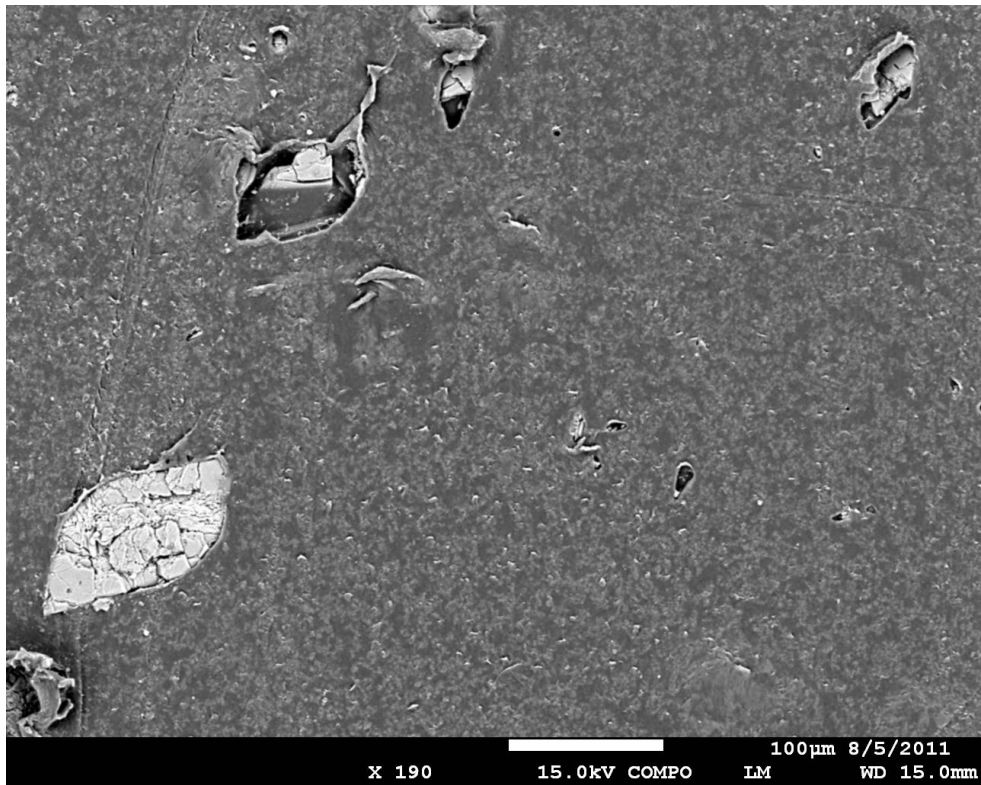


Figure 24: SEM image of 50HA at 150x magnification

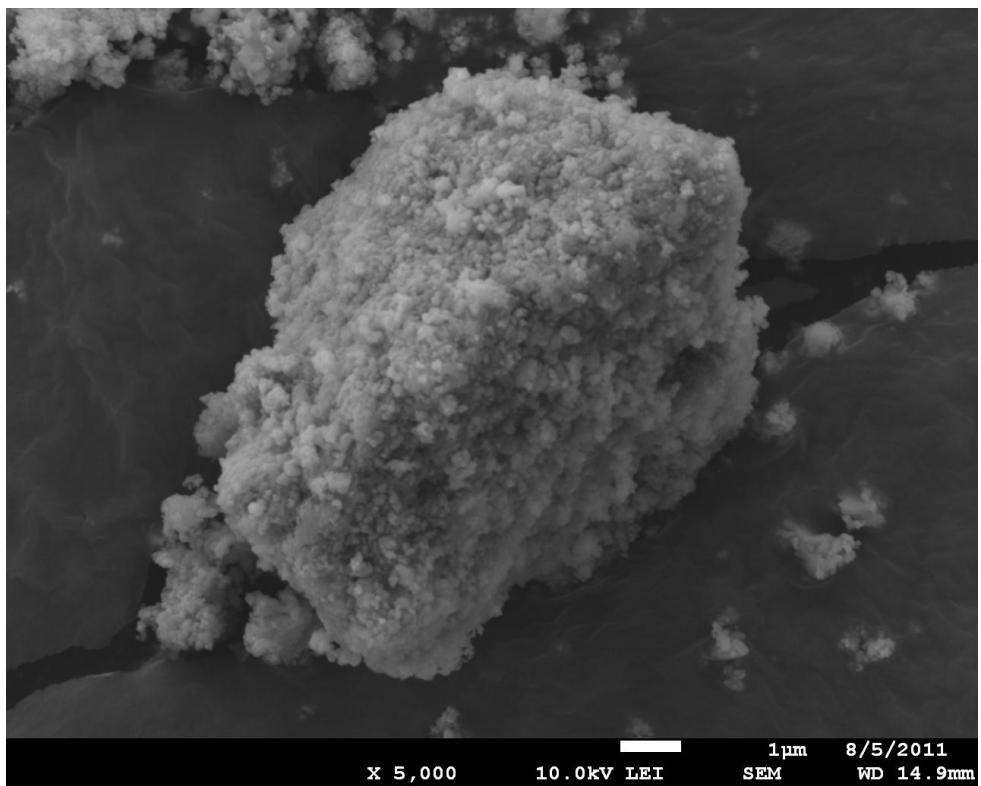


Figure 25: Shows detailed view of HA particles at 5000 magnification

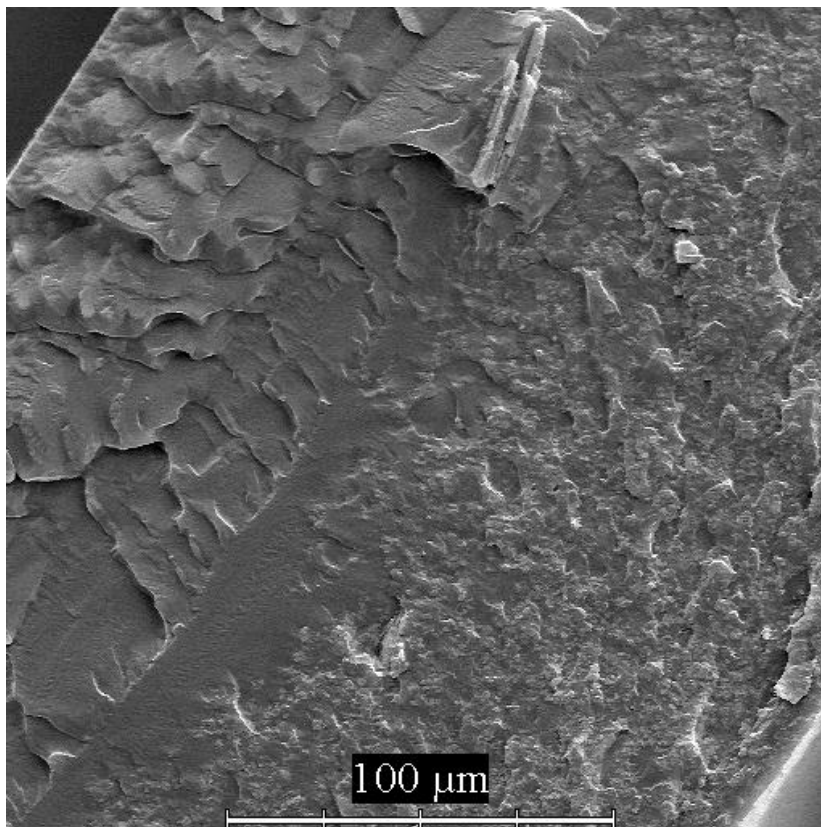


Figure 26: Cut along the membrane showing visible layer of the hydroxyapatite in the 30HA

Figure 26 depicts the cut along the 30HA membrane. The filler is visibly separated into two zones due to the action of partial sedimentation of HA particles during drying process. The morphology of HA particles in the composite membranes was changed, not only, due to the filler concentration, but also due to the temperature (30 °C) and time of membranes preparation (7 days). These conditions have greatly influenced the HA crystal growth.

5.4 Tensile properties

The mechanical behavior of the composite with various weight ratios of HA particles in terms stress-strain dependence is displayed in Fig. 27. The results show, that HA addition influences the mechanical properties of the composites. The resulted values were averaged (see Table 6) from 5 accomplished measurements.

Pure PVA shows a curve with yield point, which indicates transition between elastic and plastic deformation, in the case of composites, this point is not observed clearly.

Curves of composite have three zones - the first is characterised by an increase in the load accompanied by extension of the film, followed by a zone in which the extension occurs with slight increases in the load and the point of rupture of the membranes. The samples formed necking and white zone before rupture. The failure appears to be ductile for all the tested samples.

The significant values of the measurement are noted in Table 6. Maximum tensile stress was the highest in the case of 10HA, i.e. 55 MPa. Compared to the pure PVA, the 10HA and 20HA had higher maximum stress. The increase in the case of 10HA was 17% and 20HA was 8%. The sample 30HA had maximum tensile stress lower than that of the PVA, it was 42 MPa and the decrease was 11%, samples 40HA and 50HA had distinctly lower values of maximum

tensile stress than pure polymer, namely 32 MPa and 27 MPa for 50HA, which made the decrease up to 32% and 42% comparing to the neat polymer.

The next value is the Young's modulus, as the content of HA increased further, the Young's modulus of the composites presented decreasing trend. The pure PVA has the value at 662 MPa, very close to this value was 10HA composite with 644 MPa. Similar value of Young's modulus was observed for 20HA and 40HA composites at 383 MPa and 382 MPa and the lowest was 50HA composite with 247 MPa.

Tensile stress at break have increased in comparison with the pure PVA in the case of 10HA and 20HA composites, this followed the trend of the maximum stress values. The increase in the case of 10HA was 29% and 14% for 20 HA. When the HA content in the composite reached 30%, the stress at break decreased. For 30HA, the decrease was 5% and then steeply 39% decrease for 40HA and 51% for 50HA.

Elongation at break in % compared with the pure PVA decreased for all the composites, the decrease was non-linear. The highest value of percentage of elongation was observed for neat polymer, this was 226%, the composite elongation was lower, the lowest for 20HA, then 10HA and then in ordered from lowest to highest 50HA → 30HA → 40HA.

Zheng *et al.*[121] presented results where the tensile strength and modulus of PVA/HA composite hydrogel increased with HA content. The viscosity of composite hydrogel was enhanced and its stress relaxation performance was more similar to natural cartilage. Li *et al.*[122] showed that the tensile strength of PVA/HA composite hydrogel first increased and then decreased with the increase in HA content. It was found, that the tensile strength achieved the maximum value when HA concentration was 7.5%. As HA content further increased the tensile strength decreased.

In this survey the values of tensile strength are improved for 10HA and 20HA in comparison with the pure PVA (0HA). The increasing amount of HA deteriorates the tensile strength, this may be caused by generating of HA agglomerates.

The SEM Fig. 28 shows rough surface which belongs to direction of the loading during testing for the 30HA specimen. Figures 29 and 30 show the edge (fracture surface) after tear apart.

Table 6: Tensile properties of prepared membranes

Sample	Maximum tensile stress (MPa)	Young's modulus (MPa)	Tensile stress at break (MPa)	Elongation at break (%)
0HA	47	662	41	226
10HA	55	644	53	156
20HA	51	383	47	140
30HA	42	362	39	181
40HA	32	382	25	185
50HA	27	247	20	177

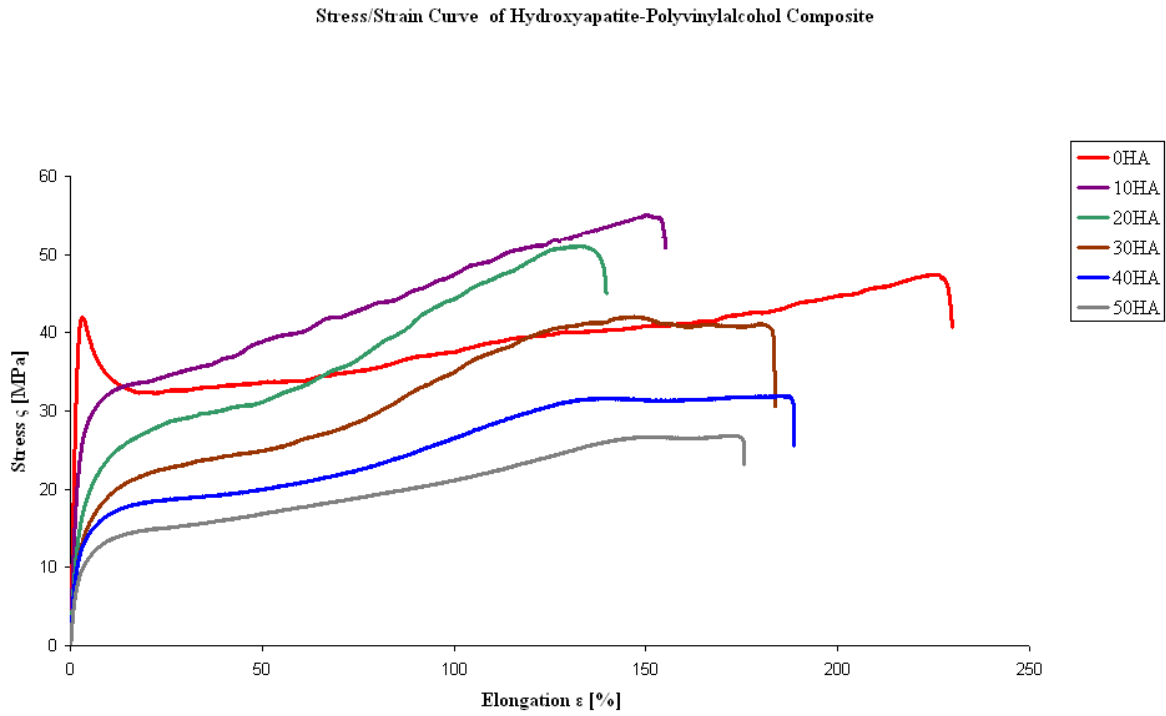
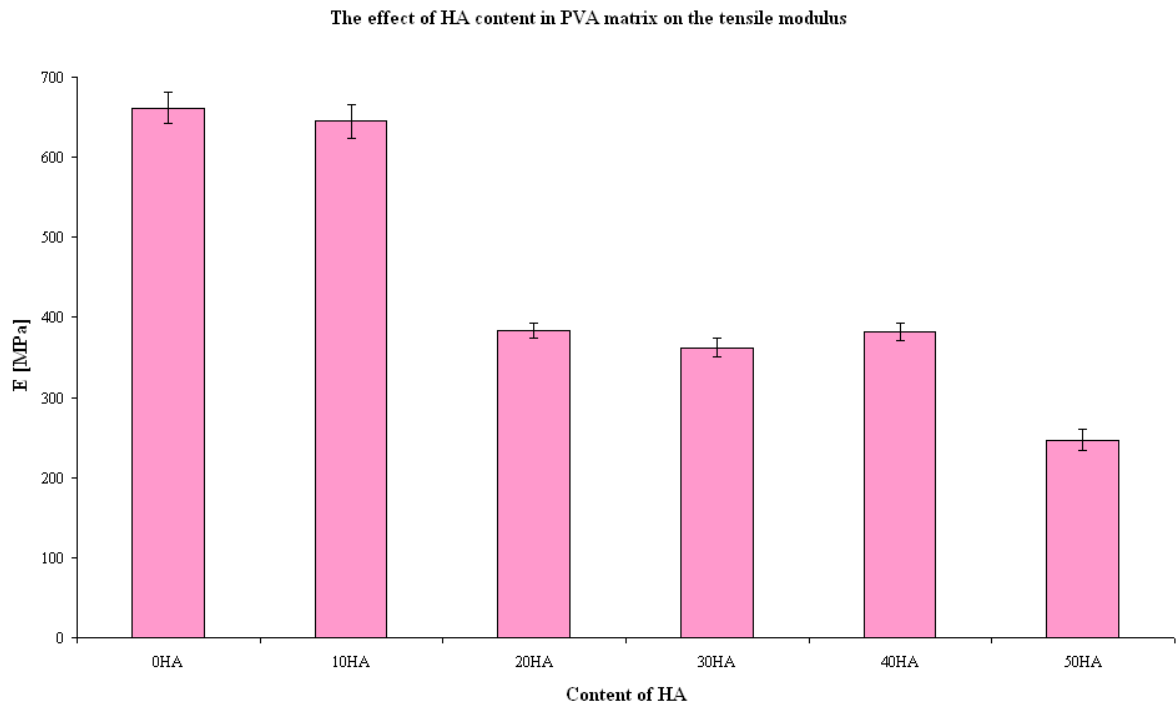


Figure 27: Stress/strain characteristics of the PVA/HA composite



Graph 2: The effect of HA content in PVA/HA composite on tensile modulus

The mechanical properties of the polymer are expected to be improved effectively by adding inorganic nanoparticles into polymer matrix due to their high mechanical strength and surface energy [98]. Ideally the interfacial bonding can effectively transfer the load from the matrix to

the reinforcement and weak interfacial bonding can deflect an advancing crack thus providing enhanced fracture toughness and avoiding catastrophic failure [44].

Contrarily, the nano-HA particles can easily agglomerate because of its high surface active energy, while the content of nano-HA exceeding a certain percent. The local agglomeration of nano-HA particles can not act as a reinforcement phase but can become the original defective region, which deteriorates the tensile strength of the composites [123].

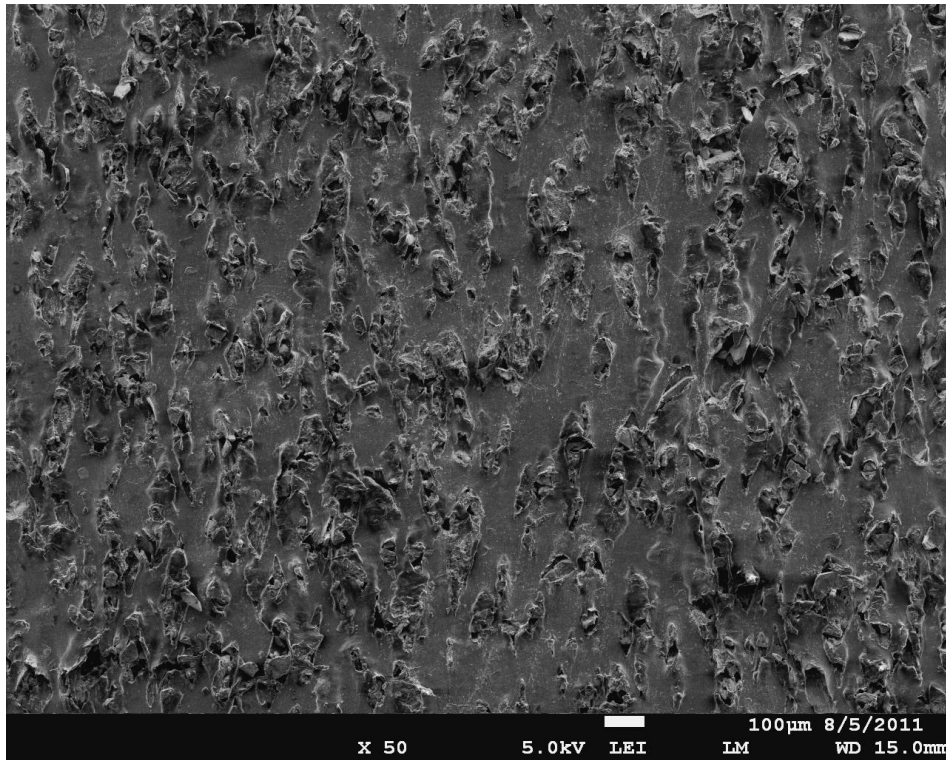


Figure 28: SEM image of the tensile impact fracture surfaces of the sample 30HA at 100 magnification

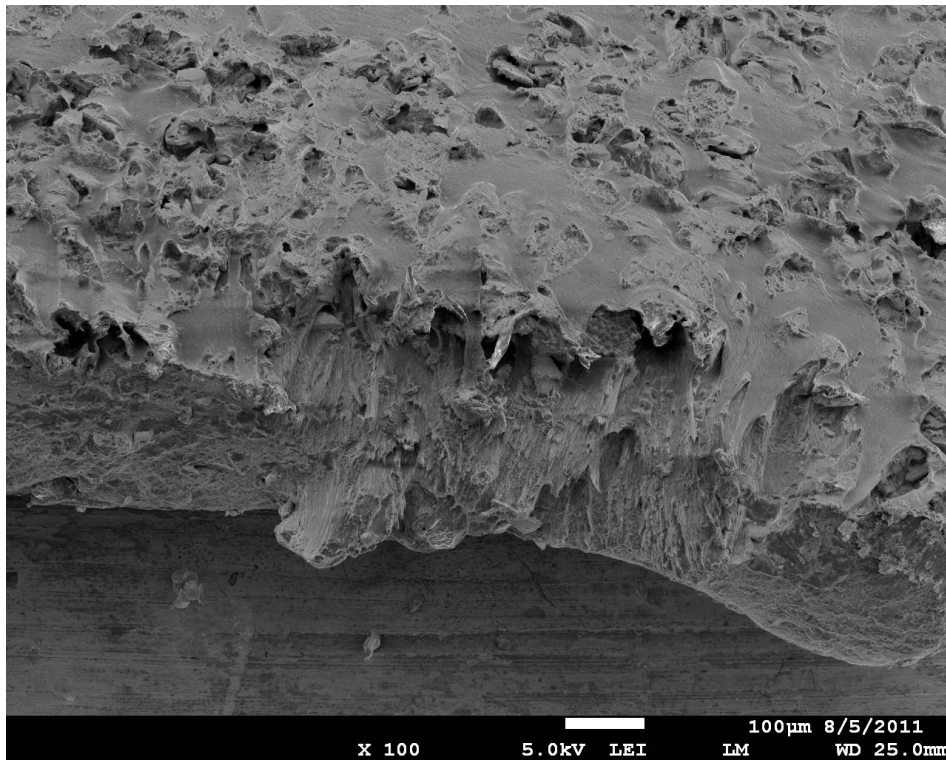


Figure 29: SEM image of sample 30HA after tensile strength testing – the impact edge at 100 magnification

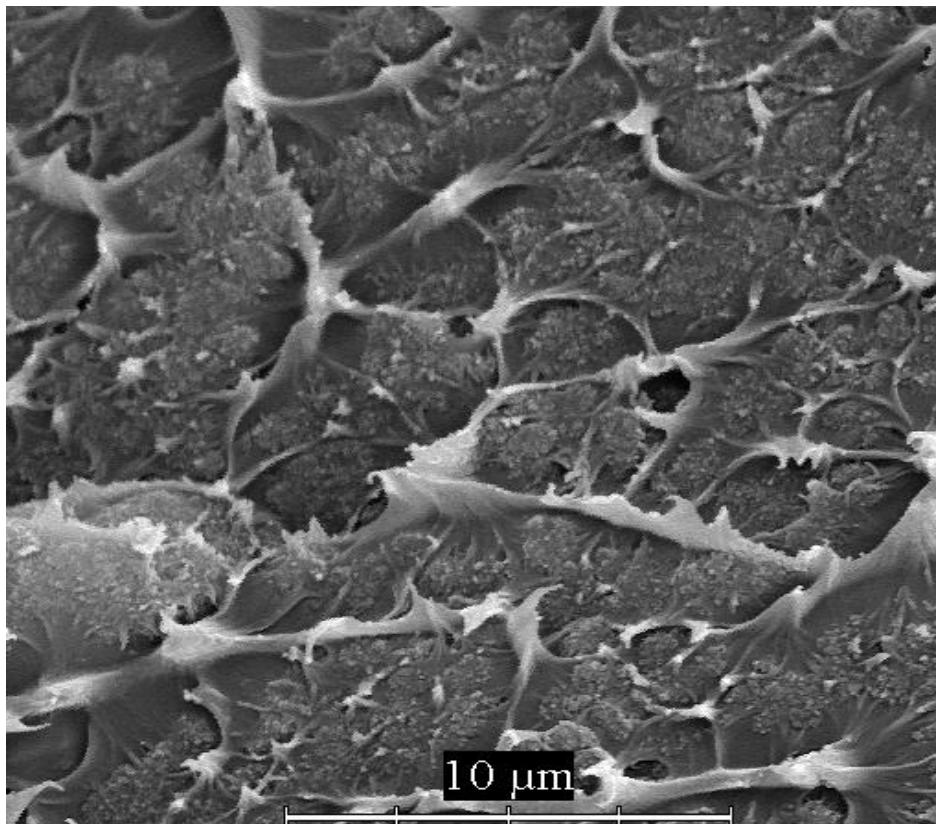


Figure 30: Detail of the impact edge with visible HA and PVA phase after tensile testing of 30HA

5.5 Thermogravimetric analysis

5.5.1 PVA thermal decomposition

The thermal degradation of PVA under 300 °C the major pyrolysis product has been reported to be water, produced by the elimination of hydroxyl side-groups [124, 125].

Peng [126] investigated PVA/SiO₂ nanocomposite, where he described two steps of PVA thermal decomposition (Fig. 31 – 33). The first degradation step are elimination reactions. The elimination reactions of linear and aliphatic polymers including PVA in the first stage of thermal degradation mainly form polyene structures via dehydration [127, 128].

The degradation temperature of the first degradation step is not high enough to break all the backbone chains of these polyenes into low-molecular-weight polyenes. Most of these polyene structures acts as intermediate products and is further degraded into other products with lower molecular weights at the next degradation step, which is chain-scission reactions. The degradation products of the second degradation step are acetaldehyde, acetic acid, polyenes, benzenoid derivatives and a small amount of furan

As the second step of thermal degradation occurs at higher temperatures compared to the first step, it becomes more complex. At this step, the degradation is dominated by the chain-scission reactions, side-reactions and cyclization reactions. A continual degradation of residual acetate groups is also found. Furan is formed by intramolecular cyclizations [126].

Table 7: *The physical appearance during thermal decomposition of PVA [129].*

Material	Appearance
PVA	White solid
250°C Char (30 min)	Yellow-orange foam
300°C Char (30 min)	Tan rigid foam
350°C Char (30 min)	Dark brown foam
400°C Char (30 min)	Black powder

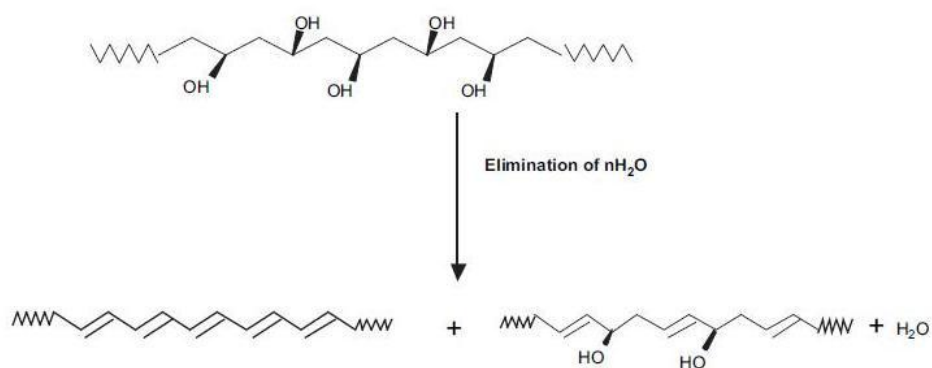


Figure 31: Elimination reaction – H_2O realising

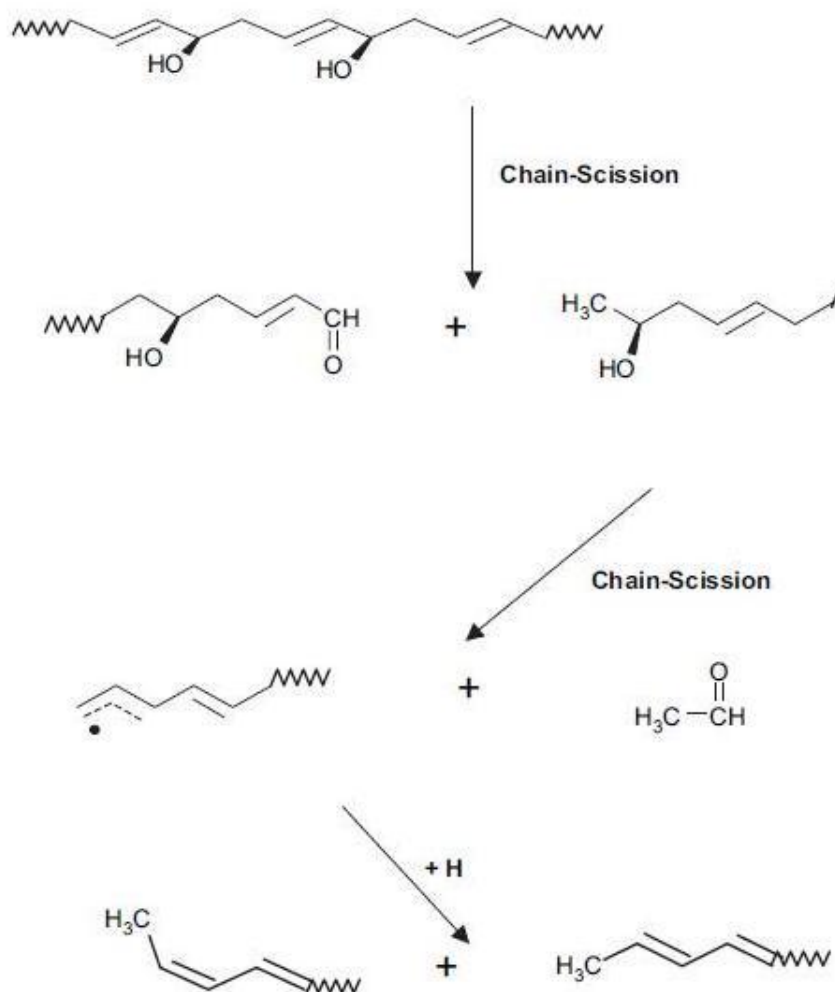


Figure 32: Chain scission reactions in the first degradation step

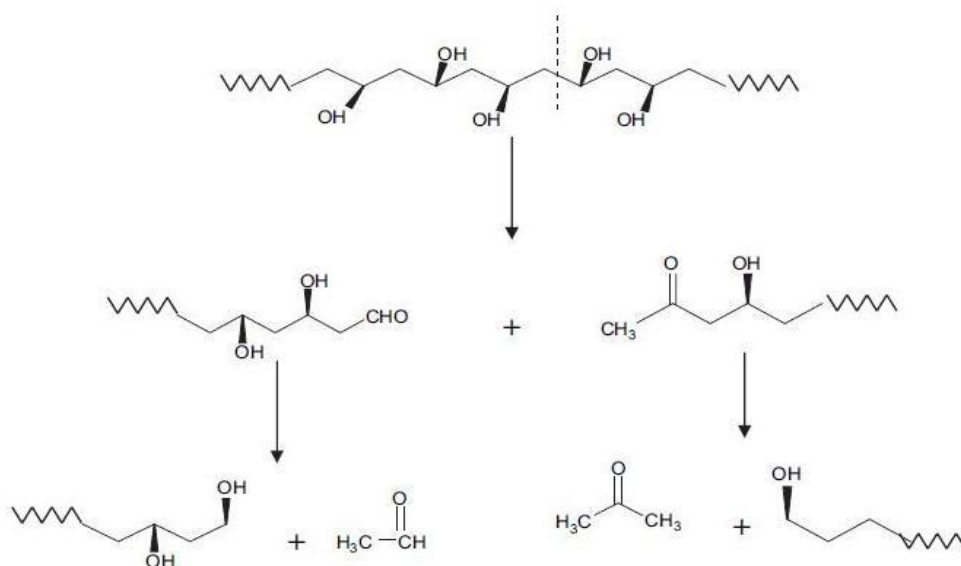


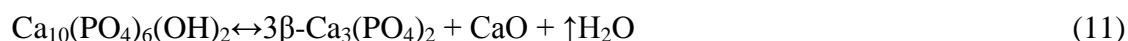
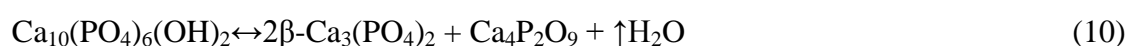
Figure 33: Chain scission reactions

5.5.2 HA thermal decomposition

The decomposition of HA proceeds in two stages: reversible expulsion of water producing oxyapatite (OA), and irreversible decomposition to HA yielding calcium phosphates [130].

HA is a hydrated calcium phosphate material. It begins to dehydroxylate at about 800 °C to form oxyhydroxyapatite, or $\text{Ca}_{10}(\text{PO}_4)_6(\text{OH})_{2-2x}\text{O}_x\Box_x$, where \Box =vacancy. Furthermore, HA also decomposes to form other calcium phosphates at elevated temperatures. Two mechanisms have been proposed for the decomposition as follows:

Further heating results in the transformation of β -tricalcium phosphate ($\beta\text{-Ca}_3(\text{PO}_4)_2$), forming α -tricalcium phosphate. This usually requires exposure to temperatures in excess of 1350 °C for this phase transformation to take place. Two mechanisms have been proposed for the decomposition as follows:



Of these, the former is the more accepted mechanism.

Regardless of which mechanism takes place, both result in the formation of soluble or resorbable calcium phosphates, which dissolve when exposed to physiological environments [131].

5.5.3 PVA thermogravimetry analysis

The course of thermogravimetric curve of pure PVA(OHA) shows 3 main degradation steps, which are clearly expressed with DTG – derivated TG curve (Fig. 34).

The initial weight loss for the pure PVA occurred at a temperature range of 37 to 200 °C with a peak at 156 °C in the DTG curve ($T_{\text{max},1} = 156\text{ °C}$), due to the evaporation of physically weak and chemically strong bound H_2O from the polymer matrix. The weight loss was about 7,5 wt%. The next major weight losses have been observed in the range of 250 to 415 °C

($T_{\max,2} = 368\text{ }^{\circ}\text{C}$). This was due to the degradation of side chain (O–H) of PVA and the weight loss at this stage was about 68 wt%. The last peak of the third stage temperature range between 450 and 500 $^{\circ}\text{C}$ ($T_{\max,3} = 461\text{ }^{\circ}\text{C}$). This may correspond to the cleavage of C–C backbone of PVA polymer or commonly called carbonation with a weight loss of 16 wt%.

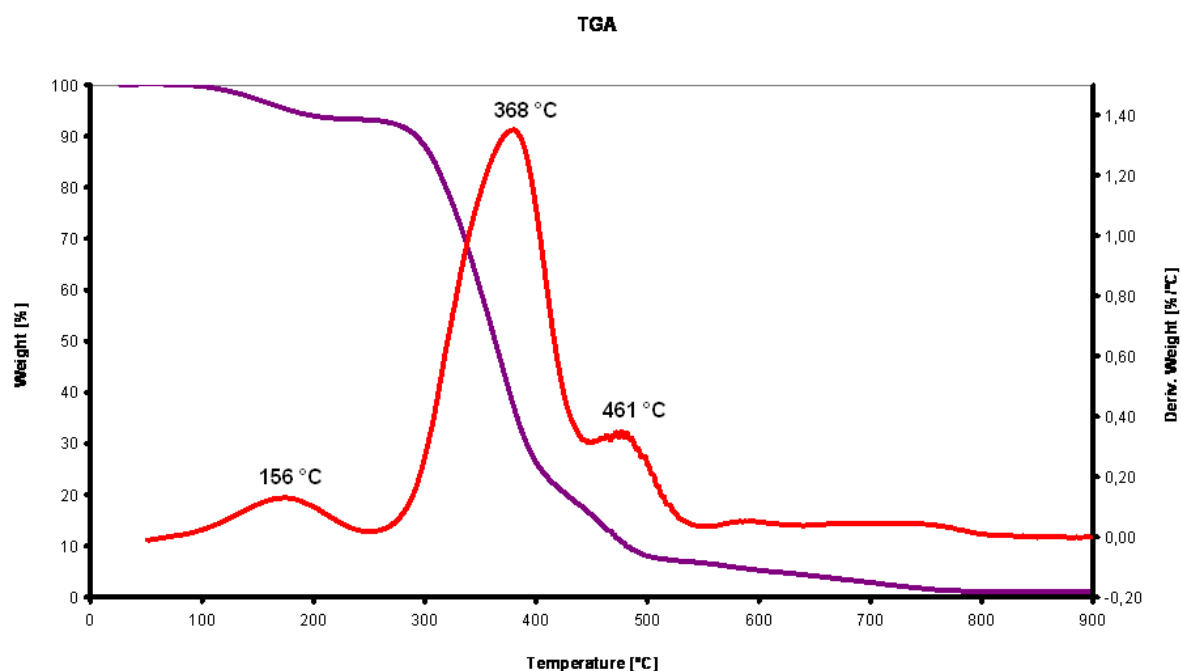


Figure 34: TGA curve of pure PVA (0HA)

5.5.4 Hydroxyapatite thermogravimetry analysis

The decomposition of the pure HA powder was monitored up to 900 $^{\circ}\text{C}$ (Fig. 35). There was revealed one significant peak at DTG curve around 272 $^{\circ}\text{C}$, which belongs to massive loss of physically bond water from hydroxyapatite structure. This mass loss was near 25 wt% in range 200 – 300 $^{\circ}\text{C}$.

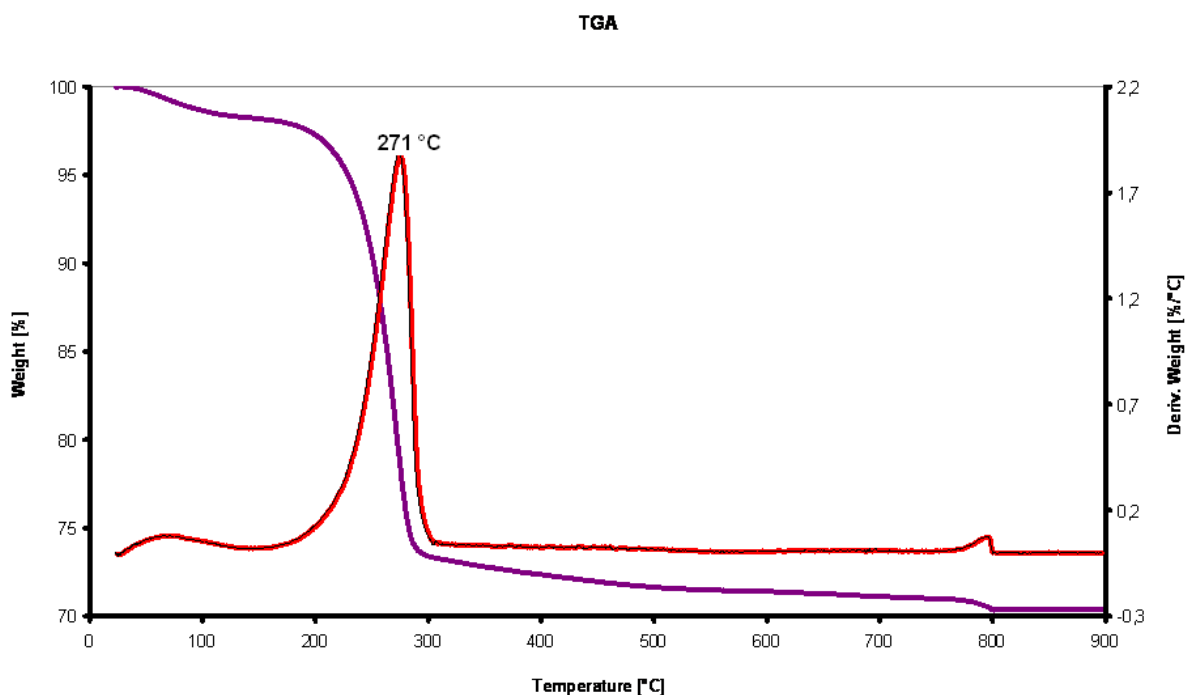


Figure 35: TGA curve of pure hydroxyapatite powder (100HA)

5.5.5 PVA/HA composite thermogravimetry analysis "

The main loss of weight in composite shows peaks in DTG curves and declination of the TGA curve. The thermograms of all measured PVA/HA composites show common features. The main weight loss carry out in three ranges. The first one takes place by 250 °C, the second range is approximately between 250 and 450 °C and the last one 450 °C and higher.

Table 8: Weight loss of PVA/HA composites with variable HA content in PVA matrix sorted into three temperature ranges

Sample	1st Range		2nd Range		3rd Range	
	T [°C]	Weight loss [%]	T [°C]	Weight loss [%]	T [°C]	Weight loss [%]
10HA	37 - 230	14.9	250 – 450	49.6	450– 540	18.9
20HA	37 - 240	17.0	260 – 430	43.1	430– 530	15.8
30HA	37 – 250	19.9	270 – 420	41.8	430– 500	10.7
40HA	37 - 210	22.9	250 – 400	35.0	500- 630	15.0
50HA	37 - 200	31.9	250 - 400	25.5	450- 600	21.0

First temperature range reveals, that with increasing hydroxyapatite in PVA matrix increases weight loss. This phenomenon might be explained as weight releasing in form of water from hydroxyapatite and breaking of weak bonds between matrix and the filler.

The second range, approx. between 250 and 450 °C shows opposite tendency comparing to previous range, so with increasing amount of HA in PVA matrix, the weight loss decreases.

It was also found out, that the interval of decomposition is shortened, so the broadest is in 10HA. The temperature range is in line from the lowest presence of HA to the highest wide 200, 160, 160, 150 and 150 °C.

The weight loss in this range is influenced by both – the filler and the matrix decomposition, as the hydroxyapatite has its main weight loss in this survey between 200 – 300 °C, and it is 25%wt. and the PVA which show in range 250 – 450 °C massive weight loss about 68%. This loss is associated with the degradation of PVA polymer membrane.

The third decomposition region is in range approx. 450 °C and higher, which is due to due to the cleavage backbone of PVA polymer membrane (or so-called carbonation).

The 20HA shows peculiar run of the curve at around 240 °C, this was recorded the bouncing measuring pan during testing which was caused by foaming of the PVA in the sample at this temperature.

The PVA/HA composite shows improved resistance in comparison with the pure PVA. Degradation temperatures of the composite are noticeably higher which is due to interfacial bonding between HA particles and the PVA polymer matrix.

The total weight loss was determined at all of the measured samples at 900 °C and as expected, the highest residue was noticed at pure HA, the lowest at pure PVA and according to amount of HA in PVA matrix. The results of the measurement are noticed in Tab. 9.

All TGA curves of PVA/HA composites are displayed in Appendix (Figures 49 - 55).

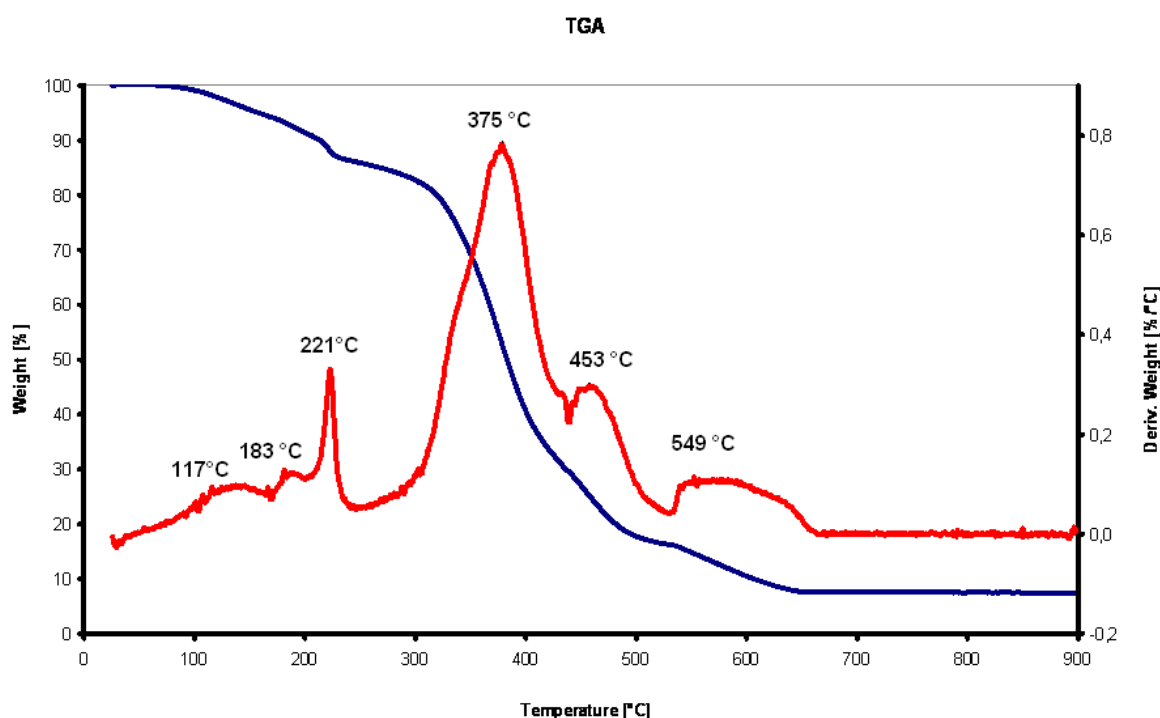


Figure 36: TGA curve of composite 10HA

Table 9: Comparison of total weight loss at 900°C

Sample	Total weight loss at 900°C in %
0HA	98.99
10 HA	92.61
20 HA	90.82
30 HA	85.40
40 HA	80.39
50 HA	79.50
100 HA	33.04

The residuum of the TGA measured samples was a white powder, which was further analysed by XRD measurement, which showed supposed results - equations (section 5.5.2). After TGA analysis, there was found rest of not fully decomposed hydroxyapatite and calcium phosphate $\text{Ca}_3(\text{PO}_4)_2$. Polyvinyl alcohol was not more found in sample, but whitlockite as product of partial decomposition of HA (Fig. 37).

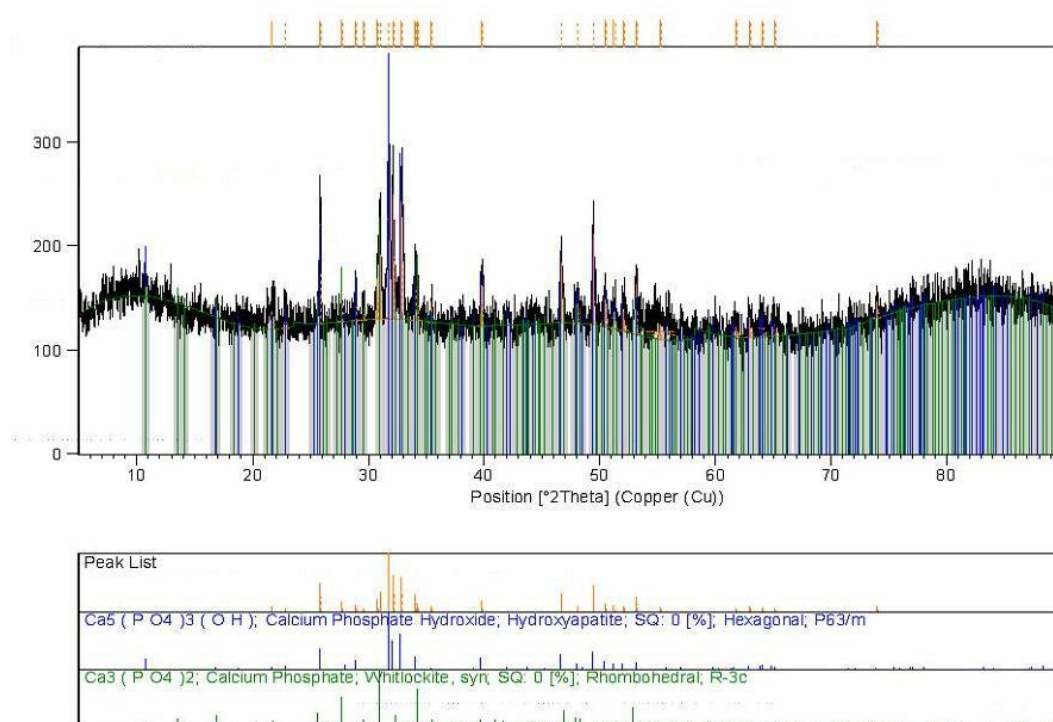


Figure 37: XRD spectrum of 20HA composite after TGA analysis

5.6 Bioactivity testing

Samples removed from the microincubator were rinsed with distilled water and dried at laboratory temperature. All the samples were weighed before and after the SBF immersion to compare weight loss respectively estimate the biodegradation of the composite. The weight loss was calculated according to percentage of initial weight. These results are depicted in Tab. 10. There are not included samples soaking for two hours as the weigh loss was negligible. It is obvious, that HA content strongly influences the degradation rate of the composite. The weigh loss was as expected highest in the case of pure PVA and stepped up with the increasing time soaked in SBF. Conversely the lowest weight loss was registered in

the case of 50HA, this is due to high content of HA in PVA matrix and because of new HA formation. Nie [132] tested foamed BCP/PVA bodies and the results described the same degradation effect, but the degradation rate was higher because of higher contact area.

Graphical representation of weight change see in Fig. 38. The limitation of PVA are obvious, including fast hydrolysis [132] and its bioinert nature [133] that hinder protein and cell adhesion [134]. This requires the incorporation of component, which reduces the rate and time of biodegradation, this demand fulfills hydroxyapatite.

Table 10: Weigh loss of PVA/HA biocomposites in testing time

	Weight loss after 7 days [%]	Weight loss after 28 days [%]
0HA	14.2	21.0
10HA	11.1	20.1
20HA	10.1	17.3
30HA	7.0	12.4
40HA	4.9	7.2
50HA	3.0	5.0

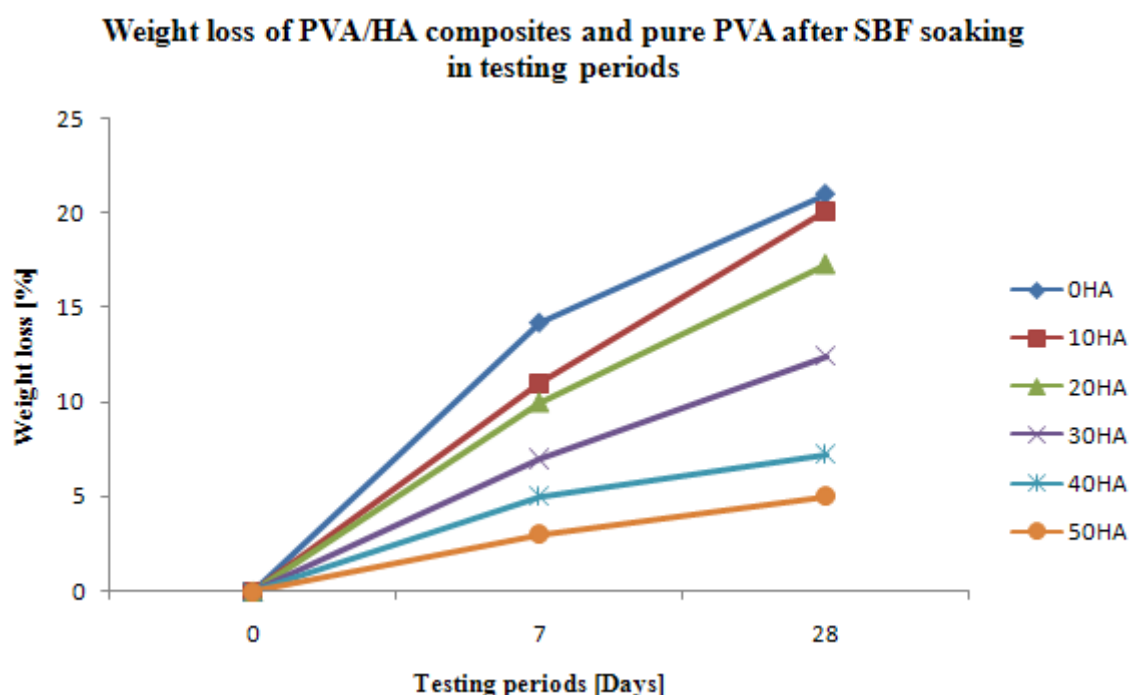


Figure 38: Increasing weight loss of composites and the pure PVA in time

The Fig. 39 displays macroscopic comparison of tested membranes after 7 days of SBF bioactivity testing. The membranes were flat before testing, the picture shows change in shape, as the samples were faced with flowing 37°C warm solution.

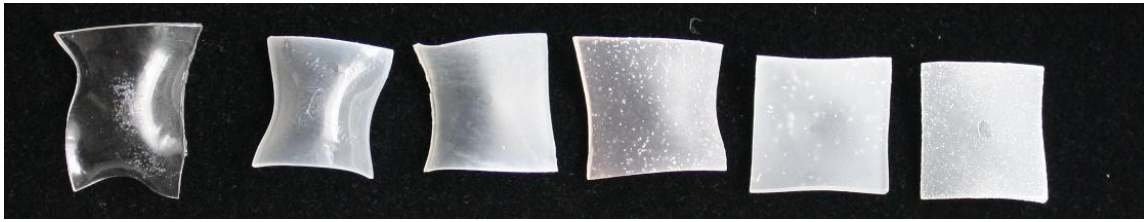


Figure 39: Shows macroscopic comparison of membranes with various HA content in PVA matrix, from left to right 0HA, 10HA, 20HA, 30HA, 40HA and 50HA after 7 days of SBF soaking.

The SEM pictures Fig. 40 - 43 display HA formation on the surface of 50HA composite during testing periods.

HA crystals were observed on all composite membranes just after 2 hours of soaking in SBF. Most of the membranes surface was entirely covered with crystals after 7 days of soaking in SBF. Fig. 44 – 46 depict corresponding change of surface roughness during testing periods.

The number of nucleation locations of apatite crystals was adequate to the experimental time and the apatite layer formed more rapidly on composite with higher content of HA.

The *in vitro* testing proved high bioactive properties of the PVA/HA composites. The possibility to manage the rate of bioactivity makes PVA/HA composite suitable to fulfill diverse requirements and can be useful as tailor-made materials for medical application.

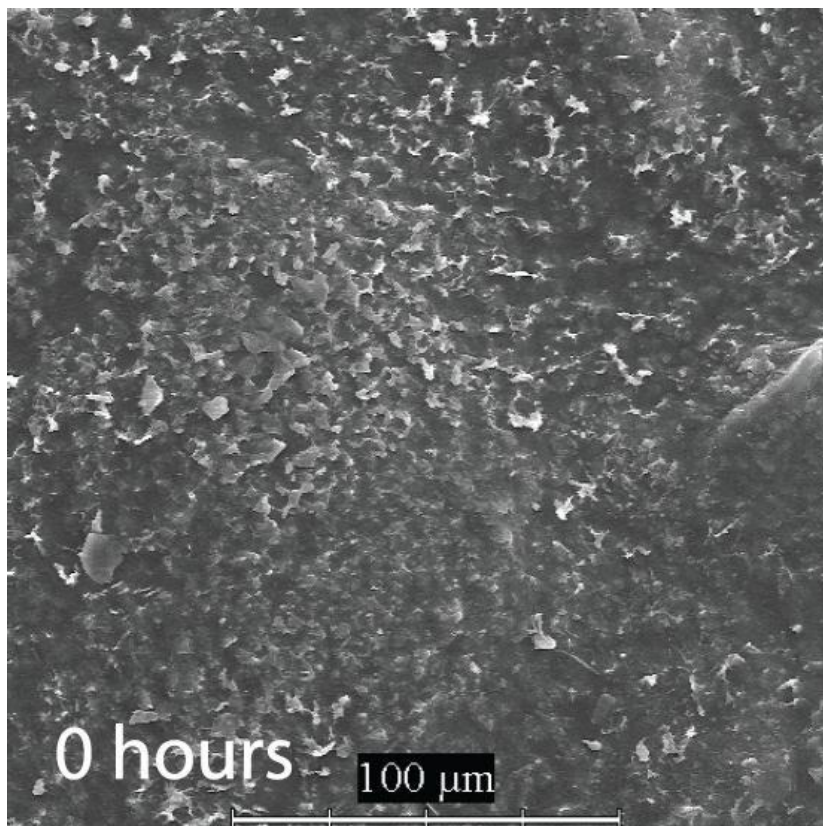


Figure 40: Surface morphology of 50HA before soaking in SBF

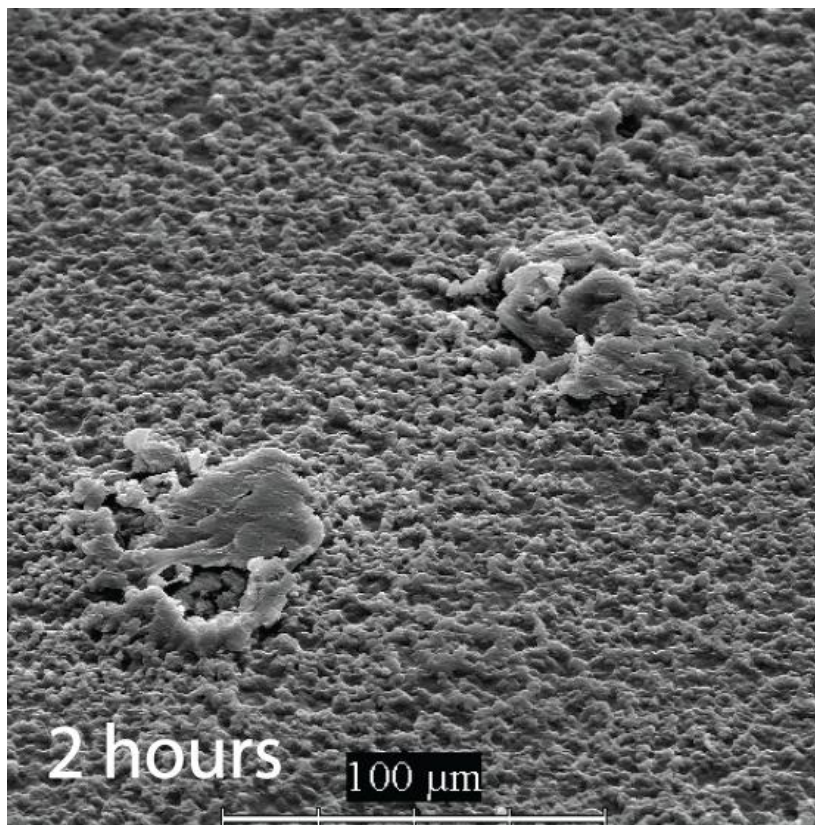


Figure 41: Surface morphology of 50HA after soaking in SBF for 2 hours

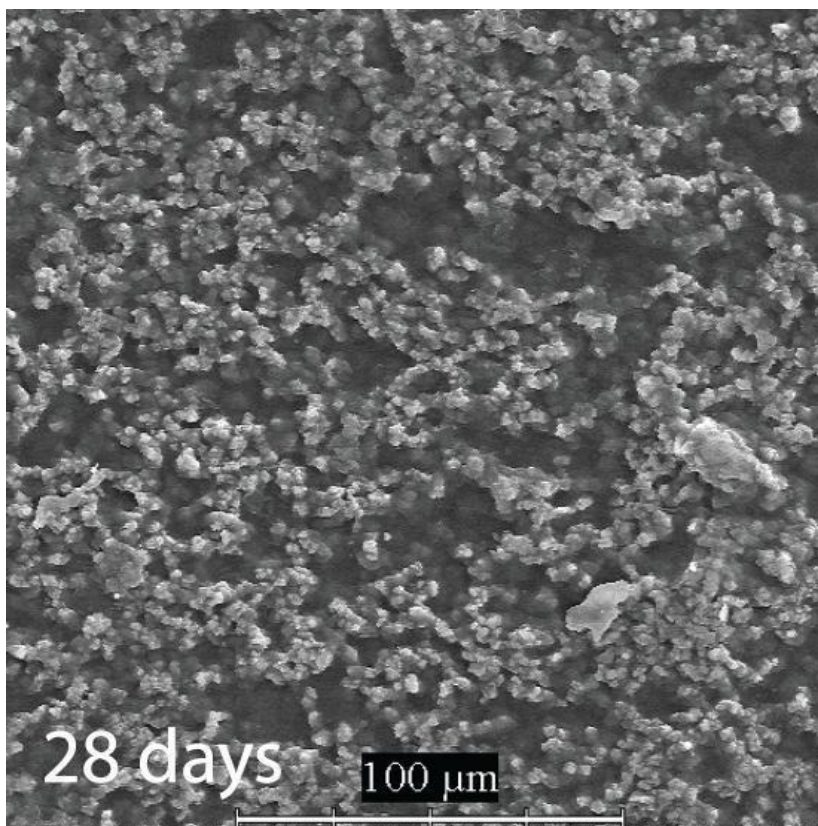


Figure 42: Surface morphology of 50HA after soaking in SBF for 28 days

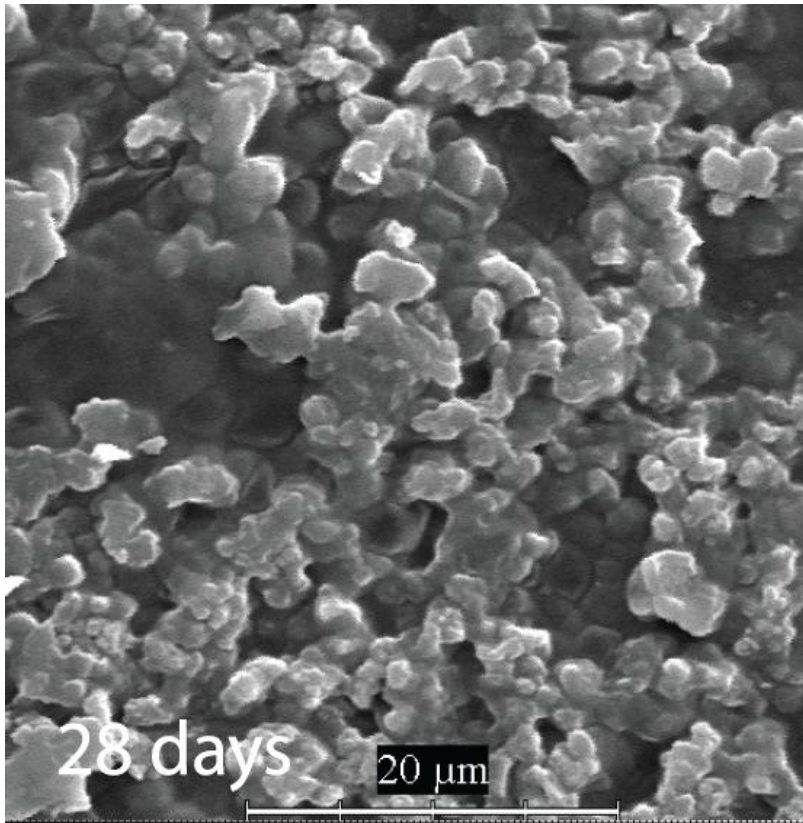


Figure 43: Detail of new formed hydroxyapatite on the surface

5.6.1 Surface Roughness

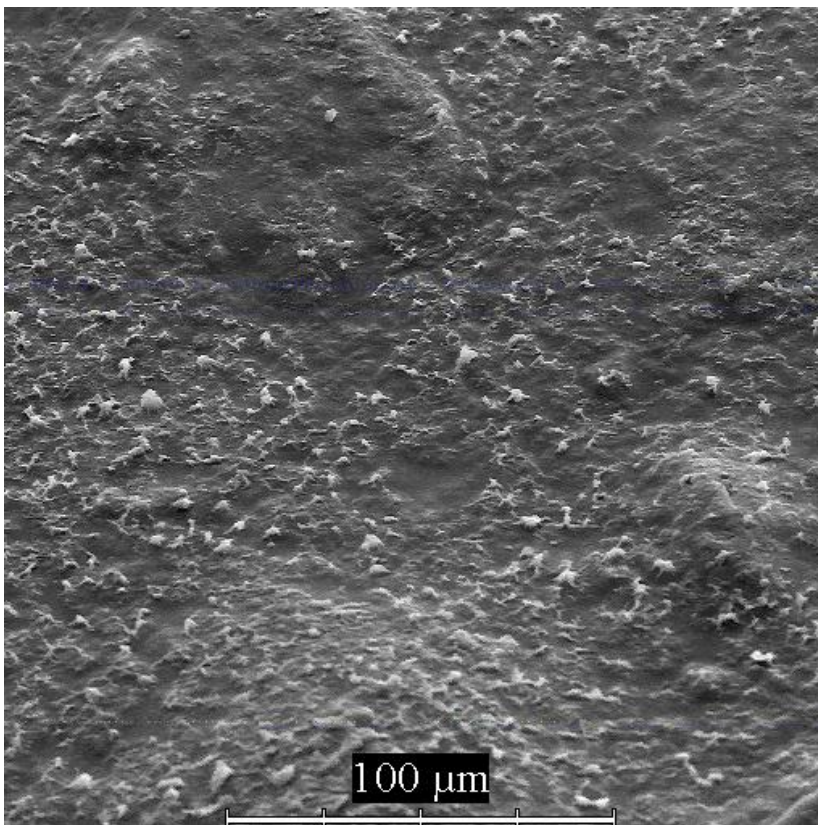


Figure 44: Study of surface change during testing periods – 50HA before soaking in SBF

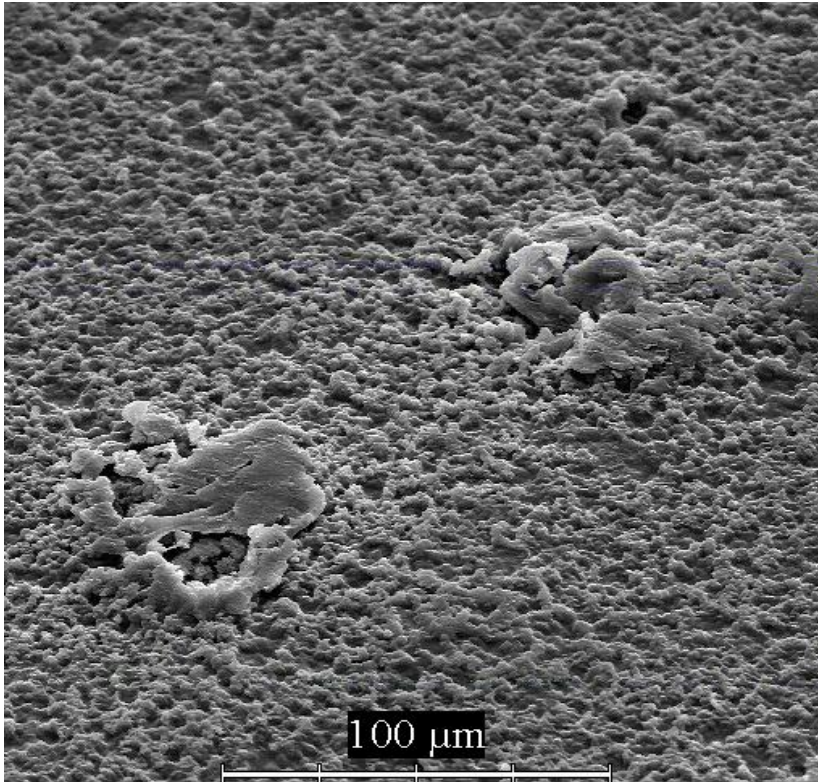


Figure 45: Study of surface change during testing periods – 50HA after 2 hours of soaking in SBF

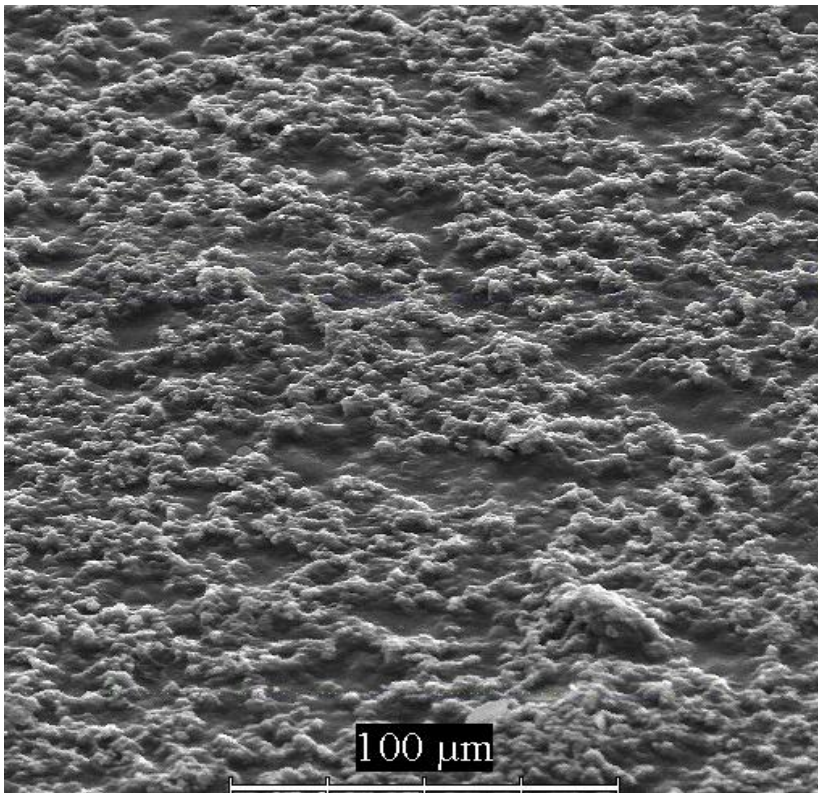


Figure 46: Study of surface change during testing periods – 50HA after 28 days of soaking in SBF

The newly formed layer was analysed by XRD analysis, which proved HA on the surface - Fig. 47 and 48. The diffractograms should be not considered as quantitative analysis, because of the high amount amorphous phase in the membranes, this misrepresents the results.

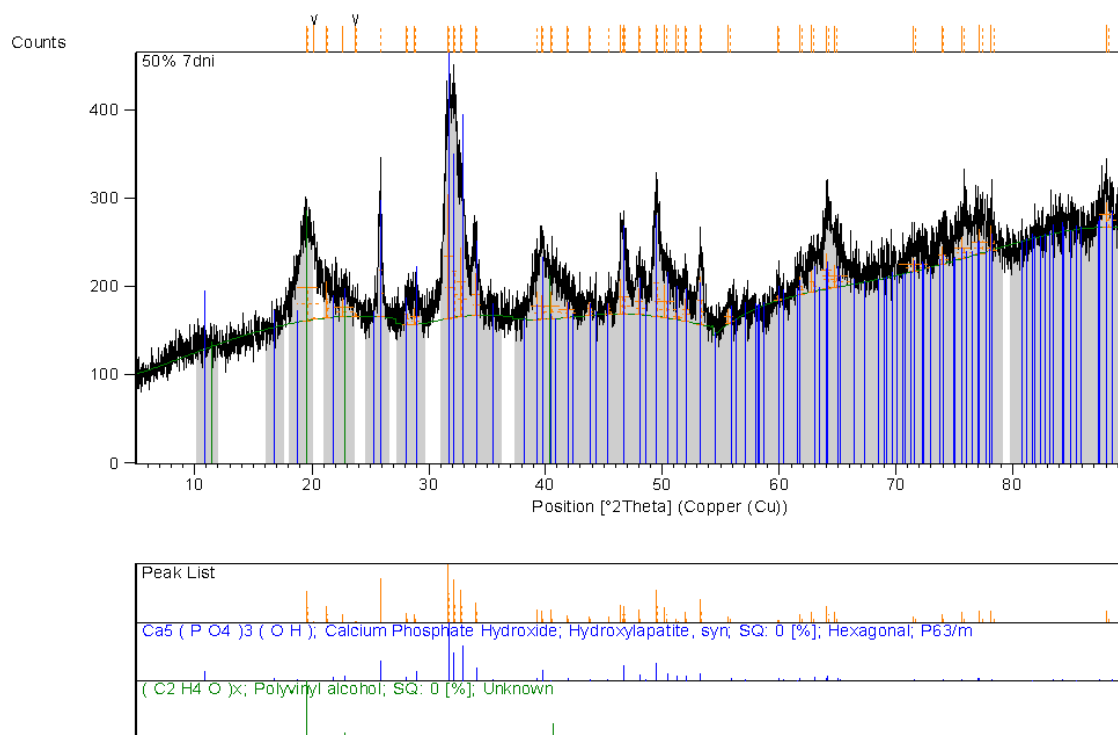


Figure 47: Diffractogram of 50HA composite surface after 7 days of soaking in SBF

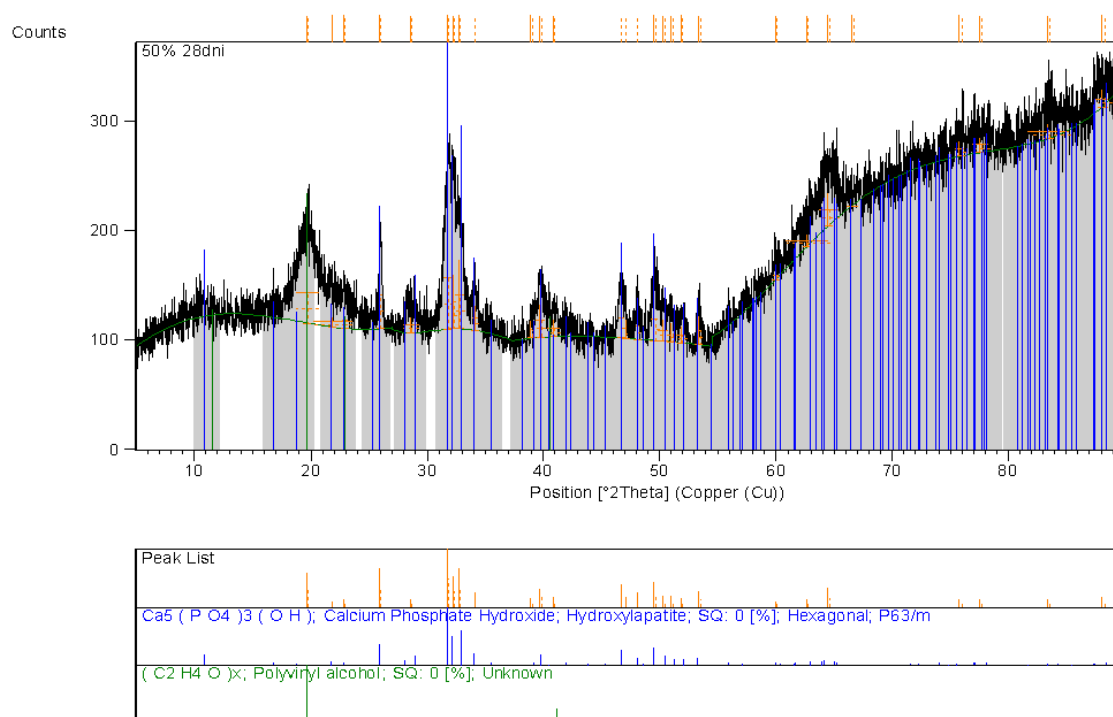


Figure 48: Diffractogram of 50HA composite surface after 28 days of soaking in SBF

6 CONCLUSION

The aim of the work was to synthesize biocomposite poly(vinyl alcohol) membranes reinforced with particles of hydroxyapatite and to characterise the properties of the composites. The main part of the work was focused on study of the *in vitro* bioactivity of synthesized membrane biocomposites.

As the first step, hydroxyapatite was prepared by action of diammonium hydrogen phosphate $(\text{NH}_4)_2\text{HPO}_4$ on calcium nitrate tetrahydrate $\text{Ca}(\text{NO}_3)_2 \cdot 4\text{H}_2\text{O}$ in the presence of ammonium hydroxide NH_4OH in water environment to form yogurt-like suspension. After washing the ammonium ions out, the solution was further used to prepare PVA/HA composite membranes with various weight HA content. The prepared composites were characterised by various methods and the bioactivity of the material was also tested.

ATR-FTIR spectroscopy was used to identify the different functional groups in composite membranes and composite components (HA filler, PVA matrix) themselves. The bonding between HA and PVA appeared in spectra after composite formation.

The SEM was used to determine surface morphology of synthesized composite membranes and the influence of HA amount on morphology. The dried HA was observed and it was round particles before processed into composite. The HA changed its structure after composite formation, there were detected needles shaped structures, which created clusters of various shapes. The agglomerates amounts increased with increasing wt% amount of HA. The change in morphology was caused not only by amount of HA in PVA matrix, but also because of the procedure, which was used to synthesize the membranes. They were dried for 7 days at 30°C. These condition caused HA crystal growth and the agglomeration trend as well.

The tensile testing was used to compare pure PVA and composites mechanical properties. There was a noticeable influence of HA filler. The values of tensile strength are improved for 10HA and 20HA in comparison with the pure PVA. The increasing amount of HA deteriorated the tensile strength, this was probably caused by HA agglomerates.

The bioactivity testing results indicated that the synthesized HA/PVA composite membranes showed the high bioactivity *in vitro* in the SBF solution. At all the tested membranes new apatite layer was formed, this was detected with SEM measurements. The tested samples showed weight loss after SBF soaking which decreases with increasing content of HA in the PVA matrix, this was caused by biodegradation ability of PVA. The bioactivity of membrane containing 50 % of HA had the highest ability to form the apatite and the layer increased with increasing soaking time. This ability makes the composite a suitable candidate for applications as artificial cartilage.

The main contributions of this work is that PVA/HA biocomposites were characterised with wide scope of methods. In the case of FTIR, the bonding between components was detected, the thermal stability of the composites was improved in comparison to the pure PVA and the mechanical properties were strongly influenced with bioceramic filler. The distribution and the arrangement of the HA crystals were observed with SEM. Finally the *in vitro* method was

used for the study of the membranes, this test allows prediction of the approximate behaviour of such materials *in vivo*. The bioactivity was proved due to formation of new HA layer on the membranes surface.

Due to rapid advances made in this research area, it was not possible to include all points of view in the work. There are still tasks which should be focused on in future work.

7 FUTURE WORK

Because of the synthesized hydroxyapatite was both micro and nano sized, the next synthesis will be focused on production of nano-sized particles only. The different technique methods to prepare the composites are required to avoid HA crystals growth and homogeneous dispersion of nanoparticle fillers in the matrix of biopolymers. Investigated samples could be membranes or porous bodies composed of hydroxyapatite with polymer as fillers. The *in vitro* bioactivity testing gave us an information about the host tissue response to the biocomposite, the future studies could be more focused on bioactivity and on *in vivo* behaviour.

8 REFERENCES

- [1] Urban, K., Strnad, Z.: Bioaktivní sklokeramika nahrazující kost : Neživé náhrady srůstající s živou tkání, *Vesmír*, 1.1.2000, vol. 79, pp. 130-133.
- [2] Vallet-Regí, M.: Evolution of bioceramics within the field of biomaterials, *Comptes Rendus Chimie*, vol. 13, issues 1-2, 2010, pp. 174-185.
- [3] William, D. F.: On the nature of biomaterials, *Biomaterials*, 2009, vol. 30, issue 30, pp. 5897-5909.
- [4] Williams, D.F.: *The Williams dictionary of biomaterials*, Liverpool: Liverpool University Press, 1999, xvii, p. 343, ISBN 08-532-3734-4.
- [5] Dorozhkin, S.V.: Calcium Orthophosphates as Bioceramics: State of the Art, *Journal of Functional Biomaterials*, 2010, vol. 1, issue 1, pp. 22-107.
- [6] Vallet-Regí, M.: Ceramics for medical applications, *J. Chem. Soc. Dalton Trans.*, 2001, pp. 97-108.
- [7] Saraydin, S.U., Saraydin, D.: *Histopatological Effect Characteristics of Various Biomaterials and Monomers Used in Polymeric Biomaterial Production*, *Biomaterials - Physics and Chemistry*, Prof. Rosario Pignatello (Ed.), 2011, 490.p ISBN: 978-953-307-418-4.
- [8] Jandt, K.D.: Evolutions, revolutions and trends in biomaterials science - A perspective, *Advanced Engineering Materials*, 2007, vol. 9, pp. 1035-1050.
- [9] Mann, S., (Ed.): *Biomimetic Materials Chemistry*, 1996, Wiley-VCH: Weinheim, Germany, p.400.
- [10] Bohner, M.: Resorbable biomaterials as bone graft substitutes, *Materials Today*, 2010, vol. 13, pp. 24-30.
- [11] Best, S. M., Porter, A.E., Thian, E.S., Huang, J.: Bioceramics: Past, present and for the future, *Journal of the European Ceramic Society*, 2008, vol. 28, pp. 1319-1327.
- [12] Heness, G., Ben-Nissan, B.: Innovative bioceramics, *Materials Forum*, 2004, vol. 27, pp. 104-114.
- [13] Biswal, S.: *Preparation of Hydroxyapatite Porous Scaffold*, Rourkela, 2010, Bachelor Thesis, National Institute of Technology Rourkela, p.44.
- [14] Puska, M., Aho, A.J., Vallittu, P.: *Polymer Composites for Bone Reconstruction*, *Advances in Composite Materials - Analysis of Natural and Man-Made Materials*, Dr. Pavla Tesinova (Ed.), 2011, InTech, ISBN: 978-953-307-449-8.
- [15] Hench, L.L.: Biomaterials, *Science*, 1980, vol. 208, issue 4446, pp. 826-831.
- [16] Navarro, M., Michiardi, A., Castano, A., Planell, J.A.: Biomaterials in orthopaedics, *Journal of The Royal Society Interface*, 2008, vol. 5, issue 27, pp. 1137-1158.
- [17] Wang, K., Zhou, C., Hong, Y., Zhang, X.: A review of protein adsorption on bioceramics. *Interface Focus*, 2012-04-23, vol. 2, issue 3, pp. 259-277.
- [18] Ho, E.Y.: *Engineering Bioactive Polymers for the Next Generation of Bone Repair*, PhD Thesis, Drexel University, 2005, p.166.
- [19] Fisher, J., Dowson, D.: Tribology of total artificial joints, *Proc. Inst. Mech. Eng. J. Eng. Med.*, 1991, vol. 205, pp.73-79.
- [20] Sutula, L.C. et al.: Impact of gamma sterilization on clinical performance of polyethylene in the hip, *Clin. Ortho*, 1995, vol. 319, pp.28-40.
- [21] Gasser, B.: About composite materials and their use in bone surgery, 2000, *Injury Int J Care Injured*, vol. 31, pp. 48-53.

- [22] Mano, J.F., Sousa, R.A., Boesel, L.F., Neves, N.M., Reis, R. L.: Bioinert, biodegradable and injectable polymeric matrix composites for hard tissue replacement: state of the art and recent developments, *Composites Science and Technology*, 2004, vol. 64, issue 6, pp. 789-817.
- [23] Hench L. L., Splinter R. J., Allen W. C., Greenlee T. K. Jr: Bonding mechanisms at the interface of ceramic prosthetic materials, *J. Biomed. Mater.*, 1971, Res. 2, pp. 117–141.
- [24] Hench, L.L., Wilson, J: Surface-active biomaterials, *Science*, 1984, vol. 226, issue 4675, pp. 630-636.
- [25] Hench, L.L., Thompson, I: Twenty-first century challenges for biomaterials, *Journal of The Royal Society Interface*, 2010, , vol. 7, Suppl_4, pp. 379-391.
- [26] Vallet-Regí, M.: Evolution of bioceramics within the field of biomaterials, *Comptes Rendus Chimie*, 2010, vol. 13, issue 1, pp. 174-185.
- [27] Nicolodo, L., Sjolander, E., Olsson, E., Jolander, K.: Biocompatible Ceramics -An Overview of Applications and Novel Materials, *Course 2B1750 - Smart Electronic Materials* 2004, [online]. [cit. 2009-09-22].
- [28] El-Ghannam, A.: Bone reconstruction: from bioceramics to tissue engineering, *Expert Review of Medical Devices*, 2005, vol. 2, issue 1, pp. 87-101.
- [29] Ginebra, M.P., Fernandez, E., De maeyer, E.A.P., Verbeek, R.M.H., Boltong, M.G., Ginebra, J., Driessens, F.C.M., Planell, J.A: Setting Reaction and Hardening of an Apatitic Calcium Phosphate Cement, *Journal of Dental Research*, 1997, vol. 76, issue 4, pp. 905-912.
- [30] Takagi, S., Chow, L.C., Ishikawa, K.: Formation of hydroxyapatite in new calcium phosphate cements, *Biomaterials*, 1998, vol. 19, issue 17, pp. 1593-1599.
- [31] Hench, L.L.: Bioceramics, *J. Am. Ceram. Soc.*, 1998, vol. 81, issue 7, pp.1705-1728.
- [32] Kokubo, T., Shigematsu, M., Nagashima, Y., Tashiro, M., Nakamura, T., Yamamuro, T., Higashi, S.: Apatite and wollastonite containing glass ceramics for prosthetic applications, *Bulletin of the Institute for Chemical Research*, 1982, Kyoto University, vol.60, pp. 260–268.
- [33] Gil-Albarova, J., Garrido-Lahigvera, R., Salinas, A.J., Roman, J., Bueno-Lozano, A.L., Gil-Albarova, R., Vallet-Regí, M.: The *in vivo* performance of a sol-gel glass and a glass-ceramic in the treatment of limited bone defects, *Biomaterials*, 2004, vol. 25, issue 19, pp. 4639-4645.
- [34] Gil-Albarova, J., Salinas, A., Bueno-Lozano, A.L., Roman, J., Aldini-Nicol, N., García-Barea, A., Giavaresi, G., Fini, M., Giardini, R., Vallet-Regí, M.: The *in vivo* behaviour of a sol-gel glass and a glass-ceramic during critical diaphyseal bone defects, *Biomaterials*, 2005, vol. 26, issue 21, pp. 4374-4382.
- [35] Dorozhkin, S.V.: Biocomposites and hybrid biomaterials based on calcium orthophosphates, *Biomatter*, 2011-07-01, vol. 1, issue 1, pp. 3-56.
- [36] Vert, M., Li, S.M., Spenlehauer, G., Guerin, P.: Bioresorbability and biocompatibility of aliphatic polyesters, *Journal of Materials Science: Materials in Medicine*, 1992, vol. 3, issue 6, pp. 432-446.
- [37] Li, S.M., McCarthy, S.: Further investigations on the hydrolytic degradation of poly(DL-lactide), *Biomaterials*, 1999, vol.20, pp.35–44.
- [38] Bonfield, W.: Composites for bone replacement, *Journal of Biomedical Engineering*, 1988, vol. 10, issue 6, pp. 522-526.
- [39] Bonfield, W., Gryn timer, M.D, Tully, A.E, Bowman, J., Abram, J.: Hydroxyapatite reinforced polyethylene - a mechanically compatible implant material for bone replacement, *Biomaterials*, 1981, vol. 2, issue 3, pp. 185-186.

- [40] Tenhuisen, K.S., Martin, R.I., Klimkiewicz, M., Brown, P.W.: Formation and properties of a synthetic bone composite: hydroxyapatite–collagen, *J. Biomed. Mater. Res.*, 1995, vol.29, pp. 803–10.
- [41] Hench, L. , Polak, J.: Third generation biomedical materials, *Science*, 2002, vol. 295, pp.1014–1017.
- [42] Tuan, H.S., Hutmacher, D.W.: Application of micro CT and computation modelling in bone tissue engineering, *Computer-Aided Design*, 2005, vol. 37, issue 11, pp. 1151–1161.
- [43] Bostman, O., Pihljamaki, H.: Clinical biocompatibility of biodegradable orthopaedic implants for internal fixation: a review, *Biomaterial*, 2000, vol. 21, 2615-2621.
- [44] M.Supová et al.: Problem of hydroxyapatite dispersion in polymer matrices: a review, *Journal of Materials Science: Materials in Medicine*, 2009, vol. 20, issue 6, pp. 1201-1213.
- [45] Kickelbick, G.: Concepts for the incorporation of inorganic building blocks into organic polymers on a nanoscale, *Prog. Polym. Sci.*, 2003, vol. 28, pp. 83-114.
- [46] Bilotti, E.: *Polymer / Sepiolite Clay Nanocomposites*, London, 2009. Dostupné z: <http://www.sems.qmul.ac.uk/research/honours/doc.php?id=324>, Dissertation Thesis, University of London, Supervisor Prof. Ton Peijs.
- [47] [Rho, J.](#), [Kuhn-Spearing, L.](#), [Ziopoulos, P.](#): Mechanical properties and the hierarchical structure of bone, *Medical Engineering & Physics*, 1998, vol. 20, issue 2, pp. 92-102.
- [48] Anandhan, S., Bandyopadhyay, S.: Polymer Nanocomposites: From Synthesis to Applications, *Nanocomposites and Polymers with Analytical Methods*, InTech, 2011-08-09, vol. 226, issue 4675, pp. 630-636.
- [49] Jančář, J.: The thickness dependence of elastic modulus of organosilane interphases., *Polymer Composites*, 2008, vol. 29, issue 12, pp. 1372-1377.
- [50] Jancar , J.: *Late Night Show with Polymer Nanocomposites I* - conference, Brno, 2008.
- [51] Recman, L.: Deformation Behavior of Nano/Micro Reinforced PMMA. Brno, 2010, p. 90, Dissertation Thesis, Faculty of chemistry BUT.
- [52] Grubs, R.B., *Natur Mat*, 2007, vol. 6, pp. 553-555.
- [53] Atkins, P., De Paula, J.: *Physical chemistry*, 2001, 7th edition, Oxford University Press , p.1180, ISBN-10: 0198792859.
- [54] Pouchlý, J: *Fyzikální Chemie Makromolekulárních a Koloidních Soustav*, 1998, VŠCHT, p. 198, ISBN 8070-803312.
- [55] Kalfus, J.: *Viscoelastic properties of polyvinylacetate-hydroxyapatite nanocomposites*, Brno, 2005, p. 106, Dissertation Thesis. Faculty of Chemistry BUT, supervisor prof. J. Jančář.
- [56] Swain, S. K.: *Processing of Porous Hydroxyapatite Scaffold*. Rourkela, 2009, Thesis. National Institute of Technology. Supervisor: Dr. S. Bhattacharyya.
- [57] Chiu, H., Wei, L.J.: HWA CHONG Institution, *Photocatalytic activity of barium and strontium hydroxyapatites* [online]. 2007 [cit. 2012-03-12]. Available from: http://pdc_archive.hci.edu.sg/2007/13-WebReport/Cat-01/1-59/site/bginfo.html
- [58] Vallet-Regí, M., Gonzalez-Calbet, J.M.: Calcium phosphates as substitution of bone tissues, *Prog. Solid State Chem.*, 2004, vol. 32, issue 1-2, pp. 1-31.
- [59] Wang, X., Nyman, J.S., Dong, X., Leng, Reyes, H: *Fundamental Biomechanics in Bone Tissue Engineering*, In: Athanasiou Ka, editor. Morgan and Claypool Publishers, 2010, p.230.
- [60] Le Geros, R.Z.: *Calcium phosphates in oral biology and medicine*, Monographs in Oral Science, vol.15. Editor, H.M.Myers, Karger, New York, 1991.

- [61] Sobczak-Kupiec, A.: Comparative study of hydroxyapatite prepared by the authors with selected commercially available ceramics, *Digest Journal of Nanomaterials and Biostructures*, 2012, vol. 7, issue. 1, pp. 385-391.
- [62] Gao, Y. et al.: Characterization and osteoblast-like cell compatibility of porous scaffolds: bovine hydroxyapatite and novel hydroxyapatite artificial bone, *Journal of Materials Science: Materials in Medicine*, 2006, vol. 17, issue 9, pp. 1372-1377.
- [63] Ruksudjarit, A., Pengpat, K., Rujijanagul, G.: Synthesis and characterization of nanocrystalline hydroxyapatite from natural bovine bone, *Current Applied Physics*, 2008, vol. 8, pp. 270-272.
- [64] Narayan, R., Ed.: *Biomedical Materials*; Springer, New York, NY, USA, 2009; p. 566, ISBN-10: 0387848711.
- [65] Ramesh, S., Tan, C.Y., Sopyan, I., Hamdi, M., Teng, W.D.: Consolidation of nanocrystalline hydroxyapatite powder, *Sci. Technol. Adv. Mater.*, 2007, vol. 8, pp. 124-130.
- [66] Pecqueux, F., Tancrét, F., Payraudeau, N., Bouler, J.M.: Influence of microporosity and macroporosity on the mechanical properties of biphasic calcium phosphate bioceramics: Modelling and experiment, *J. Eur. Ceram. Soc.*, 2010, vol. 30, pp. 819-829.
- [67] Linhart, W., Briem, D., Amling, M., Rueger, J.M., Windolf, J.: Mechanical failure of porous hydroxyapatite ceramics 7.5 years after implantation in the proximal tibia, *Unfallchirurg*, 2004, vol. 107, pp. 154-157.
- [68] Cao, W.; Hench, L.L.: Bioactive materials, *Ceramics International*, 1996, vol. 22, issue 6, pp. 493-507.
- [69] Fathi, M.H., Hanifi, A.: Evaluation and characterization of nanostructure hydroxyapatite powder prepared by simple sol-gel method, *Materials Letters*, 2007, vol. 61, issue. 18, pp. 3978-3983.
- [70] Bogdanoviciene, I., Beganskiene, A., Tonsuaadu, K., Glaser, J., Meyer, H-J, Kareiva, A.: Hydroxyapatite, $\text{Ca}_{10}(\text{PO}_4)_6(\text{OH})_2$ ceramics prepared by aqueous sol-gel processing, *Materials Research Bulletin*, 2006, vol. 41, issue. 9, pp. 1754-1762.
- [71] Ramanan, S.R., Venkatesh, R.: A study of hydroxyapatite fibers prepared via sol-gel route, *Materials Letters*, 2004, vol. 58, issue 26, pp. 3320-3323.
- [72] Sakaguchi, Y., Sawada, Z., Koizumi, M., Tamaki, K.: Effect of the Kind of Bases on Hydrolysis Rate of Polyvinyl Acetate, *Kobunshi Kagaku*; 1966, vol. 23, issue 260, pp. 890-894.
- [73] Rowe, R.C., Sheskey, P.J., Quinn, M.E.. (2006) Polyvinyl Alcohol In: Handbook of Pharmaceutical Excipients, 6th ed, Pharmaceutical Press, 2009, London, UK, p. 564. ISBN 08-536-9792-2.
- [74] Polyvinyl alcohol: Chang Chun Petrochemicals, Co., L. Taiwan. Available from: www.ccp.com/tw
- [75] Nair, B.: Cosmetic Ingredient Review. Final report on the safety assessment of polyvinyl alcohol, *International Journal of Toxicology*, 1998, vol 17 (Suppl. 5), pp. 67-92.
- [76] *Mowiol Polyvinyl Alcohol*, Sulzbach / Hessen: Clariant GmbH, 1999.
- [77] Kobayashi, M., Toguchida, J., Oka, M. Preliminary study of polyvinyl alcohol/hydrogel (PVA-H) artificial meniscus, *Biomaterials*, 2003, vol. 24, pp. 639-647.
- [78] Swiezkowski, W., Ku, D.N., Bersee H.E.N., Kurzydowski, K.J. :An elastic material for cartilage replacement in an arthritis shoulder joint, *Biomaterials*, 2006, vol. 27, pp. 1534-1541.
- [79] Sakurada, I., Nukushina, Y., Sone, Y.: Relation between crystallinity and swelling of poly(vinyl alcohol), *Kobunshi Kagaku*, 1955, vol. 12, p.510-513.

- [80] Spiller, K.L., Laurencin, S. J., Charlto, D., Maher, S.A., Kosman, A.M.: Superporous hydrogels for cartilage repair: Evaluation of the morphological and mechanical properties, *Acta Biomaterialia*, 2008, vol. 4, pp. 17-25.
- [81] Chou, L., Marek, B., Wagner, W.R.: Effects of hydroxylapatite coating crystallinity on biosolubility, cell attachment efficiency and proliferation in vitro, *Biomaterials*, 1999, vol. 20, pp. 977-985.
- [82] DeMerlis, C.C. et al.: Review of the oral toxicity of polyvinyl alcohol (PVA), *Food and Chemical Toxicology*, 2003, vol. 41, issue 3, pp. 319-326.
- [83] Bakos, D., Soldan, M., Hernandez-Fuentes, I.: Hydroxyapatite-collagen-hyaluronic acid composite, *Biomaterials*, 1999, vol. 20, issue 2, pp. 191-195.
- [84] Ragel, C. V., Vallet-Regi, M., Rodriguez-Lorenzo, L.M.: Preparation and in vitro bioactivity of hydroxyapatite/solgel glass biphasic material, *Biomaterials*, 2002, vol.23, pp. 1865-1872.
- [85] Suchanek, W., Yoshimura, M.: Processing and properties of hydroxyapatite-based biomaterials for use as hard tissue replacement implants, *J Mater Res*, 1998, vol. 13, pp. 94-117.
- [86] Kobayashi, M., Chang, Y.S., Oka, M.: A two year in vivo study of polyvinyl alcohol-hydrogel (PVA-H) artificial meniscus, 2005, *Biomaterials*, vol.26, pp. 3243-3248.
- [87] Pan, Y., Xiong, D.S., Ma, R.Y.: A study on the friction properties of poly (vinyl alcohol) hydrogel as articular cartilage against titanium alloy, *Wear*, 2007, vol. 262, issue 7, pp. 1021-1025.
- [88] Fenglan, X., Yubao, L., Xueijang, W.: Preparation and characterization of nano-hydroxyapatite/poly(vinyl alcohol) hydrogel biocomposite, *J. Mater Sci.*, 2004, vol. 39, pp. 5669-5672.
- [89] Katti, K.S.: Biomaterials in total joint replacement, *Colloids and Surfaces B: Biointerfaces*, 2004, vol.39, issue 3, pp.133-142.
- [90] Pan, Y.S., Xiong, D.S.: Recent development on biotribology of poly (vinyl alcohol) hydrogel, *Tribology*, 2006, vol.26, pp. 188-192. (in Chinese).
- [91] Yusong, P., Dangsheng, X., Xiaolin, C.: Mechanical properties of nanohydroxyapatite reinforced poly(vinyl alcohol) gel composites as biomaterial, *Journal of Materials Science*, 2007, vol. 42, issue 13, pp. 5129-5134.
- [92] Sittig, C., Textor, M., Spencer, N.D.: Surface characterization of implant materials c.p. Ti, ti-6Al-7Nb and Ti-6Al-4V with different pretreatments, *Journal of Material Science: materials in medicine*, 1999, vol. 10, pp. 35-46.
- [93] Basso, N., Heersche, J.N.M.: Characteristics of in vitro osteoblastic cell loading models, *Bone*, 2002, vol. 30, issue 2, pp.347-351.
- [94] Bayzit, V., Bayzit, M., Bayzit, E.: Evaluation of bioceramic materials in biology and medicine, *Digest Journal of Nanomaterials and Biostructures*, 2010, vol. 7, issue 3, pp. 267-278.
- [95] Hyon, S.H., Cha, W.I., Ikada, Y.: Preparation of trans-parent poly(vinyl alcohol) hydrogel, *Polym Bull*, 1989, vol. 22, pp. 119-122.
- [96] Freeman, M.E., Furey, M.J., Love, B.J., Hampton, J.M.: Friction, wear, and lubrication of hydrogels as syn-thetic articular cartilage, *Wear*, 2000, vol. 241, pp. 129-135.
- [97] Wu, G., Su, B., Wang, C., Zhang, W.: In vitro behaviors of hydroxyapatite reinforced polyvinyl alkohol hydrogel composite, *Mater Chem Phys*, 2008, vol. 2, pp. 364-369.

- [98] Paul, W., Sharma, C.P.: Nanoceramic materials: Biomedical applications, *American Journal of Biochemistry & Biotechnology*, 2006, vol. 2, pp. 41-48.
- [99] Raj, S., M., Arkin, V. H., Adalarasu, Jagannath, M.: Nanocomposites Based on Polymer and Hydroxyapatite for Drug Delivery Application, *Indian Journal of Science and Technology*, 2013, vol. 6 (5S), pp.4563-4568.
- [100] Fenglan, X., Yubao, L., Xiaoming, Y., Hongbing, L., Li, Z.: Preparation and in vivo investigation of artificial cornea made of nano-hydroxyapatite/poly (vinyl alcohol) hydrogel composite, *Journal of Materials Science: Materials in Medicine*, 2007, vol. 18, issue 4, pp. 635-640.
- [101] Fenglan, X., Yubao, L., Yingpin, D., Jie, X., Zhang, L.: Porous nano-hydroxyapatite/poly(vinyl alcohol) composite hydrogel as artificial cornea fringe: characterization and evaluation in vitro, *Journal of Biomaterials Science, Polymer Edition*, 2008, vol. 19, issue 4, pp. 431-439.
- [102] Helebrant, A., Jonášová, L., Šanda, L.: The influence of simulated body fluid composition on carbonated hydroxyapatite formation, *Ceramics - Silikáty*, 2002, vol. 46, issue 1, pp. 9-14
- [103] Lutišánová, G., Kuzielová, E., Palou, M., Kozánková, J.: Static and dynamic in vitro test of bioactivity of glass ceramics, *Ceramics – Silikáty*, 2011, vol. 55, issue 2, pp.106-113.
- [104] Durschang, B.R., Carl, G., Rüssel C., Roeder, E.: *Glastech. Ber. Glass Sci. Technol*, 1994, vol.67, pp.171-177.
- [105] Kuzielová, E., Hrubá, J., Palou, M., Smrčková, E.: Influence of P₂O₅ upon the crystallisation of lithium disilicate and fluoroapatite in bio-glass ceramics, *Ceramics-Silikaty*, vol. 50, issue 3, pp.159-162
- [106] Manivasagam, G., Dhinasekaran, D., Rajamanickam: Biomedical Implants: Corrosion and its Prevention - A Review, *Recent Patents on Corrosion Science*, 2010, vol. 2, issue. 1, pp. 40-54.
- [107] Hong, Ch., Tu, J., Liu, D., Li, R., Gu, C.: The electrochemical and mechanical properties of Ti incorporated amorphous carbon films in Hanks' solution, *Applied Surface Science*, 2010, vol. 256, issue. 16, pp. 4859-4866.
- [108] Parthiban, S.P. et al. : Effect of swift heavy ion irradiation on hydrothermally synthesized hydroxyapatite ceramics, *Nuclear Instruments and Methods in Physics Research Section B: Beam Interactions with Materials and Atoms*, 2008, vol. 266, issue 6, pp. 911-917.
- [109] Dorozhkin, S.V.: Inorganic chemistry of the dissolution phenomenon, the dissolution mechanism of calcium apatites at the atomic (ionic) level, *Comment Inorg. Chem*, 1999, vol. 20, pp. 285-299.
- [110] Best, S.M., Porter, A.E., Thian, E.S., Huang, J.: Bioceramics: Past, present and for the future, *Journal of the European Ceramic Society*, 2008, vol. 28, issue. 7, pp. 1319-1327.
- [111] Kokubo, T., Takadama, H.: How useful is SBF in predicting in vivo bone bioactivity?, *Biomaterials*, 2006, vol. 27, issue 15, pp. 2907-2915.
- [112] *Introduction to Attenuated Total Internal Reflectance(ATR)*. NicoletCZ.cz [online]. 2012, 3.8.2012 [cit. 2012-08-07]. Available from: <http://www.nicoletcz.cz/userfiles/file/Aplikace/Introduction%20ATR%20SpectraTech.pdf>
- [113] Bragg's law. In: *Wikipedia: the free encyclopedia* [online]. San Francisco (CA): Wikimedia Foundation, 2001-, 26 July 2013 [cit. 2013-07-28], Available from: https://en.wikipedia.org/wiki/Bragg%27s_law

- [114] ISO 527-1:2012(en). *Plastics — Determination of tensile properties*. 2. vyd. Madrid: Asociación Española de Normalización y Certificación, 2012. Available from: <https://www.iso.org/obp/ui/#iso:std:iso:527:-1:ed-2:v1:en>
- [115] Haines, J.P.: *Principles of thermal analysis and calorimetry*, 2002, Royal Society of chemistry, p. 320, ISBN 978-085404610.
- [116] Willard, H.: *Instrumental methods of analysis*, 7th ed. Belmont, Calif.: Wadsworth Pub. Co., c1988, xxi, p.895, ISBN 05-340-8142-8.
- [117] Ramachandran, V.S., Paroli, R.M., Beaudoin, J.J., Delgado, A.H.: *Handbook of thermal analysis of construction materials*, New York: 2002, William Andrew Publishing, p. 702 ISBN 0-8155-1487-5.
- [118] Brown, M.E.: *Introduction to thermal analysis techniques and applications*, 1988, Chapman and Hall, p. 212, ISBN 0-412-30230-6.
- [119] Pramanik, N., Mohapatra, S., Alam, S., Pramanik, P.: Synthesis of hydroxyapatite/poly(vinyl alcohol phosphate) nanocomposite and its characterization, *Polymer Composites*, 2008, vol. 29, issue 4, pp. 429-436.
- [120] Wang, T., Turhan, M., Gunasekaran, S.: Selected properties of pH-sensitive, biodegradable chitosan-poly(vinyl alcohol) hydrogel, *Polym. Int*, 2004, vol. 53, pp. 911-918.
- [121] Zheng, Y, Wang Y, Chen X, Liu Q, Lu Y. Studies of poly(vinyl alcohol)/hydroxylapatite hydrogels compounds for cartilage implantation, *Journal of Biomedical Engineering*, 2003, vol. 20, pp. 401–403. (in Chinese).
- [122] Li, H.D., Xiao, J., Cheng, F.M., Chen, X.X.: Preparation and properties of hydroxyapatite/polyvinyl alcohol compound hydrogels, *Journal of Changchun University of Technology (Natural Science Edition)*, 2007, vol. 28, pp. 338–340 (in Chinese).
- [123] Yusong, P., Dangsheng, X., Xiaolin, C.: Mechanical properties of nanohydroxyapatite reinforced poly(vinyl alcohol) gel composites as biomaterial, *Journal of Materials Science*, 2007, vol. 42, issue 13, pp. 5129-5134.
- [124] Gilbert, J. B., Kipling, J. J., *Fuel*, 1962, vol.12, pp. 249-260.
- [125] Ballistreri, A., Foti, S., Montaudo, G., Scamporrin, E.: Evolution of aromatic compounds in the thermal decomposition of vinyl polymers, *Journal of Polymer Science: Polymer Chemistry Edition*, vol. 18, issue 4, pp. 1147-1153
- [126] Peng, Z., Kong, L.X.: A thermal degradation mechanism of polyvinyl alcohol/silica nanocomposites, *Polymer Degradation and Stability*, 2007, vol. 92, issue. 6, pp.1061-1071.
- [127] Alexy, P., Bakos, D., Crkonova, G., Kolomaznik, K., Krsiak, M.: Blends of poly(vinyl alcohol) with collagen hydrolysate thermal degradation and processing properties, *Macromolecular Symposia*, 2001, vol. 170, issue 1, pp. 41-50.
- [128] Zhao, W.W., Yamamoto, Y., Tagawa, S.: Radiation effects on the thermal degradation of poly(vinyl chloride) and poly(vinyl alcohol), *Journal of Polymer Science Part A Polymer Chemistry*, 1998, vol. 36, pp. 3089-3095.
- [129] Holland, B.J., Hay, J.N.: The thermal degradation of poly(vinyl alcohol), *Polymer*, 2001, vol. 42, issue 16, pp. 6775-6783.
- [130] Cihlár, J., Buchal, Trunec, M., Pramanik, P: Synthesis of hydroxyapatite/poly(vinyl alcohol phosphate) nanocomposite and its characterization, *Journal of Materials Science*, 2008, vol. 34, issue 24, pp. 6121-6131.
- [131] Chai, C., Ben-Nissan, B.: *Thermal Stability of Synthetic Hydroxyapatites* by, International Ceramic Monographs, 1994, vol. 1, issue 1, pp. 79-85, Available from: <http://www.azom.com/details.asp?ArticleID=1462>.

- [132] Nie, L., Chen, D., Suo, J., Zou, P., Feng, S., Yang, Q., Yang, S., Ye, S.: Physicochemical characterization and biocompatibility in vitro of biphasic calcium phosphate/polyvinyl alcohol scaffolds prepared by freeze-drying method for bone tissue engineering applications: characterization and evaluation in vitro, *Colloids and Surfaces B: Biointerfaces*, 2012, vol. 100, issue 4, pp. 169-176.
- [133] Yao, L., Haas, T. W., Guiseppi-Elie, A., Bowlin, G. L., Simpson, D. G., Wnek, G. E.: Electrospinning and stabilization of fully hydrolyzed poly(vinyl alcohol) fibers, *Chem. Mater.*, 2003, vol.15, pp. 1860-1864.
- [134] Asran, A.S., Henning, S. ,Michler, G.H. : Polyvinyl alcohol-collagen-hydroxyapatite biocomposite nanofibrous scaffold: mimicking the key features of natural bone at the nanoscale level, 2010, *Polymer*, vol.51, pp. 868-876.
- [135] Gil, F.J, Padrós, A, Manero, J.M, Aparicio, C, Nilsson, M. Planell, J.A: Growth of bioactive surfaces on titanium and its alloys for orthopaedic and dental implants, *Materials Science and Engineering: C*, 2002, vol. 22, issue 1, pp.53-60.

9 LIST OF FIGURES

Figure 1: Classification of bioceramics according to their bioactivity; (a) bioinert, alumina dental implant, (b) bioactive, hydroxyapatite ($\text{Ca}_{10}(\text{PO}_4)_2(\text{OH})_2$) coating on a metallic dental implant, (c) surface active, bioglass, (d) bioresorbable tri-calcium phosphate implant ($\text{Ca}_3(\text{PO}_4)_2$) [12]	12
Figure 2: Four types of mutual arrangements of nanoparticles to a polymer chain according to Kickelbick: (1) inorganic particles embedded in an inorganic polymer, (2) incorporation of particles by bonding to the polymer backbone, (3) interpenetrating network with chemical bonds, (4) inorganic-organic hybrid polymer [45]	18
Figure 3: Hierarchical structure of bones: a) cortical and cancellous bone; b) osteons with Haversian systems; c) lamellae; d) collagen fibre assemblies of collagen fibrils; e) bone mineral crystals, collagen molecules and non-collagenous proteins. From [46, 47]	19
Figure 4: Increasing size and decreasing specific surface area of nanoparticles - From nanocomposites on the right to a micro composite on the left. Simplified example of hierarchically organized structures found in nanocomposites [52].	20
Figure 5: Crystal structure of hydroxyapatite [59].	22
Figure 6: A schematic diagram illustrating the assembly of collagen fibers and bone mineral crystals [71].	23
Figure 7: Preparation route of polyvinyl alcohol from polyvinyl acetate	25
Figure 8: Polyvinyl (alcohol) structure formula	26
Figure 9: Sakurada's structural model of polyvinyl alcohol [79].	26
Figure 10: The schematic diagrams of the interaction between hydroxyapatite and PVA polymers [88].	28
Figure 11: Tensile strength vs. modulus of materials with relevance for composite design when considering biomedical applications [93]	30
Figure 12: Schematic diagram of the process of formation of apatite on HAp surface. (a) HAp surface exposed to SBF under normal conditions, (b) calcium ions settle on HAp surface from the SBF to form Ca-rich ACP, (c) calcium-rich HAp surface attracts phosphate groups from SBF to form Ca-poor ACP and (d) ageing produces apatite on the HAp surface [108]	32
Figure 13: Two cases of the impact of X-ray beam at the crystal lattice: left Bragg condition is fulfilled - the emergence of diffraction maxima, the right is not fulfilled - destructive interference [113].	37
Figure 14: Dog-bone sample for tensile properties testing according to standard (ISO 527-2)	38
Figure 15: Typical stress strain curves [114]	38
Figure 16: XRD analysis of synthesized hydroxyapatite	40
Figure 17: XRD pattern of poly(vinyl alcohol) used in membrane preparation	41
Figure 18: Spectra of HA powder(100HA), pure PVA(0HA) and PVA/HA composites with various amount of hydroxyapatite (10HA, 20HA, 30HA, 40HA, 50HA)	42
Figure 19: Membranes with various HA content in PVA matrix, from left to right 0HA, 10HA, 20HA, 30HA, 40HA and 50HA	43
Figure 20: SEM image of 10HA at 150x magnification	44
Figure 21: SEM image of 20HA at 150x magnification	44
Figure 22: SEM image of 30HA at 150x magnification	45
Figure 23: SEM image of 40HA at 150x magnification	45
Figure 24: SEM image of 50HA at 150x magnification	46

Figure 25: Shows detailed view of HA particles at 5000 magnification	46
Figure 26: Cut along the membrane showing visible layer of the hydroxyapatite in the 30HA	47
Figure 27: Stress/strain characteristics of the PVA/HA composite	49
Figure 28: SEM image of the tensile impact fracture surfaces of the sample 30HA at 100 magnification	50
Figure 29: SEM image of sample 30HA after tensile strength testing – the impact edge at 100 magnification	51
Figure 30: Detail of the impact edge with visible HA and PVA phase after tensile testing of 30HA	51
Figure 31: Elimination reaction – H_2O realising	53
Figure 32: Chain scission reactions in the first degradation step	53
Figure 33: Chain scission reactions	54
Figure 34: TGA curve of pure PVA (0HA)	55
Figure 35: TGA curve of pure hydroxyapatite powder (100HA)	56
Figure 36: TGA curve of composite 10HA	57
Figure 37: XRD spectrum of 20HA composite after TGA analysis	58
Figure 38: Increasing weight loss of composites and the pure PVA in time	59
Figure 39: Shows macroscopic comparison of membranes with various HA content in PVA matrix, from left to right 0HA, 10HA, 20HA, 30HA, 40HA and 50HA after 7 days of SBF soaking.	60
Figure 40: Surface morphology of 50HA before soaking in SBF	60
Figure 41: Surface morphology of 50HA after soaking in SBF for 2 hours	61
Figure 42: Surface morphology of 50HA after soaking in SBF for 28 days	61
Figure 43: Detail of new formed hydroxyapatite on the surface	62
Figure 44: Study of surface change during testing periods – 50HA before soaking in SBF	62
Figure 45: Study of surface change during testing periods – 50HA after 2 hours of soaking in SBF	63
Figure 46: Study of surface change during testing periods – 50HA after 28 days of soaking in SBF	63
Figure 47: Diffractogram of 50HA composite surface after 7 days of soaking in SBF	64
Figure 48: Diffractogram of 50HA composite surface after 28 days of soaking in SBF	64
Figure 49: TGA curve of pure PVA (0HA)	80
Figure 50: TGA curve of pure hydroxyapatite powder (100HA)	80
Figure 51: TGA curve of composite 10HA	81
Figure 52: TGA curve of composite 20HA	81
Figure 53: TGA curve of composite 30HA	82
Figure 54: TGA curve of composite 40HA	82
Figure 55: TGA curve of composite 50HA	83

10 LIST OF TABLES

Table 1: The main material categories to reconstruct bone, and some of their typical disadvantages[14]	13
Table 2: List of mechanical properties of some materials [94]	30
Table 3: The ion concentrations (mol/l) of SBF in comparison with ions in blood plasma (BP), Ringer's solution (RS) and Hank's solution (HBSS).	32
Table 4: Characterisation of used PVA Mowiol 10-98 [76]	35
Table 5: Designation of prepared composites	35
Table 6: Tensile properties of prepared membranes	48
Table 7: The physical appearance during thermal decomposition of PVA [129].	52
Table 8: Weight loss of PVA/HA composites with variable HA content in PVA matrix sorted into three temperature ranges	56
Table 9: Comparison of total weight loss at 900°C	58
Table 10: Weight loss of PVA/HA biocomposites in testing time	59

11 LIST OF SYMBOLS

ACP	Amorphous calcium phosphate
A-W	Apatite-wollastonite
ATR-FTIR	Attenuated Total Reflectance Fourier Transform Infrared Spectroscopy
BMP	Bone morphogenic protein
BG	Bioactive glass
CHAp	Carbonate apatite
CaP	Calcium phosphate
CDHA	Calcium deficient hydroxyapatite
CPC	Calcium phosphate cement
FA	Fluorapatite
FDA	Food and Drug Administration
HAPEX	PE matrix reinforced with HA particles
HCA	Hydroxycarbonated apatite
HA	Hydroxyapatite
HCl	Hydrochloric acid
NOAEL	No Observed Adverse Effect Level
OA	Oxyapatite
PCL	Poly(3-caprolactone)
PDS	Polydioxanone
PE	Polyethylen
PEEK	Poly(etheretherketone)
PGA	Polyglycolide
PHB	Polyhydroxybutyrate
PHEMA	poly(2-hydroxyethyl- methacrylate)
PLA	Poly lactide
PP	Polypropylene
PSU	Polysulfone
PVAc	Polyvinyl acetate
PVA	Polyvinyl alcohol
SEM	Scanning electron microscopy
SBF	Simulated Body Fluid
TTCP	Tetracalcium phosphate
TCP	Tricalcium phosphate
TGA	Thermogravimetric Analysis
UHMWPE	Ultra-high-molecular-weight polyethylene
XRD	X-ray Diffraction

12 APPENDIX

12.1 TGA results

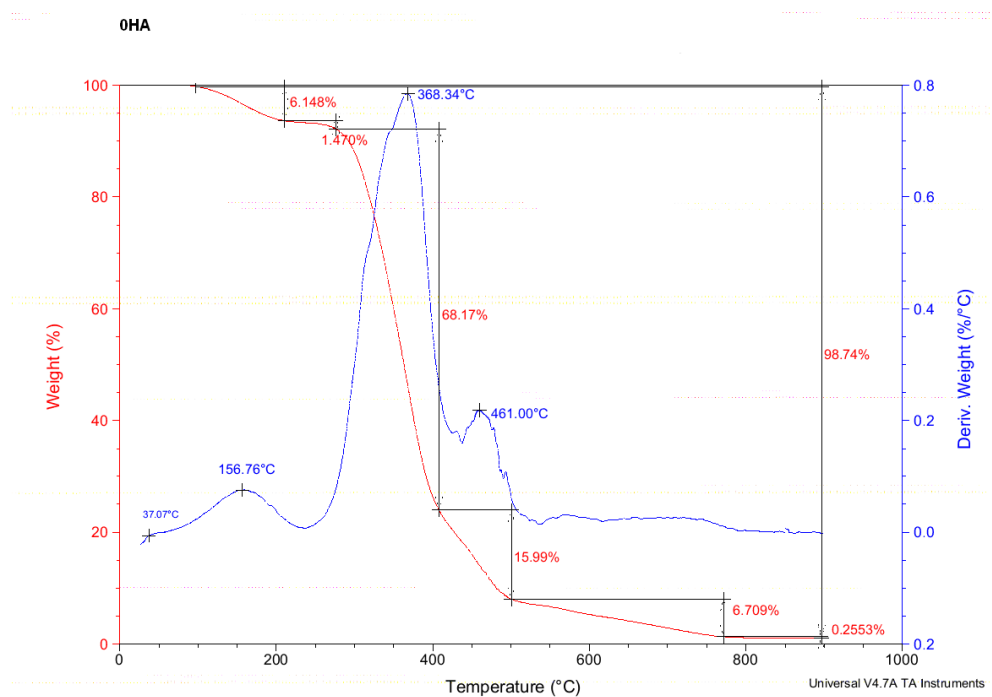


Figure 49: TGA curve of pure PVA (0HA)

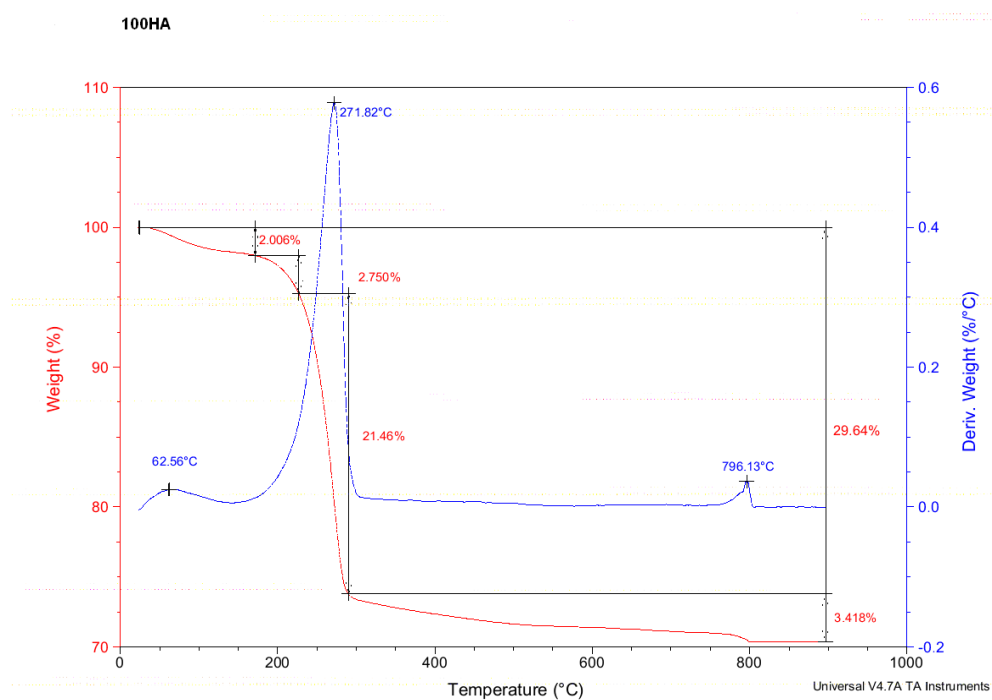


Figure 50: TGA curve of pure hydroxyapatite powder (100HA)

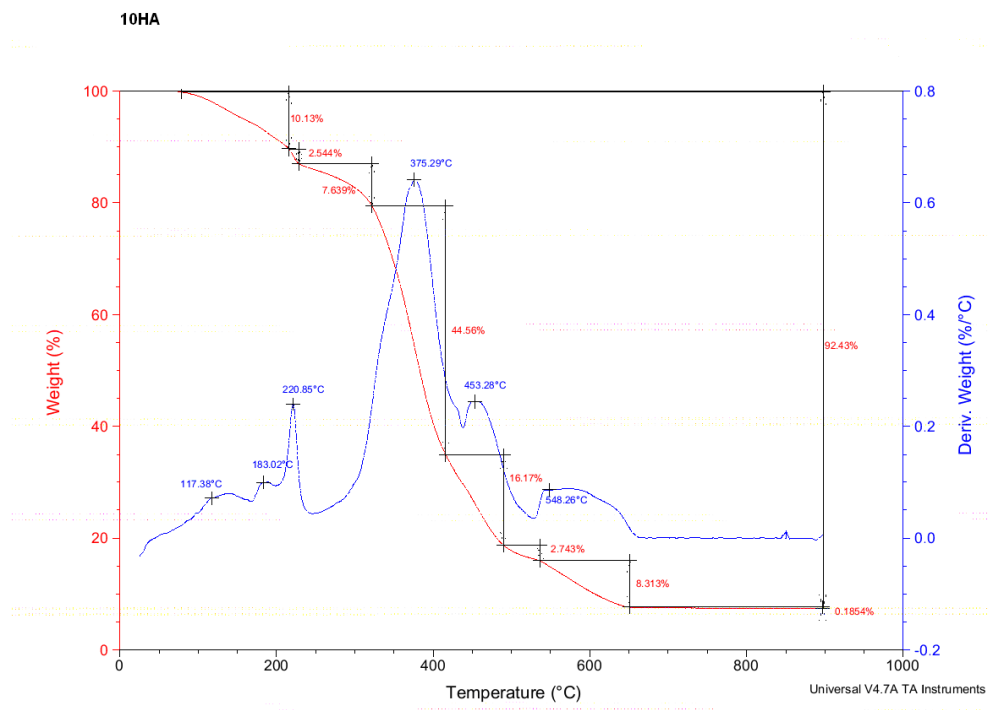


Figure 51: TGA curve of composite 10HA

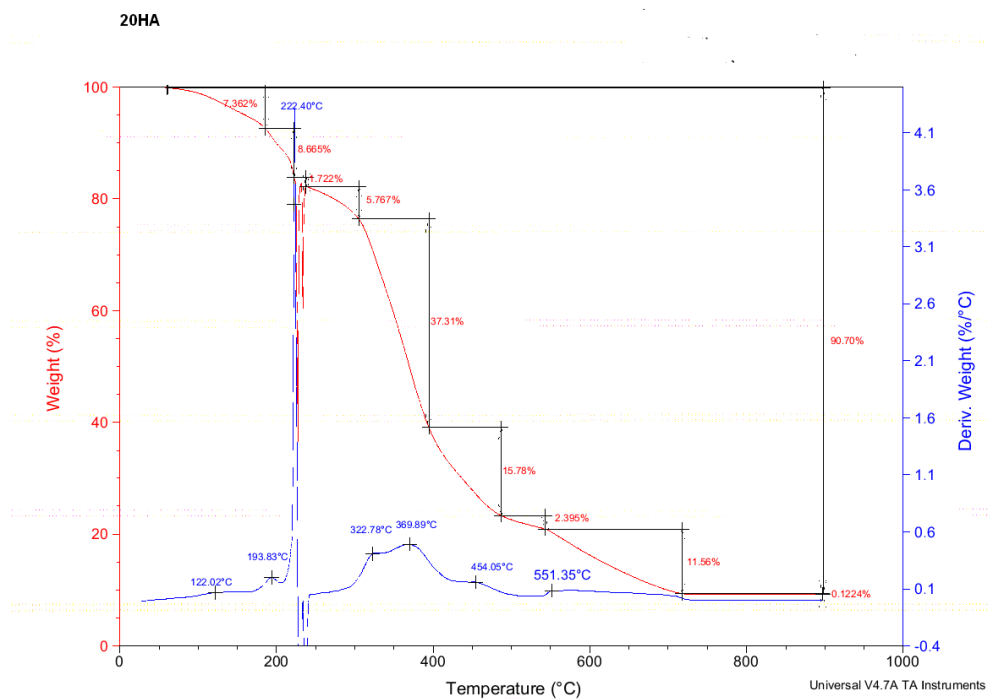


Figure 52: TGA curve of composite 20HA

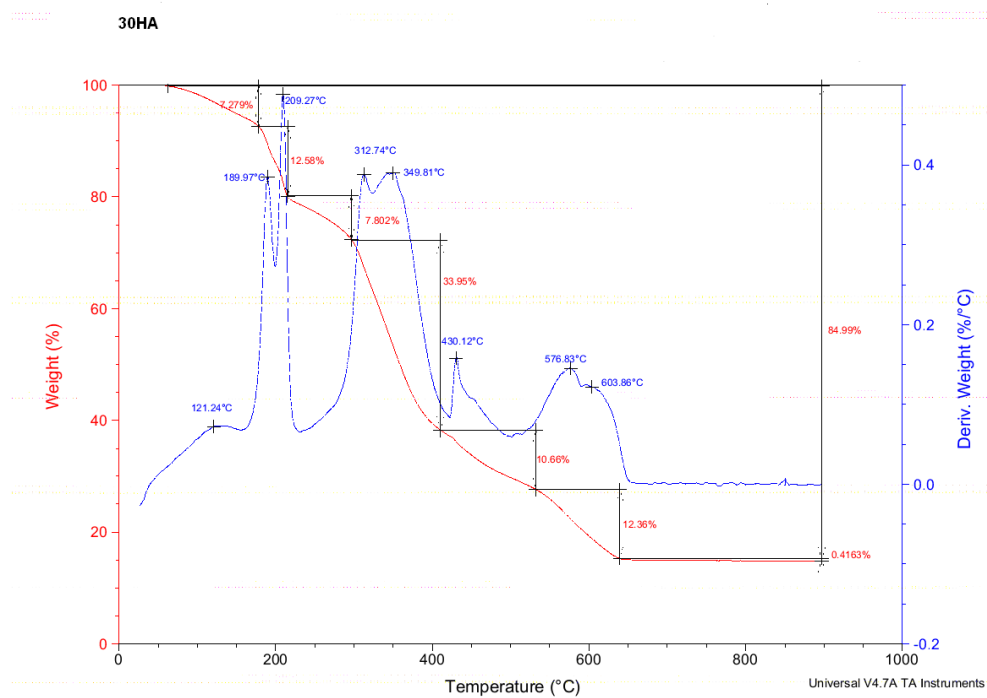


Figure 53: TGA curve of composite 30HA

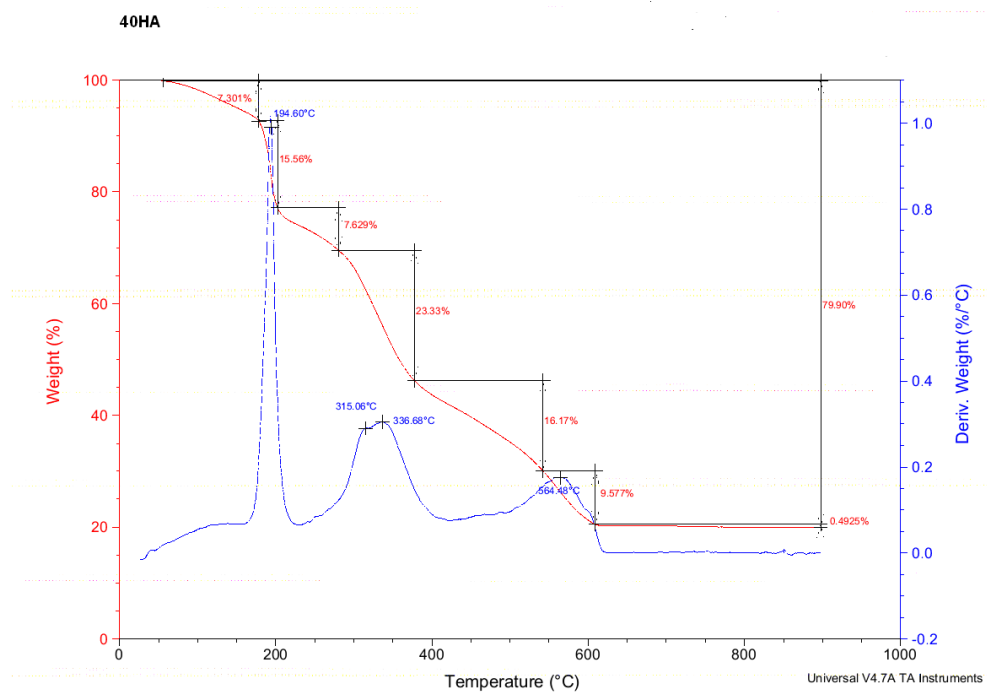


Figure 54: TGA curve of composite 40HA

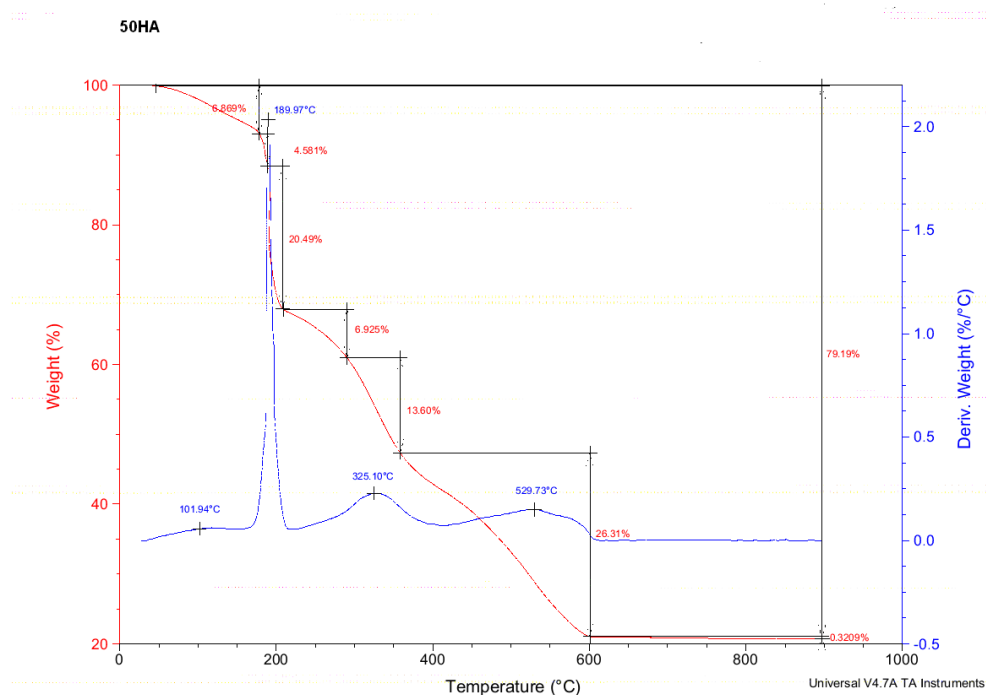


Figure 55: TGA curve of composite 50HA

12.2 List of publications

Publications

BALGOVÁ, Z.; PALOU, M.; WASSERBAUER, J.; KOZÁNKOVÁ, J.; LUTIŠANOVÁ, G. Preparation, characterization and in vitro bioactivity of polyvinyl alcohol- hydroxyapatite biphasique membranes. *Acta Chemica Slovaca*, 2013, roč. 6, č. 1, s. 8-14. ISSN: 1337- 978X.

BALGOVÁ, Z.; PALOU, M.; WASSERBAUER, J.; KOZÁNKOVÁ, J. Synthesis of poly(vinyl alcohol) - hydroxyapatite composites and characterization of their bioactivity. *CENTRAL EUROPEAN JOURNAL OF CHEMISTRY*, 2013, roč. 11, č. 9, s. 1403-1411. ISSN: 1644- 3624.

Conference proceedings

OPRAVIL, T.; HAVLICA, J.; BRANDŠTETR, J.; PTÁČEK, P.; ŠOUKAL, F.; BALGOVÁ, Z. Preparation and properties of binders based on roman cement. In *11th INTERNATIONAL CONFERENCE Ecology and new building materials and product*. 2007.s. 255-259. ISBN: 978-80-239-9347- 9.

BALGOVÁ, Z.; PALOU, M. *Synthesis of polyvinyl alcohol- hydroxyapatite membranes*. Chemické listy. Brno: Česká společnost chemická, 2011. s. 943-943. ISSN: 0009- 2770.

BALGOVÁ, Z.; PALOU, M. Thermal Characterisation of Polyvinyl alcohol/ Hydroxyapatite Composite. In *4th Joint Czech-Hungarian-Polish-Slovak Thermoanalytical Conference, Book of Contributions*. 1. University of Pardubice, 2013.s. 222-225. ISBN: 978-80-7395-603- 5.

Research report

BALGOVÁ, Z.; ŠOUKAL, F.; HAVLICA, J. *Spoluspalování masokostní moučky v cementářských pecích - vliv obsahu P_2O_5 na vlastnosti cementu*. 2006.